uOttawa

L'Université canadienne
Canada's university

FACULTÉ DES ÉTUDES SUPÉRIEURES ET POSTOCTORALES

uOttawa

L'Université canadienne
Canada's university

FACULTY OF GRADUATE AND POSDOCTORAL STUDIES

Jennifer Lam

AUTEUR DE LA THÈSE / AUTHOR OF THESIS

M.Sc. (Cellular and Molecular Medicine)

GRADE / DEGREE

Department of Cellular and Molecular Medicine

FACULTÉ, ÉCOLE, DÉPARTEMENT / FACULTY, SCHOOL, DEPARTMENT

D*ll*1 is a Potential CDX2 Target Gene

TITRE DE LA THÈSE / TITLE OF THESIS

David Lohnes

DIRECTEUR (DIRECTRICE) DE LA THÈSE / THESIS SUPERVISOR

CO-DIRECTEUR (CO-DIRECTRICE) DE LA THÈSE / THESIS CO-SUPERVISOR

Marc Ekker

Valerie Wallace

Gary W. Slater

Le Doyen de la Faculté des études supérieures et postdoctorales / Dean of the Faculty of Graduate and Postdoctoral Studies

Dll1 is a Potential CDX2 Target Gene

Jennifer S. Lam

Thesis submitted to the Faculty of Graduate and Postdoctoral Studies

in partial fulfillment of the requirements for the

degree of Master's of Science in Cellular and Molecular Medicine

Department of Cellular and Molecular Medicine

Faculty of Medicine

University of Ottawa

April 29, 2010

© Jennifer Lam, Ottawa, Canada, 2010

Library and Archives Canada

Published Heritage Branch

395 Wellington Street
Ottawa ON K1A 0N4
Canada

Bibliothèque et Archives Canada

Direction du Patrimoine de l'édition

395, rue Wellington
Ottawa ON K1A 0N4
Canada

Your file Votre référence
ISBN: 978-0-494-79668-9
Our file Notre référence
ISBN: 978-0-494-79668-9

NOTICE:

The author has granted a non-exclusive license allowing Library and Archives Canada to reproduce, publish, archive, preserve, conserve, communicate to the public by telecommunication or on the Internet, loan, distribute and sell theses worldwide, for commercial or non-commercial purposes, in microform, paper, electronic and/or any other formats.

The author retains copyright ownership and moral rights in this thesis. Neither the thesis nor substantial extracts from it may be printed or otherwise reproduced without the author's permission.

AVIS:

L'auteur a accordé une licence non exclusive permettant à la Bibliothèque et Archives Canada de reproduire, publier, archiver, sauvegarder, conserver, transmettre au public par télécommunication ou par l'Internet, prêter, distribuer et vendre des thèses partout dans le monde, à des fins commerciales ou autres, sur support microforme, papier, électronique et/ou autres formats.

L'auteur conserve la propriété du droit d'auteur et des droits moraux qui protège cette thèse. Ni la thèse ni des extraits substantiels de celle-ci ne doivent être imprimés ou autrement reproduits sans son autorisation.

In compliance with the Canadian Privacy Act some supporting forms may have been removed from this thesis.

While these forms may be included in the document page count, their removal does not represent any loss of content from the thesis.

Conformément à la loi canadienne sur la protection de la vie privée, quelques formulaires secondaires ont été enlevés de cette thèse.

Bien que ces formulaires aient inclus dans la pagination, il n'y aura aucun contenu manquant.

Canada

ABSTRACT

The functional redundancy and peri-implantation lethality inherent to members of the CDX family has traditionally limited their investigation. As such, the development by our lab of a conditional null mutant, obliterating CDX activity in the mouse, has opened up an exploration of their additional roles. Along with the loss of caudal tissue and failure of neural tube closure, *Cdx1/2* null mutants exhibit abnormal somites, an observation which is echoed by the misregulation of many somitic players including members of the Wnt and Notch signaling pathways upon microarray analysis. The replication of altered expression patterns *in situ* and identification of consensus CDX response elements (CDRE) in the proximal promoter regions validated many of these genes as potential CDX targets. Characterization of one candidate in particular, *Dll1*, revealed reduced expression in the absence of CDX and overlapping expression domains with CDX members as well as somitic anomalies in *Dll1* null mutants. The identification of two highly conserved putative CDRE in the proximal promoter region, in addition to the ability of CDX2 to occupy the promoter in the vicinity of these sites *in vivo* and specifically bind the identified motifs *in vitro*, was consistent with direct regulation. Functional analysis of CDX2 in association with the *Dll1* promoter has so far proven inconclusive, but synergistic induction of the wildtype promoter in the presence of TBX6 supports a potential co-regulation. Overall, this thesis presents evidence for delta-like 1 (*Dll1*) as a potential direct target of CDX2. Moreover, these findings support the possibility that CDX may regulate players in the Notch and Wnt signaling pathways and thereby play an important role in somitogenesis.

TABLE OF CONTENTS

LIST OF FIGURES

LIST OF TABLES

LIST OF ABBREVIATIONS

5'UTR	5' Untranslated Region
Ab	Antibody
AP	Anterior-Posterior
APC	Adenomatous Polyposis Coli
AS-C	Achaete Scute and Lethal of Scute
ATCC	American Type Culture Collection
βCAT	β-Catenin
βGAL	β-Galactosidase
bHLH	Basic Helix-Loop-Helix
Bp	Base Pair
BSAP	B-Cell-Specific Activator Protein
CAD	Caudal
cDNA	Complementary Deoxyribonucleic Acid
CDX	Caudal-Related Homeobox
CDRE	Cdx Response Element
ChIP	Chromatin Immunoprecipitation
CK1α	Casein Kinase 1 Alpha
Cpm	Counts Per Minute
CPRG	Chlorophenolred-β-D-Galactopyranoside
CRE	Cre Recombinase
CSL	CBF1 and RBPjκ, Suppressor of Hairless (Su(H)), and Lag-1

CYP26A1	Cytochrome P450, Family 26, Subfamily A, Polypeptide 1
DEPC	Diethylpyrocarbonate
DLL1	Delta-Like 1
DMSO	Dimethyl Sulfoxide
DNA	Deoxyribonucleic Acid
DSL	Delta-Serrate-Lag-2
DOS	Delta and OSM-11-Like Proteins
DVL	Dishevelled
E	Embryonic Day
EDTA	Ethylenediaminetetraacetic Acid
EGF	Epidermal Growth Factor
EMSA	Electrophoretic Mobility Shift Assay
ERT2	Estrogen Receptor Ligand Domain modified to respond to Tamoxifen
ES	Embryonic Stem
EST	Expressed Sequence Tag
FGF	Fibroblast Growth Factor
FRZB	Frizzled-Related Protein
FZD	Frizzled
GSK3	Glycogen Synthase Kinase 3
GST	Glutathione *S*-Transferase
HOX	Homeobox
Hsp	Heat Shock Protein

ISH	*In Situ* Hybridization
JAG1	Jagged 1
Kb	Kilobase
LacZ	β-Galactosidase Gene
LEF1	Lymphoid Enhancer Binding Factor 1
LoxP	Locus of Crossover in P1
LRP	Low-Density Lipoprotein Receptor-Related Protein
MAM	Mastermind
MES	Mesodermal Enhancer Domain
mRNA	Messenger Ribonucleic Acid
Msd	Mesodermal Enhancer Domain
NCoR	Nuclear Receptor Co-Repressor
NICD	Notch Intracellular Domain
NEXT	Notch Extracellular Truncation
NP-40	Nonyl Phenoxylpolyethoxylethanol
NRARP	Notch-Regulated Ankyrin Repeat Protein
PBS	Phosphate-Buffered Saline
PCR	Polymerase Chain Reaction
PFA	Paraformaldehyde
PIS	Pre-Immune Serum
PITX2	Paired-Like Homeodomain Transcription Factor 2
PS	Primitive Streak
PSM	Presomitic Mesoderm

RA	Retinoic Acid
RARE	Retinoic Acid Response Element
RNA	Ribonucleic Acid
Rpm	Revolutions Per Minute
RSV-βGAL	RSV-β-galactosidase
RT-PCR	Reverse Transcriptase Polymerase Chain Reaction
RV	Rib-Vertebrae
SDS	Sodium Dodecyl Sulfate
SPSB4	SpIA/Ryanodine Receptor Domain and SOCS Box Containing 4
SS	Supershift
SUV39H1	Suppressor of Variegation 3-9 Homolog 1
TBST	Tris-Buffered Saline Tween-20
TBX6	T-box 6
TCF	T-Cell Factor
TE	Tris EDTA Buffer
TESS	Transcription Element Search System
TSHZ1	Teashirt Zinc Finger Family Member 1
VP16	Herpes Simplex Virus Protein vmw65; Trans Inducing Factor (α-TIF)
WNT	Wingless-Related
WT	Wildtype

ACKNOWLEDGMENTS

The following work would not have been possible without the help and encouragement of a great number of individuals. First and foremost, I would like to thank my supervisor Dr. David Lohnes for his guidance and support over the past three years. His understanding of my peculiar working hours, support for my non-scientific interests, as well as the countless hours he has dedicated to helping me achieve success in my scientific endeavours has not gone unnoticed.

I would also like to express my sincere gratitude to the many members of the Lohnes lab past and present who have helped me throughout my Master's career. I am particularly grateful to Joanne and Stephanie, for teaching me the ropes and bearing with my endless streams of questions. I would also like to thank Beta, Jen, and Sabrina my late-night lab partners and close friends, as well as Christine, Donna, Colin, Cat, James, Nadine, Melissa, Leon the fish, Alexa, and Caitlin for their company and friendship. I would like to make particular mention of my committee members Dr. Christine Pratt and Dr. Marc Ekker, for their direction and advice over the course of my project, as well as CIHR for funding my work.

Finally, I am indebted to my parents and my brother, as well as close friends for helping me to endure the ups and downs of scientific research. I'm also grateful for my personal cheering squad and housemates Matt, Minette, Stella and Bereket, for their unfaltering love and encouragement. The present work would simply not have been possible without this network of love and support. Thank you.

CHAPTER 1

INTRODUCTION

1.1 Introduction

Shortly following implantation, the developing mammalian embryo undergoes a series of morphogenetic changes that collectively give rise to the primitive body plan. This process, known as gastrulation, relies on cell proliferation and migration in order to form three germinal layers: the endoderm, mesoderm and ectoderm (Beddington and Robertson, 1998; Tam and Behringer, 1997). Each of these layers subsequently acquires distinct fates as a result of subsequent specification and patterning events (Mitiku and Baker, 2007). These events rely on the concerted activity of numerous transcription factors, including the family of Caudal-related homeobox (CDX) transcription factors, which are involved in patterning the posterior embryo (Lohnes, 2003).

1.2 Somitogenesis

During gastrulation, the development of the mesodermal layer in particular arises as a result of the ingression of cells from the external surface through a raised structure on the posterior end of the embryo known as the primitive streak (PS) (Alexander *et al.*, 2009; Tam and Behringer, 1997). Some of these cells contribute to the paraxial mesoderm (Kinder *et al.*, 1999; Wilson and Beddington, 1996), which gives rise to transient structures known as somites that flank the prospective neural tube. Once formed, the epithelial somites undergo subsequent differentiation into the dermatome, myotome, and sclerotome, which are the anlagen of the future dermis, skeletal muscles of the trunk and limbs, and vertebrae, respectively

(Dequeant and Pourquie, 2008). Following the closure of the neural tube around E10.5, cells no longer ingress through the primitive streak (Wilson and Beddington, 1996). Subsequently, paraxial mesoderm is sustained by a stem-cell-like population in the tailbud (Cambray and Wilson, 2007; Gridley, 2006).

During somitogenesis, the presomitic paraxial mesoderm (PSM) condenses periodically to form the epithelial metameric somites (Gridley, 2006) (Figure 1.1 A). Segmentation of somites occurs in a regular cyclical manner due to regulation by a molecular "clock". This molecular clock, in turn, interacts with a "wavefront" of graded gene expression which dictates where somites will condense, a region termed the determination front (Olivera-Martinez and Storey, 2007; Wahl *et al.*, 2007).

The molecular clock is reflected by the oscillating expression of a number of genes, including members of the Notch pathway (e.g. *Lfng, Hes1*, and *Hes7*), the Wnt negative regulator *Axin2,* as well as other Wnt genes, and Fgf pathway players (e.g. *Spry2* and *Dusp6)* (Feller *et al.*, 2008; Gomez *et al.*, 2008; Gridley, 2006). Expression of such genes typically initiates in the caudal region of the tailbud and propagates anteriorly through the presomitic mesoderm until it reaches the determination front where segmentation begins (Olivera-Martinez and Storey, 2007) (Figure 1.1 B). The determination front is established by the opposing action of FGF8 in the caudal embryo and RA emanating from the trunk region (Olivera-Martinez and Storey, 2007).

Figure 1.1: Mechanisms in somitogenesis.

A: Schematic of somite formation, with an emphasis on graded gene expression and the segmentation process. The "wavefront" is depicted on the left, consisting of opposing gradients of gene expression from members of the Fgf/Wnt and RA signaling cascades. The "determination front" indicates the threshold whereby cells become competent to a signal to begin differentiation, and this marks the point where somite border formation is initiated. The regeneration of mesodermal tissue is also illustrated in the tailbud as new presomitic mesoderm (PSM) is produced to sustain continued segmentation in the caudal end of the embryo. Image based and adapted from (Dubrulle and Pourquie, 2004).

B: Schematic illustrating the periodicity of somite formation resulting from oscillating gene expression. Shading depicts transcript levels as they originate in the tailbud and die out at the level of the formed somites. As the posterior presomitic mesoderm continues to extend in the caudal direction, the signal starts anew. Within any individual cell this results in periodic waves of gene expression that have been likened to a "molecular clock". Genes with cyclic expression from the Notch, Wnt and Fgf pathways have been listed in the table. Image based and adapted from (Kageyama *et al.*, 2007).

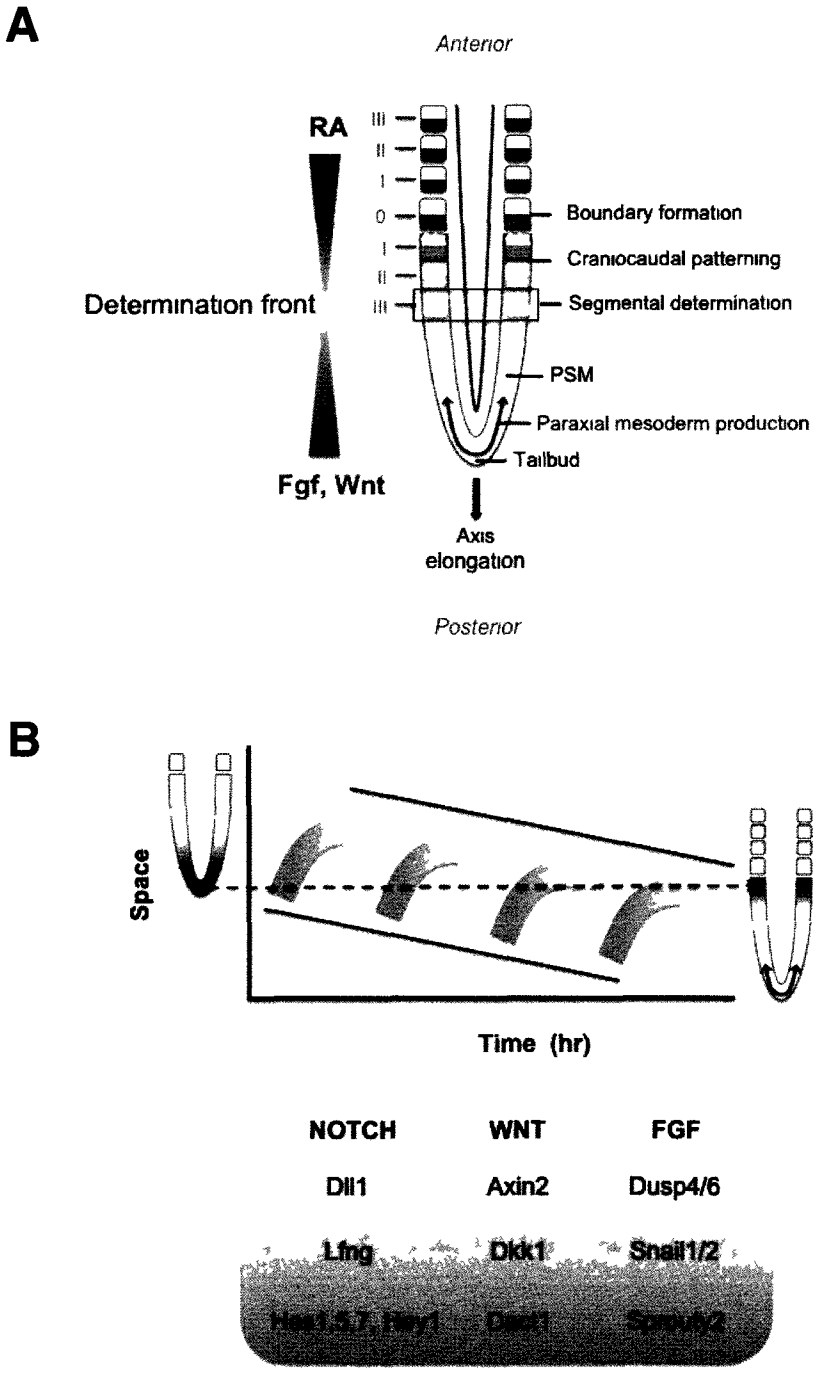
A
Anterior
RA
III
II
I
0
I
II
III
Boundary formation
Craniocaudal patterning
Segmental determination
Determination front
PSM
Paraxial mesoderm production
Tailbud
Fgf, Wnt
Axis elongation
Posterior
B
Space
Time (hr)
NOTCH
WNT
FGF
Dll1
Axin2
Dusp4/6
Lfng
Dkk1
Snail1/2

Figure 1.1

Wnt and Notch pathways play key roles in somitogenesis, and are potential targets of CDX, as described later in this discussion. I will therefore focus on a description of some of these pathways with particular emphasis on their roles in somitogenesis.

1.3 The CDX transcription factors

Caudal-related homeobox (CDX) proteins are a family of transcription factors containing a highly conserved homeodomain that binds DNA. The 180 bp homeobox sequence contains an evolutionary conserved α-helix that is presumed to bind the major groove of DNA and transmit sequence specificity (Mlodzik *et al.*, 1985). *Cdx* genes are said to have arisen from an ancestral *ProtoHox* gene cluster that also gave rise to the *Hox* genes, another family of homeodomain transcription factors (Ferrier and Holland, 2001). CDX factors play important roles during embryogenesis, and have been implicated in posterior specification, intestinal development, and anteroposterior (AP) patterning among other things (Lohnes, 2003).

Drosophila Caudal (CAD) was the first member of the CDX family to be identified (Mlodzik *et al.*, 1985). Caudal is a 472 amino acid transcription factor containing the highly conserved homeodomain (Mlodzik and Gehring, 1987). Caudal has been implicated in both patterning of the anterior-posterior (AP) axis and specification of the posterior fly embryo, and *cad* mutants exhibit severe defects in these processes,

often lacking differing combinations of posterior segments (Macdonald and Struhl, 1986).

The mouse and human have three CAD orthologues: CDX1 (Duprey *et al.*, 1988), CDX2 (James and Kazenwadel, 1991), and CDX4 (Gamer and Wright, 1993). While the spatial and temporal expression of each *Cdx* gene is distinct, there is typically extensive overlap among family members, particularly in the posterior embryo (Figure 1.2). *Cdx1* transcripts are first detected around embryonic day (E) 7.5 in the ectoderm and nascent mesoderm of the primitive streak region, and reach an anteriormost boundary at the preotic sulcus. Later expression is seen in the dorsal neural folds, the mesonephros, proximal limb buds, and the presumptive dermamyotome of the somites until the signal is extinguished around twelve days post-coitum (Meyer and Gruss, 1993). *Cdx1* expression is reinitiated in the hindgut endoderm at E12.5 in a caudal-high gradient in the developing intestine, and it retains this expression postnatally (Grainger *et al.*, 2009; Silberg *et al.*, 2000).

Cdx2 expression initiates slightly later in the embryo proper, and encompasses a more posterior domain relative to *Cdx1*. At E8.5 *Cdx2* is expressed in all tissues of the primitive streak remnant, including the tailbud, the unsegmented paraxial mesoderm, the hindgut endoderm and the base of the allantois (Beck *et al.*, 1995; Chawengsaksophak *et al.*, 1997). At E12.5, *Cdx2* becomes restricted to the

Figure 1.2: Expression patterns of murine *Cdx*.

Representation of the expression domains of each of the murine *Cdx* members at different stages of development. *Cdx1* is expressed earlier and more anteriorly relative to *Cdx2*, and *Cdx4* is more restricted in the posterior embryo. Image from (Lohnes, 2003).

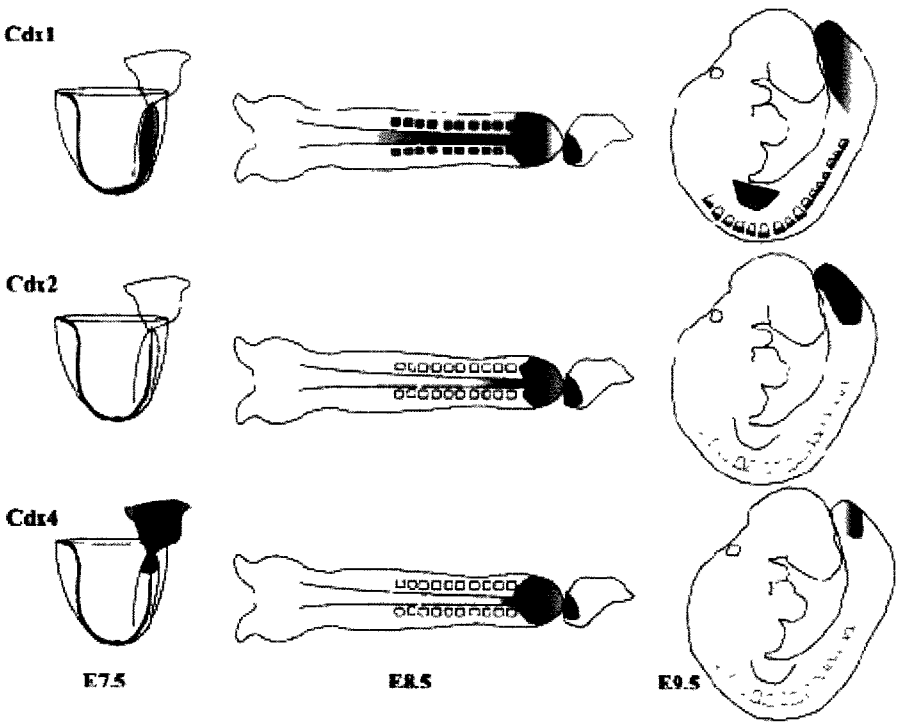

(Lohnes, 2003)

Figure 1.2

developing intestine, with peak expression occurring in the proximal colon. Similar to *Cdx1*, expression in the intestinal epithelium is maintained through adulthood (Silberg *et al.*, 2000). Interestingly, and distinct from the other *Cdx* members, *Cdx2* is also expressed in the trophectoderm commencing at E3.5 where it plays an essential role as discussed below (Beck *et al.*, 1995; Chawengsaksophak *et al.*, 1997).

Cdx4 is expressed between E7.5 and E10.5 and is observed at low levels in the allantois and in the posterior tip of the primitive streak. *Cdx4* reaches an anterior limit of expression at the level of the most recently formed somites, and unlike the other murine *Cdx* members, is absent from the intestinal epithelium (Gamer and Wright, 1993; Grainger *et al.*, 2009). Details related to CDX function in the intestine will not be covered in this discussion, as they are peripheral to the thesis.

1.4 Models of *Cdx* loss-of-function

Loss-of-function mouse models are frequently used to elucidate critical functions of a given gene product (Thomas and Capecchi, 1987). Accordingly, knockout mutants have been generated for *Cdx1* (Subramanian *et al.*, 1995), *Cdx2* (Chawengsaksophak *et al.*, 1997) and *Cdx4* (van Nes *et al.*, 2006). Homozygous null *Cdx1* mutants are viable and fertile but display vertebral patterning defects representing anterior homeotic transformations affecting the cervical and upper thoracic regions (Subramanian *et al.*, 1995) (Figure 1.3). Mice heterozygous for *Cdx1* also exhibit

Figure 1.3: Homeotic transformations in *Cdx* mutants.

Anterior homeotic transformations in mouse *Cdx1* null mutants. The C1 vertebra has taken on a more occipital localization, and the remaining cervical vertebrae have assumed morphologies of more anteriorized vertebrae relative to the wildtype control. Image from (Lohnes, 2003).

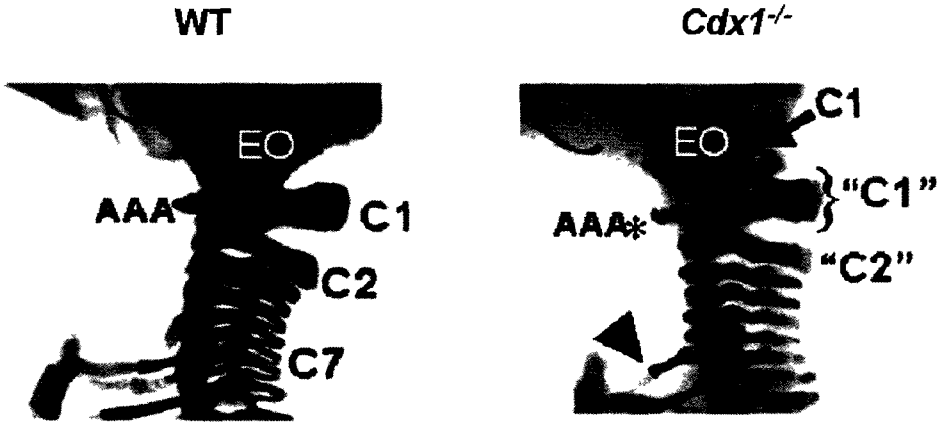

(Lohnes, 2003)

Figure 1.3

vertebral homeotic transformations, but with lower penetrance, while additional tissues expressing *Cdx1*, such as the limb buds, the intestine and the mesonephros, are unaffected (Subramanian *et al.*, 1995). Collectively, these observations suggest that *Cdx1* is haploinsufficient and plays a role in vertebral patterning.

In contrast to the *Cdx1* homozygotes, *Cdx2* null mice are embryonic lethal and die between E3.5 and E5.5 due to a critical requirement for CDX2 in the trophectoderm (Chawengsaksophak *et al.*, 1997). C*dx2* heterozygotes, however, have a similar phenotype to their *Cdx1* counterparts, exhibiting homeotic vertebral transformations that affect the posterior cervical and anterior thoracic vertebrae (Chawengsaksophak *et al.*, 1997). The more caudal localization of these mutations compared to the transformations seen in the *Cdx1* null embryos is in agreement with the later onset of expression of *Cdx2* relative to *Cdx1* (Lohnes, 2003). Additionally, *Cdx2* heterozygotes display a "kinky" or truncated tail, neonate weights are two standard deviations below their wildtype littermates, and 90% of the offspring develop intestinal lesions suggestive of an anterior transformation of the intestinal epithelia (Chawengsaksophak *et al.*, 1997). Altogether, these observations imply that the *Cdx2* gene is haploinsufficient and that it is essential for AP patterning of both mesodermal and endodermal derivatives (Chawengsaksophak *et al.*, 1997). Furthermore, loss of *Cdx2* seems to have a greater penetrance and more widespread effects than loss of its paralogue *Cdx1*.

In contrast to *Cdx1* and *Cdx2*, *Cdx4* null mutants do not exhibit any overt phenotype (van Nes *et al.*, 2006). However, loss of *Cdx4* exacerbates the phenotypes of both *Cdx1* and *Cdx2* mutants, indicative of functional redundancy among the CDX members (van Nes *et al.*, 2006). Consistent with this, *Cdx1*$^{+/-}$/*Cdx2*$^{+/-}$ and *Cdx1*$^{-/-}$ *Cdx2*$^{+/-}$ compound mutants also exhibit more progressive mutations compared to their single mutant counterparts, particularly with respect to truncation of the tail (van den Akker *et al.*, 2002). In addition, "knock-in" of *Cdx2* into the *Cdx1* locus revealed functional equivalence between these paralogues, at least as regards vertebral patterning (Savory *et al.*, 2009b).

1.5 CDX regulation of *Hox* genes

The vertebral homeoses seen in *Cdx* mutants likely reflects their function as regulators of homeobox (*Hox*) gene expression (Davidson *et al.*, 2003; van Nes *et al.*, 2006). Like *Cdx* members, *Hox* genes encode homeodomain transcription factors that regulate AP patterning (Guazzi *et al.*, 1994; Iimura and Pourquie, 2007; Wellik, 2007). The 39 mammalian *Hox* genes are arranged in 4 chromosomal clusters (*Hoxa* - *Hoxd*). They are further divided into 13 paralogous groups based on the sequence of their homeodomains and physical position of each gene within a cluster. Interestingly, *Hox* genes are expressed along the AP axis in a spatiotemporal fashion that reflects their physical order on the chromosome, a phenomenon termed colinearity (Duboule and Dolle, 1989; Duboule, 1998; Krumlauf, 1994). The *Hox* genes are responsible for specifying vertebral identities, and this is achieved

through a genre of "*Hox* code" (McGinnis and Krumlauf, 1992). While developing somites appear originally indistinct, the final vertebrae acquire individual fates on account of the differing arrangements of *Hox* genes in association with each segment.

In addition, direct correlations have been observed between the expression domains of individual *Hox* genes and vertebral patterning defects seen in *Cdx* mutants. A number of studies now offer strong evidence that CDX transcription factors directly regulate *Hox* expression, and the close phenocopy of vertebral homeotic transformations presented in *Cdx* mutants to those of certain H*ox* mutants is consistent with such a mechanism of action (Lohnes, 2003; Subramanian *et al.*, 1995).

CDX transcription factors function through binding to *cis*-acting CDX response elements (CDRE) (Dearolf *et al.*, 1989), and consensus motifs have been identified in *Drosophila* and other species. The sequence TTTATG is recognized as a binding motif for CAD in *Drosophila* (Dearolf *et al.*, 1989), while random primers tested by *in vitro* binding assays and DNase I footprinting have identified $\underset{A\ A\ \ A}{A\underline{T}\underline{T}\underline{T}A\underline{T}\underline{G}}$ as the chicken CDXA CDRE (Margalit *et al.*, 1993). Potential CDREs have been detected in many *Hox* loci, including the promoter regions for *Hoxa7*, *Hoxb8*, and *Hoxc8* (Charite *et al.*, 1998; Subramanian *et al.*, 1995; Taylor *et al.*, 1997). Deletion of one of the two CDREs in the *Hoxa7* promoter reduces its response to CDX1 in transient transfection (Subramanian *et al.*, 1995), while the CDREs identified in the *Hoxb8* locus were

shown to play a key role in the spatial expression of a transgenic reporter (Charite *et al.*, 1998). Collectively, these findings present strong support for the notion of direct regulation of *Hox* genes by CDX transcription factors.

1.6 Development of novel *Cdx2* mouse models

While the aforementioned *Cdx* mutants clearly suggest a role for CDX in AP vertebral patterning, the functional overlap between CDX members impedes our understanding of the full scope of their activity. Additionally, our comprehension of the role of CDX2 in later development has been limited due to the peri-implantation lethality of the *Cdx2* knockout, and a novel model is necessary to circumvent this restriction. To this end, the Rossant lab utilized a tetraploid aggregation approach, which can rescue lethal mutations caused by defects in extraembryonic tissues (Nagy *et al.*, 1990; Rossant and Spence, 1998). In this model, *Cdx2* null ES cells were aggregated with wildtype tetraploid embryos, which form the embryo and the extraembryonic tissues, respectively (Figure 1.4 A). *Cdx2* null embryos created in this manner begin to show abnormalities around embryonic day 8.5 (E8.5) with an underdeveloped allantois leading to the lack of chorio-allantoic fusion and eventual placental failure. Mutants also display a caudal truncation posterior to the forelimb bud, smaller and irregular-shaped somites posterior to the fifth somite, with some mice exhibiting extensive necrosis in the posterior endoderm and the caudal mesenchyme. Mutant embryos remain viable until approximately E11.5 but are

Figure 1.4: Alternative methods in the creation of *Cdx2* null embryos.

A: Model of the tetraploid aggregation technique that has been used to produce *Cdx2* null embryos. *Cdx2* null embryonic stem (ES) cells are aggregated to wildtype tetraploid cells. ES cells produce the embryo proper while the wildtype tetraploid cells form a normal trophoblast and allow the embryo to implant. This effectively circumvents the lethality inherent to the requirement for *Cdx2* in proper implantation. Image recreated from (Kunath et al., 2003).

B: Schematic of the CRE/*loxP* system of conditional *Cdx2* inactivation. CRE is fused to a modified estrogen receptor (ERT2) ligand domain that only responds to tamoxifen (hereby termed *Cre-ERT2*), and is expressed universally under the control of the *β-actin* promoter. In the absence of tamoxifen it is believed that Heat-shock protein 90 (Hsp90) associates with the estrogen receptor and effectively sequesters the chimeric protein [2]. This binding is reversed upon tamoxifen administration [3]. A *Cre-ERT2* male is crossed with a female containing a "floxed" *Cdx2* allele, where exon 2 of the *Cdx2* locus (*Cdx2* E2) is flanked by two location of crossover (*loxP*) sites not present in mammalian genomes [1]. Following the period of blastocyst implantation the pregnant female is administered a dose of tamoxifen and the *Cre-ERT2* protein is allowed to translocate to the nucleus. Presence of the *Cre-ERT2* transgene leads to a recombination event resulting in the excision of the *Cdx2* DNA-binding domain [4]. The onset of *Cdx2* loss is controlled by the timing of tamoxifen administration, and, in this way, this method is also able to circumvent the peri-implantation lethality.

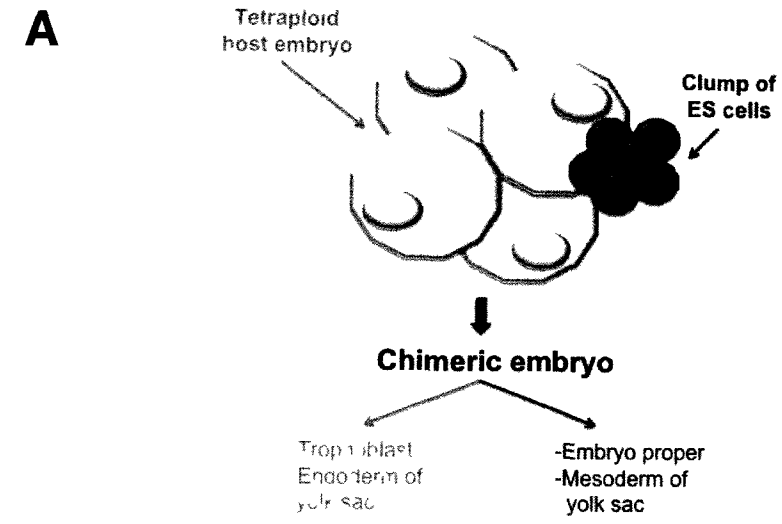
A
Tetraploid host embryo
Clump of ES cells
Chimeric embryo
-Embryo proper
-Mesoderm of yolk sac

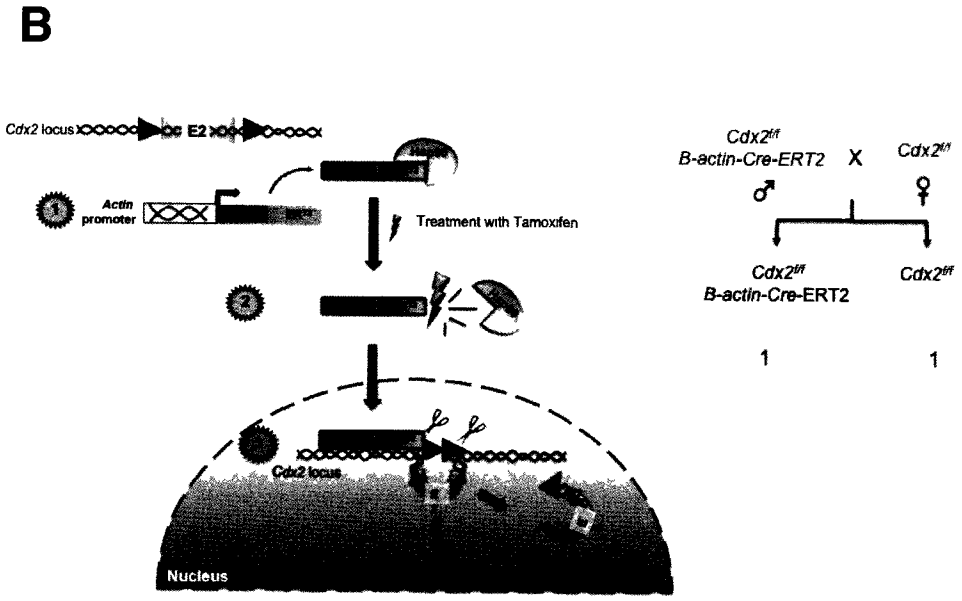
B
Cdx2 locus
E2
Actin promoter
Treatment with Tamoxifen
Cdx2 locus
Nucleus
Cdx2f/f B-actin-Cre-ERT2
X
Cdx2f/f
Cdx2f/f B-actin-Cre-ERT2
Cdx2f/f
1
1

Figure 1.4

developmentally 1.5 to 2 days behind their nominal age (Chawengsaksophak *et al.*, 2004). Despite the information gleaned from these studies, creation of tetraploid mutants is technically demanding, labor intensive, temporally limiting, and yields relatively few null embryos. To evade these difficulties, our lab has developed an alternative model, as discussed below.

To circumvent the shortcomings of the tetraploid construct, our lab used the CRE/*loxP* recombinase system to restrict loss of *Cdx2* to the post-implantation period (Figure 1.4 B). In the CRE/*loxP* system the Cre recombinase enzyme catalyzes a recombination event between two *loxP* sites (Hamilton and Abremski, 1984). When these sites are in *cis* and in the same orientation, this leads to excision of the intervening sequences (Nagy, 2000). In our model we flanked exon 2 of the *Cdx2* locus, which harbours the DNA-binding homeodomain, with *loxP* sites and effected its excision throughout the embryo using a widely expressed β-*actin-Cre-ERT2* transgene. This transgene also allowed temporal activation of CRE through its fusion to an estrogen receptor ligand domain (ERT2) modified to respond exclusively to tamoxifen, a synthetic modulator of the estrogen receptor. *Cdx2$^{f/f}$* (*i.e.* *Cdx2* "floxed" - also known as "flanked by *loxP*" sites) females were paired with *Cdx2$^{f/f}$; Cre-ERT2* males in timed matings, and pregnant dams were treated at E5.5 with 2 mg of tamoxifen by oral gavage in order to inactivate the *Cdx2* floxed allele following the period of implantation (Savory *et al.*, 2009a).

Embryos were harvested at E8.5 and E9.5, at which time the CDX2 protein could no longer be detected. Interestingly, while levels of CDX1 protein remained the same, CDX4 was severely attenuated (Savory *et al.*, 2009a); this was also true of the mutants generated by tetraploid aggregation (Chawengsaksophak *et al.*, 2004). Conditional *Cdx2* null embryos did not survive past E11.5, and displayed a severe caudal truncation. Somites posterior to the first 5-7 pairs appeared smaller than wildtype littermate controls, and extended nearly to the tip of the tail at later stages due to the loss of presomitic mesoderm (Savory *et al.*, 2009a). Thus, CDX2 was shown to play an essential role in axial elongation, and this was likely via the direct regulation of genes responsible for the formation of paraxial mesoderm such as *Wnt3a*, *T* (brachyury), and *Cyp26a1* (Savory *et al.*, 2009a).

Subsequent to these findings, we generated a *Cdx1/Cdx2* double homozygote to address the issue of CDX functional overlap. To this end, the *Cdx2$^{f/f}$; Cre-ERT2* line was crossed into a *Cdx1* null background (Subramanian *et al.*, 1995), and tamoxifen was administered to pregnant females at E5.5 to inactivate *Cdx2* post-implantation. Embryos were later harvested at E7.5 and E8.5. At this time, CDX2 protein was completely extinguished, and in comparison to the attenuation of CDX4 expression in *Cdx2* single null embryos, CDX4 protein was now absent. The loss of CDX4 intimated the creation of a mutant model representing complete loss of the murine CDX family, and hence a prototype to investigate the full scope of CDX activity in the absence of functional complementarity.

Cdx1/2 null mutants survived to E10.5, which was shorter than their *Cdx2* single null counterparts, and displayed more progressive anomalies. *Cdx1/2* compound mutants were characterized by a more severe caudal truncation as well as an open neural tube that extended along the length of the AP axis. While markers of mesoderm and/or paraxial mesoderm such as *T* (brachyury), *Wnt3a* and *Cyp26a1* were downregulated in the *Cdx2* single null mutants (Savory *et al.*, 2009a), they were essentially extinguished in the doubles at E8.5. Finally, while the segmentation of somites was not perturbed, somitogenesis ceased prematurely, and the more caudal somites appeared slightly broader and sometimes asymmetric (Figure 1.5) compared to their wildtype littermate controls (our unpublished data).

1.7 Identification of novel CDX target genes

Following the establishment of the CDX1/2 double mutants, we were interested in determining the molecular basis for the *Cdx1/Cdx2* null phenotype. Since CDX proteins are transcription factors, we performed a microarray in order to identify genes that were misregulated in the mutant background. For this screen, we collected *Cdx1/2* null embryos and used their wildtype littermates as controls. The embryos were harvested at E8.5 to coincide with the onset of the full complement of CDX proteins, as well as the stage at which many of the anomalies were observed. Additionally, we performed our screen using only the presomitic tissue since CDX proteins are expressed predominantly in this region. The microarray was

Figure 1.5: Morphology of the *Cdx1*$^{-/-}$*Cdx2*$^{-/-}$ mutant.

Representation of irregular somite formation in the compound mutant embryos. Somites appear wider (black bars) and the regularity of border formation is disturbed compared to littermate controls. Somites have been labeled for *Paraxis*, which marks the sclerotome and dermatome of condensed somites, and images were shot under identical lighting conditions and magnification using a Leica MZ16FA microscope.

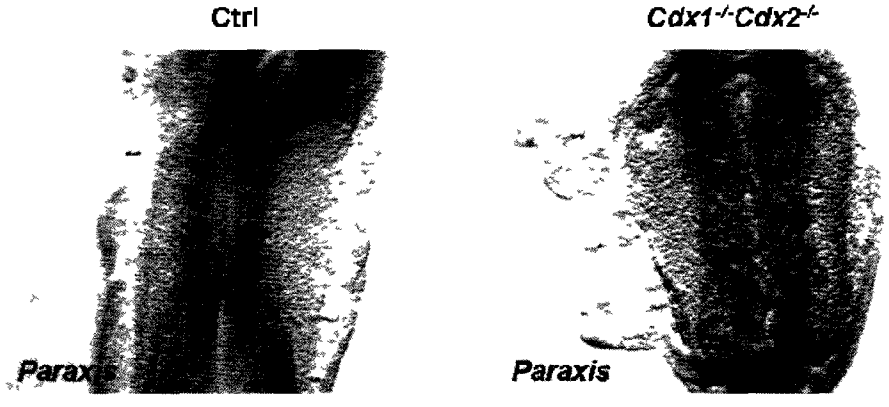

Figure 1.5

subsequently analysed using a stringent triple algorithm filtration with MAS5, RMA, and GC-RMA, in collaboration with Dr. Alan Mears. This screen revealed at least 80 genes with a high probability of downregulation in the mutants. Importantly, several of these genes are known (or suspected) CDX targets, including a number of the *Hox* genes (e.g. *Hoxa5, Hoxa9, Hoxb8, Hoxc8, and Hoxd8*) and CDX target genes previously identified by our group such as brachyury (*T*), and cytochrome P450, family 26, subfamily A, polypeptide 1 (*Cyp26a1*) (our unpublished data).

One intriguing result from the microarray analysis was the appearance of a number of players from the Notch and canonical Wnt signaling pathways, both of which have been implicated in posterior fate determination, and, in particular, the process of somitogenesis. As evidenced by the premature termination of somitogenesis and the presence of broader and sometimes asymmetric somites in *Cdx1/Cdx2* double null mutants, this process appears to be impacted by CDX function.

1.8 Mechanism of canonical Wnt signaling

The Wnt pathway is an example of paracrine signaling, and conveys its actions through the transmission of signaling molecules from cell to cell. The canonical pathway is so-named because it was the first form of Wnt signaling to be discovered, and is distinguished from other mechanisms by its dependence on β-catenin for signal transduction (Angers and Moon, 2009; MacDonald *et al.*, 2009). Thus, non-canonical Wnt pathways have also come to be known as β-catenin independent. The

present discussion focuses solely on canonical signaling since the implications of this pathway on somite development have been well described.

The WNT family was first discovered in *Drosophila*, and received its name as a cross between Wingless, a *Drosophila* segment polarity protein and Wnt ligand, and Integrated 1, a vertebrate homologue of WNT (Hausmann *et al.*, 2007). The WNT ligands are a group of conserved cysteine-rich glycoproteins that are shuttled to the plasma membrane for secretion (Angers and Moon, 2009; MacDonald *et al.*, 2009). WNT ligands are slightly hydrophobic, due to post-translational lipidation, but they are capable of close range and even long-range signaling through binding to lipoproteins or the formation of multimers in order to shield their lipid groups (Katanaev *et al.*, 2008; Lin, 2004; Panakova *et al.*, 2005).

At the plasma membrane of target cells, WNT ligands interact with Frizzled (FZD) receptors. Frizzled proteins have 7 transmembrane domains and are part of the G protein-coupled receptor family (Bjarnadottir *et al.*, 2006; Logan and Nusse, 2004). There are 10 members in mammals (Binnerts *et al.*, 2007; Logan and Nusse, 2004), and WNT ligands bind to these receptors with particularly high affinity (1-10 nm). Together with Low density lipoprotein receptor-related protein (LRP) and other receptor cofactors, Wnt and Frizzled activate a signaling cascade (Logan and Nusse, 2004; MacDonald *et al.*, 2009) (Figure 1.6).

Figure 1.6: Schematic of canonical Wnt signaling.

Diagram of the canonical Wnt signaling pathway. In the absence of WNT ligand a cytosolic complex containing Axin, APC, GSK3 and CK1α phosphorylates β–catenin, resulting in its ubiquitylation and degradation through β-TrCP. Additionally, the transcriptional co-repressor Groucho binds to LEF/TCF transcription factors in the nucleus and inhibits the transcription of Wnt target genes. When WNT ligand is present, signaling through the family of Frizzled (FZD) transmembrane receptors bound to LRP co-receptors removes GSK3 and members of the cytosolic complex. This allows β–catenin to accumulate and translocate to the nucleus where it can replace Groucho on LEF/TCF factors and induce the transcription of Wnt target genes. Image based and modified from (Clevers, 2006).

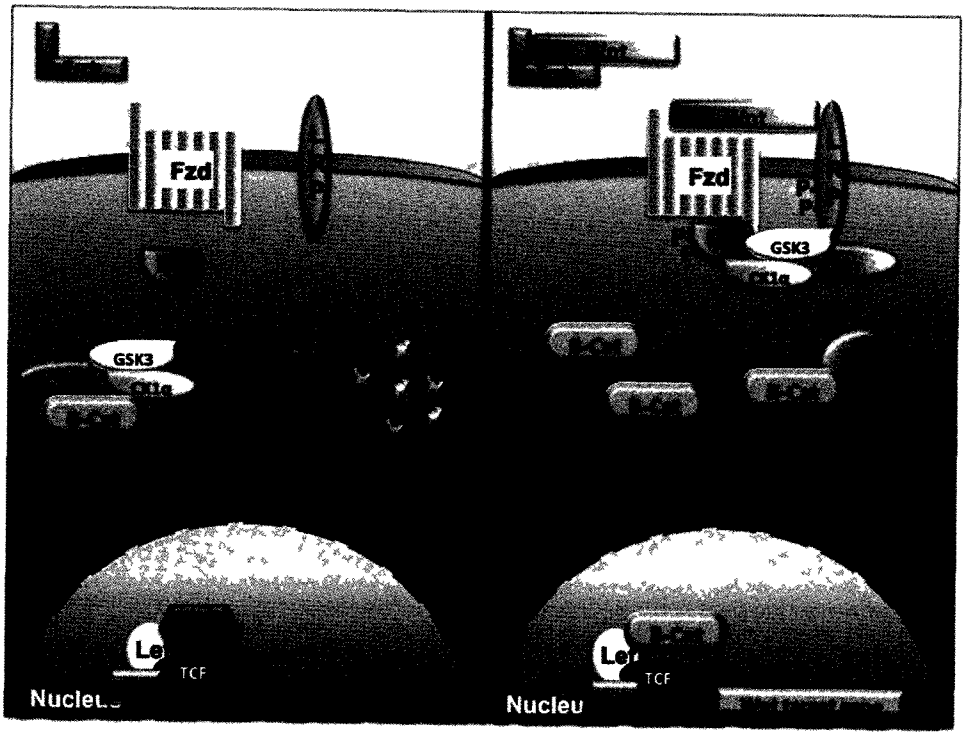

Figure 1.6

As mentioned previously, canonical Wnt signaling is dependent on β-catenin. In fact, the mechanism of canonical signaling is dependent on the stabilization of this protein in the cytoplasm. In the absence of WNT ligand, β-catenin is bound by the Axin complex, consisting of the scaffolding proteins Axin and Adenomatous polyposis coli (APC) as well as kinases Glycogen synthase kinase 3 (GSK3) and Casein kinase 1 alpha (CK1α). CK1α and GSK3 phosphorylate Axin and APC to facilitate their association with β-catenin, and also phosphorylate β-catenin itself (Huang and He, 2008; Kimelman and Xu, 2006). This latter phosphorylation process creates binding sites for β-TrCP, an E3 ubiquitin ligase, leading to ubiquitylation and degradation of β-catenin by the 26S proteosome (Kimelman and Xu, 2006). This continual elimination of β-catenin prevents its nuclear accumulation, thus inhibiting the activation of Wnt target genes.

When WNT ligand is present, however, a different sequence of events takes place. WNT binds a Frizzled (FZD) transmembrane receptor inducing the association of FZD with its co-receptor LRP5/6 (MacDonald *et al.*, 2009). This binding promotes the scaffolding protein Dishevelled (DVL) to recruit Axin and associated members of the destructor complex. GSK3 and CK1 now phosphorylate LRP (Davidson *et al.*, 2005; Zeng *et al.*, 2005), allowing it to bind and recruit more Axin and create a positive feed-forward reaction (Baig-Lewis *et al.*, 2007; Wallingford and Habas, 2005; Zeng *et al.*, 2008). With Axin and other members of the destructor complex now bound to the receptor elements, β-catenin degradation is inhibited. Cytoplasmic β-catenin then accumulates and translocates to the nucleus where it

displaces the co-repressor Groucho from LEF/TCF members and functions as a transcriptional co-activator to turn on Wnt target genes (Angers and Moon, 2009). Subsequently, the Wnt signal is transmitted from one cell to another and able to perpetuate a message within a tissue.

The Lymphoid enhancer binding factor/T-cell factor (LEF/TCF) family consists of four members in mammals: TCF1, 3, 4 and LEF1, and these factors are responsible for translating the signal from β-catenin to activate target genes (Arce *et al.*, 2006; MacDonald *et al.*, 2009). Members of the LEF/TCF family are high-mobility group (HMG) DNA-binding proteins that can cause DNA to physically bend (Hatzis *et al.*, 2008). Deletion of one of these members, *Lef1*, results in relatively mild defects such as the loss of body hair and certain craniofacial features, although the production of mesoderm and somite patterning remain unperturbed. This latter phenotype is presumably due to functional redundancy between members of the LEF/TCF family (van Genderen *et al.*, 1994). In agreement with this, the deletion of multiple LEF/TCF members results in more severe defects. *Lef1/Tcf1* double null mutants are characterized by abnormal somites with disrupted border formation anterior to the forelimb bud, as well as several ectopic neural tubes indicative of an earlier interruption in the production of persomitic mesoderm (Galceran *et al.*, 1999). The formation of ectopic neural tubes phenocopies the loss of *Wnt3a* (Galceran *et al.*, 1999) or *Tbx6* (Chapman and Papaioannou, 1998). Collectively, these defects underline the essential role of LEF/TCF factors and Wnt signaling in

mouse development, and particularly in the production of paraxial mesoderm and its derivatives.

1.9 The multiple roles of canonical Wnt signaling

The canonical Wnt pathway is associated with many cellular decisions, including the determination of cell fate, cell proliferation and stem cell renewal (Logan and Nusse, 2004). Wnt signaling also plays an integral role in somitogenesis, and *Axin2*, dickkopf homologue 1 (*Dkk1*) and several other Wnt pathway genes display oscillating expression patterns and contribute to the periodicity of somite formation (Dequeant and Pourquie, 2008). Another Wnt player, *Wnt3a*, is expressed as a gradient along the AP axis, and helps to establish the determination front (Aulehla *et al.*, 2008; Dequeant *et al.*, 2006).

Wnt signaling operates throughout the lifespan of the organism, affecting tissue homeostasis, regeneration following injury, and the continued renewal of stem cells in adults (Angers and Moon, 2009; Logan and Nusse, 2004). It has also been linked to various human diseases. Loss of TCF transcription factors has been linked to type II diabetes (Grant *et al.*, 2006) and constitutively active β-catenin is associated with colorectal cancer (Polakis, 2007).

1.10 Notch signaling in development and disease

Like the Wnt pathway, Notch signaling is implicated in many developmental processes. In particular, Notch signaling is often associated with cell-fate decisions. These include the binary differentiation of single groups of cells, as in the development of the nematode vulva, or the convergent patterning of originally distinct populations, as evidenced through the inductive patterning of cone cells in *Drosophila* (Fortini, 2009). Notch signaling is also involved in other fundamental cell processes, enhancing or repressing cell proliferation and apoptosis (Fortini, 2009; Kopan and Ilagan, 2009), and maintaining normal neurogenesis, as highlighted by the neuronal hyperplasia exhibited by homozygous *Notch* mutants in *Drosophila* (Poulson, 1940). Likewise, the process of somitogenesis is highly dependent on Notch activity, with Notch pathway members forming part of the core network of oscillating genes believed to underlie somite segmentation (Aulehla *et al.*, 2003; Dequeant *et al.*, 2006). The formation and maintenance of somite borders also requires Notch activity (D'Souza *et al.*, 2008; Lai, 2004; Machka *et al.*, 2005).

Defects in Notch signaling have been associated with a number of human disorders, from congenital conditions like the vertebral segmentation anomalies of spondylocostal dysostosis (Gridley, 2003; Cornier, 2008), to adult-onset disorders such as CADASIL, a hereditary stroke condition associated with aberrant NOTCH3 (Louvi *et al.*, 2006). Abnormal Notch signaling has also been implicated in certain types of cancers, including colon cancer (van Es *et al.*, 2005) and T cell acute

lymphoblastic leukemia (Weng *et al.*, 2004). These diseases collectively arise as a result of abnormal cell differentiation (D'Souza *et al.*, 2008; Fortini, 2009).

1.11 Players in Notch signaling

NOTCH was first discovered in *Drosophila melanogaster* and so christened after the irregular notched wing-tips in mutants (Morgan and Bridges, 1916). Four NOTCH homologues have been described in mammals, and each member appears to serve both distinct and redundant functions (Kopan and Ilagan, 2009). Notch family members are single-pass transmembrane, type I proteins that function as cell-surface receptors. Notch receptors are composed of an extracellular domain containing between 29 and 36 epidermal growth factor (EGF)-like repeats as well as a negative regulatory region (NRR) which harbours an important cleavage site, discussed further below. The NOTCH protein also has an intracellular region containing sequences for nuclear binding and localization (Kopan and Ilagan, 2009). Notch proteins are synthesized as 300 kDa fragments that are cleaved and recombined by noncovalent interactions to form a mature receptor with an extracellular and transmembrane/intracellular domain prior to translocation to the cell surface (Fortini, 2009; Kopan and Ilagan, 2009).

In the canonical pathway, Notch receptors bind ligands of the Delta-Serrate-Lag-2 (DSL) family. DSL members include Delta and Serrate in *Drosophila* as well as their Delta-like and Jagged homologues in mammals, and Lag-2 in *C. elegans* (D'Souza *et*

al., 2008; Fortini, 2009). These ligands share a structurally similar DSL motif at their N-terminus, which is used in the binding interaction with Notch (Rebay *et al.*, 1991). DSL ligands also share many structural similarities with Notch receptors; they are type 1 single-pass membrane proteins containing various EGF-like tandem repeats, including several that are more specialized and cooperatively known as the DOS (Delta and OSM-11-like proteins) domain (Cordle *et al.*, 2008; Komatsu *et al.*, 2008). Indeed, DSL ligands are often characterized based on the presence or absence of the DOS domain or even the DSL domain in the case of certain non-canonical ligands (D'Souza *et al.*, 2008; Kopan and Ilagan, 2009).

1.12 Mechanism of canonical Notch signaling

Non-canonical mechanisms of Notch signaling are peripheral to this treatise, and as such will not be discussed. Canonical Notch signaling is an example of a juxtacrine interaction, requiring direct contact between the inducing and responding cell to enable the binding of membrane-bound ligands and receptors (Rozante *et al.*, 2007). Binding occurs between the DSL ligand domain and EGF repeats 11 and 12 on the Notch receptor (Rebay *et al.*, 1991). DSL ligands are also capable of binding Notch receptors from the same cell "in *cis*", but this typically results in inhibition of signaling (Jacobsen *et al.*, 1998).

The interaction between NOTCH and DSL ligands is unusually strong, and can effect a change in the conformation of the Notch receptor to reveal an extracellular

cleavage site in the negative regulatory region (Ahimou *et al.*, 2004) that is recognized by ADAM, a metalloprotease. The excision of this external domain engenders the membrane-bound intermediate Notch extracellular truncation (NEXT) (Fortini, 2009; Kopan and Ilagan, 2009). A second proteolysis follows, resulting in the release of the entire Notch intracellular domain (NICD) by the intramembrane protease complex γ-secretase (Bray, 2006; Gordon *et al.*, 2008; Wolfe and Kopan, 2004). NICD then translocates to the nucleus where it participates in the transcriptional regulation of Notch target genes via association with CSL transcription factors (Figure 1.7).

In the absence of DSL ligands, CSL transcription factors (for instance CBF1 in mammals, also known as Recombination signal binding protein for immunoglobulin kappa J region (RBPJκ)) occupy the promoters of target genes in association with co-repressors such as Corepressor interacting with RBPJ (CIR1), Nuclear receptor co-repressor (NCOR), and Groucho/TLE complexes (Bray, 2006; Kovall, 2008). Upon activation of Notch signaling, there is an exchange of NICD for the co-repressors and subsequent recruitment of Mastermind (MAM), a co-activator (Kovall, 2008; Petcherski and Kimble, 2000; Wu *et al.*, 2000). These three proteins, RBPJκ, NICD, and MAM, subsequently recruit general enhancers of transcription such as the histone acetyltransferase p300 and additional transcription factors in order to induce target gene expression (Fortini, 2009; Fryer *et al.*, 2002; Wallberg *et al.*, 2002). Following the activation of target genes, the active complex is disassembled and NICD undergoes ubiquitylation and

Figure 1.7: Simplified schematic of canonical Notch signaling.

Simplified illustration of the canonical Notch signaling pathway. In the absence of a DSL ligand such as Delta-like 1 (DLL1) or Jagged1 (JAG1) from an inducing cell, the transcription of Notch genes is repressed by CSL transcription factors in concert with co-repressors. In the presence of DLL1 or JAG1, ligand binding leads to the cleavage of an intracellular portion of the Notch transmembrane receptor (NICD), which is able to translocate to the nucleus and activate Notch target genes.

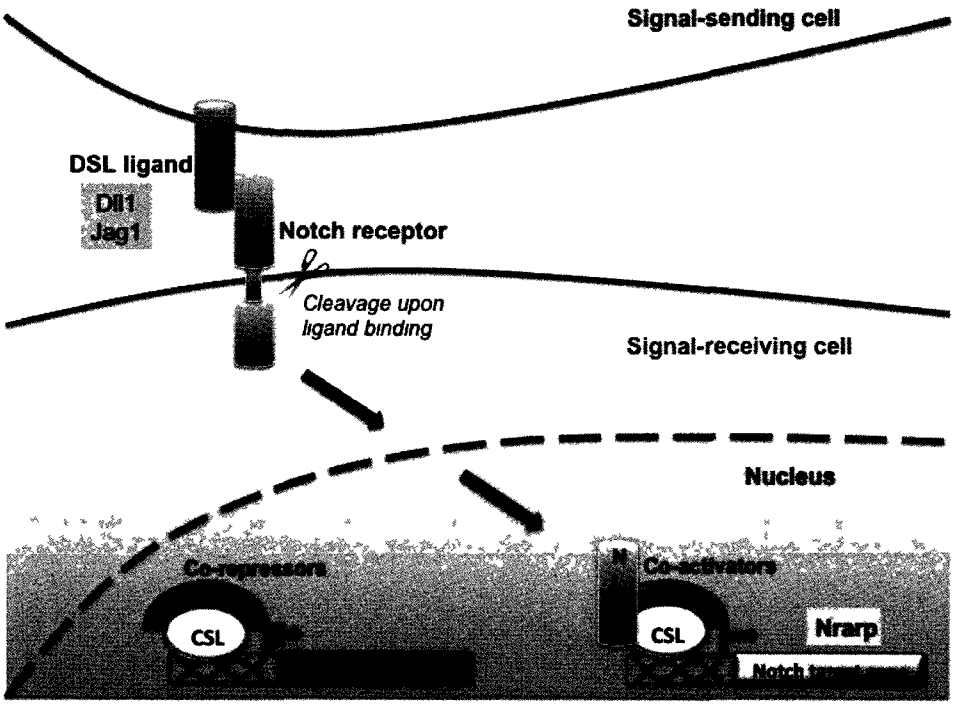
Signal-sending cell
DSL ligand
Dll1
Jag1
Notch receptor
Cleavage upon
ligand binding
Signal-receiving cell
Nucleus
Co-repressors
CSL
N
Co-activators
CSL
Nrarp

Figure 1.7

proteosomal degradation (Tsunematsu et al., 2004).

1.13 Delta-like 1 (DLL1)

Analysis of the candidate CDX targets from the microarray screen of *Cdx1/2* null embryos revealed many genes associated with Wnt and Notch signaling. In particular, these included the Notch ligand Delta-like 1 (DLL1).

Delta-like 1 (DLL1) is a murine homologue of *Drosophila* Delta (Bettenhausen *et al.*, 1995). Three Delta-like members have been identified in the mouse: DLL1 (Bettenhausen *et al.*, 1995), DLL3 (Dunwoodie *et al.*, 1997), and DLL4 (Rao *et al.*, 2000; Shutter *et al.*, 2000), although this review will focus primarily on DLL1.

DLL1 shares 40% overall homology with its fly counterpart, with even higher conservation in certain functional domains. DLL1 retains 70% identity in its EGF-like repeats, as well as high homology in its Delta-Serrate-Lag2 (DSL) receptor-binding region (Bettenhausen *et al.*, 1995). Hence, DLL1 is a member of the DSL ligand family and is a major component of the Notch signaling pathway.

1.14 Expression of *Dll1* during development

Dll1 expression appears transiently during embryonic development (Bettenhausen *et al.*, 1995) in cells of the neurectoderm and the paraxial mesoderm in patterns that

are both complex and dynamic. Interestingly, *Dll1* also shares overlap with the CDX members in the caudal embryo (Beck *et al.*, 1995; Gamer and Wright, 1993; Meyer and Gruss, 1993), consistent with a direct interaction.

Dll1 first appears around the mid-streak stage, approximately E7, in the mesoderm and primitive streak. Subsequently, expression becomes confined to the tail bud and posterior mesoderm, with an anterior boundary just rostral to the node. A strong stripe of expression accumulates at this anterior border, with more diffuse levels of transcript occupying the more caudal domains. The node itself appears to be devoid of *Dll1* transcript (Bettenhausen *et al.*, 1995).

Dll1 is one of several Notch players that display oscillating patterns of expression during somitogenesis, and it belongs to a core group of cyclic genes that constitute the "molecular clock" involved in somite formation (Dequeant and Pourquie, 2008; Maruhashi *et al.*, 2005). Cyclic expression is visualized as a moving band of *Dll1* transcripts that initiates at the caudal tip of the embryo and proceeds to the anterior boundary of the presomitic mesoderm (Maruhashi *et al.*, 2005). Within condensed somites *Dll1* becomes restricted to the caudal halves, and persists only through the first 12-14 somite pairs. At approximately E12.5 *Dll1* expression becomes constrained to the caudal tip of the embryo, and by E15.5 it disappears altogether. Although it appears that *Dll1* is not involved in the later stages of embryonic development, expression reappears after birth when *Dll1* becomes reactivated in specific tissues (Bettenhausen *et al.*, 1995).

Like some of the *Cdx* genes, *Dll1* is also expressed in the hindgut, appearing in the intestinal mesenchyme and epithelium at approximately E13.5 and persisting through adulthood (Schroder and Gossler, 2002). Details relating to *Dll1* function in these tissues will not be discussed, however, since they are peripheral to this thesis.

1.15 The role of DLL1 in somitogenesis

As with other Notch proteins, DLL1 ligands have been implicated in a number of processes, often involving the choice between different fates, or the promotion of an epithelial identity (Bettenhausen *et al.*, 1995). Much of this information has been procured through loss-of-function mutants.

Experiments using *Dll1*^{lacZ}, a loss-of-function allele with an in-frame fusion of *lacZ* in the *Dll1* coding region, have revealed a requirement for DLL1 in many aspects of somite formation (Hrabe de Angelis *et al.*, 1997). *Dll1*^{lacZ} homozygotes do not survive past E12, and somite segmentation is greatly perturbed. Although epithelial somites form initially they appear highly irregular, and by the later stages segmentation no longer occurs. The caudal halves of somites fail to condense and lack cranio-caudal polarity. Additionally, myoblasts connect adjacent segments, and somite boundaries are lost. Since the formation and elongation of the AP axis appear normal, as determined by the expression of Sonic hedgehog (*Shh*) in the tailbud, it was concluded that DLL1 was required for the formation of epithelial somites and somite polarity (Hrabe de Angelis *et al.*, 1997).

In addition to the other patterning defects, *Dll1* null mutants also exhibit an excessive differentiation of neurons (Hrabe de Angelis *et al.*, 1997). Additionally, a haploinsufficient model *Dll1*$^{tm1Gos/+}$, used to investigate the role of DLL1 in adult mice, revealed that even a relatively small reduction in the levels of this protein have an impact on weight and metabolic and immunological functions (Rubio-Aliaga *et al.*, 2009).

Dll1 mutations were also found to genetically interact, or compound the severity of mutants of another Delta-like family member, *Dll3* (Beckers and Gossler, 2000, unpublished observation; Beckers *et al.*, 2000b), as well as particular murine models affecting somitogenesis such as the rib-vertebrae (*rv*) mutant (Beckers *et al.*, 2000b). *Dll1*^{lacZ} - *rv* double heterozygotes display anomalies not present in either single mutant and as such exhibit nonallelic noncomplementation. These mice are characterized by the appearance of vertebral anomalies and a kinky tail, presumably as a result of the additional reduction in *Dll1* expression by *rv*. The addition of *Dll1*^{lacZ} to the *rv* null mutant line leads to a greater number of fused vertebrae and a caudal truncation (Beckers *et al.*, 2000b), while the combination of *Dll1*^{lacZ} with *Dll3* homozygotes increases the severity of the respective single mutant phenotypes, resulting in lethality *in utero* (Beckers *et al.*, 2000b). In contrast, compound *Dll1/Dll3* mutants maintain a wildtype appearance (Geffers *et al.*, 2007, unpublished observation; Geffers *et al.*, 2007).

1.16 Regulation of *Dll1*

One of the first studies investigating *Dll1* transcriptional regulation in the mouse identified a promoter region beginning 4.3 kb upstream of the translational start site that is sufficient to reproduce most of the endogenous expression from the primitive streak stage through early organogenesis (Beckers *et al.*, 2000a). This region contains several regulatory domains, including the mesodermal enhancer "msd", which directs *Dll1* expression in the paraxial mesoderm and its derivatives, and could thus relay tissue-specific activity (Beckers *et al.*, 2000a). Studies in *Drosophila* have revealed some of the players that may act on these regulatory regions. Proneural proteins of the Achaete scute and lethal of scute complex (AS-C) can activate transcription of *Delta* in neuroblasts, while HLH-M5 and other Basic helix-loop-helix (bHLH) transcription factors of the enhancer of split complex (E(spl)-C) negatively regulate the proneural genes through lateral inhibition, downregulating *Delta* expression (Beckers *et al.*, 2000a; Ghysen and Dambly-Chaudiere, 1988; Heitzler *et al.*, 1996; Oellers *et al.*, 1994).

Studies in murine models have defined additional regulators of *Dll1* expression, including canonical Wnt signaling via LEF1 (Galceran *et al.*, 2004). Indeed, homozygous *Lef1-βgal* mutants exhibit a reduction in *Dll1* expression and defects in somite polarity reminiscent of certain aspects of the *Dll1* null mutant phenotype (Galceran *et al.*, 2004). Although *Lef1-βgal* mutants do not completely phenocopy *Dll1* mutants, this is perhaps due to functional redundancy with other LEF/TCF members.

T-box 6 (TBX6) is another potential regulator of *Dll1* transcription. TBX6 is a transcription factor that contains a conserved T-box DNA binding domain (Papaioannou, 2001). TBX6 is expressed in the primitive streak, the tail bud and the presomitic mesoderm and is required for the specification of posterior paraxial mesoderm (Chapman *et al.*, 1996). Corroboration for TBX6 function as a regulator of *Dll1* expression is also multifold. *Dll1* activity was shown to be greatly diminished or lost in TBX6 mutants (White and Chapman, 2005). In addition, *Dll1* was able to genetically interact with *Tbx6*, as double heterozygotes exhibit vertebral fusions and a kinky tail, defects not seen in either single heterozygote background (White *et al.*, 2003). Indeed, the rib-vertebrae (*rv*) mutant (Beckers *et al.*, 2000b) is actually a hypomorphic allele of TBX6 (Watabe-Rudolph *et al.*, 2002; White *et al.*, 2003), and this allele also exhibits nonallelic noncomplementation with *Dll1*, as described above.

A regulatory relationship between TBX6 and *Dll1* is further supported by the finding of multiple putative TBX6 binding sites (5'– AGGTGTBRNNNN – 3'; where B represents any base pair with the exception of adenosine, and R is A or G), in the *Dll1* promoter. TBX6 can bind to two of these sites based on electrophoretic mobility shift assays (EMSA) (White and Chapman, 2005). Transgenic analysis also demonstrated that the TBX6 binding sites in the msd are essential for maintaining *Dll1* expression in the tailbud (Hofmann *et al.*, 2004). Collectively, these findings also support a direct regulatory role for TBX6 on *Dll1* activity. The lack of a phenocopy between the *Dll1* and *Tbx6* null embryos may be a reflection of an earlier

role for TBX6 in effecting specification of paraxial mesoderm, while DLL1 impacts later somite polarity.

Relevant to the above findings additional evidence suggests that LEF1 and TBX6 interact on the *Dll1* promoter, resulting in a synergistic induction of transcriptional activity. This synergy was β-catenin-dependent and required the TBX6 binding sites in the mesodermal enhancer region (Hofmann *et al.*, 2004). These findings further strengthen the argument that TBX6 and LEF1 are critical regulators of *Dll1* expression.

1.17 Rationale

Murine CDX members are critical for vertebral AP patterning, via direct regulation of *Hox* gene expression. However, a better understanding of their function has been hampered by the crucial role for CDX2 in trophectoderm and the inherent peri-implantation lethality of a cognate null mutant (Chawengsaksophak *et al.*, 1997). The creation of a conditional *Cdx2* transgenic model by our group (Savory *et al.*, 2009a) has revealed novel functions for CDX in development and has identified several non-*Hox* targets involved in these processes. *Cdx1/2* double null mutants also exhibit severe anomalies affecting the caudal embryo, including a truncated tail, an open neural tube, and abnormal somitogenesis. A microarray analysis of these mutants revealed many known or suspected CDX targets, including several *Hox* genes. Importantly, it also indicated that many players in the Wnt and Notch

signaling pathways, central to somitogenesis, were dependent on CDX function. Among these candidates *Dll1*, an important Notch ligand, was identified.

Dll1 expression in the presomitic mesoderm overlaps with each of the *Cdx* members (Beck *et al.*, 1995; Gamer and Wright, 1993; Meyer and Gruss, 1993). Although *Dll1* mutants do not exactly phenocopy the *Cdx1/2* double nulls, the genetic interaction between the *Dll1* null allele and a *Tbx6* hymomorph results in caudal truncation (White *et al.*, 2003) reminiscent of the *Cdx2* null (Savory et al., 2009a) and *Cdx1/2* null phenotypes. Together with the identification of *Dll1* as CDX-dependent, by microarray analysis, these observations are consistent with *Dll1*, and potentially other Wnt and Notch pathway members isolated by the screen, as direct CDX target genes.

1.18 Hypothesis

I hypothesize that murine CDX members regulate somitogenesis through direct transcriptional control of players in the Wnt and Notch signaling pathways.

1.19 Objectives

1) Confirm the misregulation of Wnt and Notch candidates revealed by the microarray screen using whole mount *in situ* hybridization.
2) Identify and characterize CDX response elements (CDRE) in a small number of affected candidates.
3) Investigate the capacity of CDX to bind the CDREs in one of these target genes *in vivo* and *in vitro,* and assess the putative binding sites for functionality.

CHAPTER 2

MATERIALS AND METHODS

2.1 Mice

CD-1 ® wildtype mice aged 6-8 weeks were obtained from Charles River. For timed matings mice were paired overnight and successful couplings were determined by the presence of a vaginal plug the following morning; noon of the day of evidence for a vaginal plug was denoted E0.5. Pregnant females were sacrificed on E7.5 or E8.5 and the embryos were collected for subsequent experimentation.

Cdx1$^{-/-}$*Cdx2*$^{-/-}$ mice were generated through the crossing of several mutant and transgenic lines and the implementation of the CRE/*loxP* recombinase system of conditional gene inactivation. One of the core mutants, *Cdx2*$^{f/f}$, was developed previously by our laboratory (Savory *et al.*, 2009a). Briefly, a targeting vector harbouring a "floxed" (*i.e.*: flanked by *loxP* sites) version of the *Cdx2* locus was electroporated into embryonic stem (ES) cells, and positive cell lines were injected into C57BL/6 blastocysts in order to generate chimeras. The resulting *Cdx2*$^{+/f}$ mice were intercrossed to produce *Cdx2*$^{f/f}$, or alternatively, paired with *CMV-β-actin-Cre-ERT2* (hereafter denoted *Cre-ERT2*) transgenic animals obtained from Filippo Rijli (Santagati *et al.*, 2005) to create *Cdx2*$^{+/f}$; *Cre-ERT2* mice. The *Cdx2*$^{+/f}$; *Cre-ERT2* progeny were then backcrossed in order to obtain the desired *Cdx2*$^{f/f}$; *Cre-ERT2* genotype. This strategy utilized the CRE/*loxP* system of conditional gene inactivation. Stud males harboured a *Cre* recombinase transgene under the control of the *β-actin* promoter. *Cre* was fused to an estrogen receptor ligand domain (ERT2) that was modified to respond exclusively to tamoxifen, a synthetic modulator of the estrogen receptor.

To create the *Cdx1/2* compound null line, *Cdx2$^{f/f}$; Cre-ERT2* mice were subsequently crossed into a *Cdx1$^{-/-}$* transgenic obtained from Peter Gruss (Subramanian *et al.*, 1995) to produce *Cdx1$^{-/-}$Cdx2$^{f/f}$* and *Cdx1$^{-/-}$Cdx2$^{f/f}$; Cre-ERT2* animals. Timed matings were arranged between a male *Cdx1$^{-/-}$Cdx2$^{f/f}$; Cre-ERT2* and a female *Cdx1$^{-/-}$Cdx2$^{f/f}$*, and pregnant dams were treated at E5.5 by oral gavage with a single dose of 2 mg of tamoxifen prepared in corn oil. Tamoxifen was administered in order to conditionally activate the Cre recombinase driven excision of *Cdx2* in the developing embryos, and effectuate the creation of the *Cdx1$^{-/-}$Cdx2$^{-/-}$* knockout line. Pregnant females were sacrificed from E7.5-E8.5 and embryos harvested in phosphate-buffered saline (PBS) supplemented with diethylpyrocarbonate (DEPC, Sigma) for further processing.

2.2 Whole mount *in situ* hybridization (ISH)

While probes against many of the candidate genes were available in the laboratory, the remainder were obtained as expressed sequence tags (ESTs) from the American Type Culture Collection (ATCC). Among the Wnt candidates, *Lef1*, *Pitx2*, and *Tshz1* were generated from constructs provided by Liliana Attisano, Jacques Drouin, and Terry Yamaguchi respectively, while *Frzb* was ordered as an expressed sequence tag. Likewise, among the Notch players *Dll1* and *Jag1* were donated by Domingos Henrique, whereas *Nrarp* was obtained as an EST. Sequences of approximately 1 kb were used to generate anti-sense digoxigenin-labeled RNA probes. Riboprobes

were assessed for faithful replication of endogenous expression in wildtype CD-1 embryos prior to their use in the *Cdx1/2* null mutants.

Whole mount *in situ* hybridization (ISH) was performed as previously described (Houle *et al.*, 2000; Pilon *et al.*, 2007; Prinos *et al.*, 2001). In brief, embryos were collected and fixed overnight at 4°C in 4% paraformaldehyde (PFA, Bioshop) in PBS-DEPC. The following day they were dehydrated in a methanol series and stored at -20°C. Subsequently, embryos were sorted according to stage and genotype, rehydrated, bleached, and post-fixed for 20 minutes in a mixture of 0.2% glutaraldehyde (Sigma) and 4% PFA in PBS-DEPC. Embryos were hybridized overnight with the digoxigenin-labeled RNA probe at 64°C. The next day, the samples were washed, blocked with a mixture of 1% blocking reagent (Roche), 10% heat-inactivated goat serum (Chemicon, Millipore), and TBST-levamisole hydrochloride (0.48 mg/ml, MP Biomedicals) and incubated overnight at 4°C with anti-digoxigenin-alkaline phosphatase AP Fab fragments (Roche). The embryos were then washed and reacted with 500 µl of BM Purple AP Substrate (Roche). Subsequent washing stopped the reaction when an appropriate level of signal strength was attained. Stage-matched embryos to be compared were processed in parallel to control for signal strength variation. Embryos were then dehydrated, rehydrated, and cleared in glycerol in CMFET (0.8 g NaCl, 0.02 g KCl, 0.115 g Na_2HPO_4, 0.02 g KH_2PO_4, 0.02 g EDTA, 100 µl Tween-20, completed with 100 ml H_2O). Embryos were photographed using a Leica MZ16FA microscope.

2.3 Semi-quantitative reverse-transcriptase polymerase chain reaction (RT-PCR)

Cdx1$^{-/-}$*Cdx2*$^{-/-}$ embryos and their wildtype littermates were collected at E8.5 and RNA was extracted using TRIzol® Reagent (Invitrogen). cDNA was generated through standard procedures and amplified by PCR. Oligonucleotides for *Dll1*: 5' - ATGGGCCGTCGGAGCGCGCTA - 3' (sense) and 5' - TGTGCGGCCGCTACTGTGAAGG - 3' (antisense), amplified a 504-bp fragment, while the 228-bp section of *β-actin* served as a loading control: 5' - AGCCATGTACGTAGCCATCC - 3' (sense) and 5' - CTCTCAGCTGTGGTGGTGAA - 3' (antisense). The sequences were amplified using 80 – 100 ng of each primer in a 25 μl reaction, and a PCR program with an initial 2 minute denaturation at 94°C followed by 35 or 50 cycles, for *β-actin* and *Dll1* respectively, of 94°C for 30 sec, 58°C for 30 sec, and 72°C for 1 min. The products were resolved by gel electrophoresis on a 1% agarose gel, stained with SYBR Safe Nucleic Acid Stain I (Invitrogen) and quantified using the Luminescent Image Analyzer LAS-4000 miniseries (Fujifilm) microscope along with Image reader LAS-4000 and Multi Gauge Ver. 3.x software (Fujifilm). Quantitation of transcript levels between *Cdx1/2* null mutants and their littermate controls was achieved using ImageJ software.

2.4 Identification and phylogenetic analysis of CDX response elements (CDREs)

Prospective Cdx targets from the microarray screen were analysed for the presence of potential CDX response elements using the Transcription Element Search System (TESS) (Schug, 2008) available online (http://www.cbil.upenn.edu/cgi-bin/tess/tess). A region spanning 5 kb upstream of the transcriptional start site was selected from each gene for initial review. Following this assessment, potential binding sites were investigated for interspecies conservation using ClustalW2 software (Larkin *et al.*, 2007).

2.5 Chromatin immunoprecipitation (ChIP) on embryos

ChIP was performed as described (Pilon *et al.*, 2006) with minor modifications. Briefly, approximately 50 CD-1 wildtype embryos were harvested at day E8.5 in PBS-DEPC and prepared immediately for chromatin immunoprecipitation. Embryos were fixed with 1% formaldehyde (Fisher) in PBS and the reaction was stopped through the addition of glycine (Bioshop) to a final concentration of 0.125 M. The tissue was resuspended in RIPA buffer (10 mM Tris pH 8.0, 140 mM NaCl, 1 mM EDTA, 1% Triton® X-100, 0.1% Sodium dodecyl sulfate, 0.1% sodium deoxycholate) supplemented with protease inhibitors, and disrupted by three passages through a $26^{1/2}$ gauge needle (Becton Dickinson & Co). Additionally, the samples were sonicated four times for 30 seconds with the Branson Sonifer 450 (settings: Duty Cycle 20%, Output 2.0) while keeping the tubes on ice. At this time, a sample of

Input DNA was collected and the remaining chromatin was divided into the intended number of aliquots for precipitation before being stored at -80°C for later processing.

Next, the samples were precleared at 4°C for 1-4 hours using 2 μg of sheared herring sperm DNA (Sigma), 10 μg of rabbit pre-immune serum, and 50 μl of Protein A/G Plus Agar beads (Santa Cruz), and supplemented with 5 μg of an appropriate antibody (α-Cdx2 or rabbit pre-immune serum), including the additional "mock" or no chromatin control, overnight at 4°C with inversion. On the 3rd day, samples were again incubated for 1-4 hours in the cold room with 2 μg of sheared herring sperm DNA and 50 μl of Protein A/G Plus Agar beads and washed sequentially in 1 ml of a series of buffers for 10 minutes with inversion: 2 x TSEI (0.1% SDS, 1% Triton® X-100, 2 mM EDTA, 20 mM Tris-HCl pH 8.1, 150 mM NaCl), 2 x TSEII (0.1% SDS, 1% Triton® X-100, 2 mM EDTA, 20 mM Tris-HCl pH 8.1, 500 mM NaCl), 3 x TSEIII (0.25 M LiCl, 1% NP-40, 1% sodium deoxycholate, 1 mM EDTA, 10 mM Tris-HCl pH 8.1), and 3 x TE pH 8.1. Once the samples had been washed, the DNA-protein complexes were eluted off of the beads in 3 x 100 μl of Elution Buffer (1% SDS, 0.1 M $NaHCO_3$) for 20 minutes at room temperature. Finally, samples and input DNA were incubated at 65°C overnight to reverse the formaldehyde cross links, and then purified over a column using the QIAquick PCR Purification Kit (Qiagen).

Determination of CDX2 occupancy of the *Dll1* promoter was carried out by PCR amplification. Primers 5' - TTGGCTAGGCCAACATTCAGGC - 3' (sense) and 5' -

TTCCTCCTCCTCATCCTCCTGT - 3' (antisense) were selected to amplify a 457-bp genomic region between the two potential CDREs in order to account for either site in the screen of immunoprecipitated chromatin. A smaller area was also selected in order to maximize the detection of either site among 1 kb fragments of sheared chromatin. An area approximately 12 kb upstream of the transcriptional start site was used as a negative control, with primers 5' - GGTAGGGGATGGTTGGGTTCC - 3' (sense) and 5' - GGTCTGCCTACCTCCACAGTC - 3' (antisense) encompassing a 642-bp fragment. PCR was conducted using 100 ng of each primer and GoTaq® Green Master Mix (Promega) in a 25 µl volume, and a program with an initial denaturation step at 95°C for 5 minutes, followed by 35 cycles of: 95°C 1 min, 60°C 45 sec, 72°C 1 min, and a 5 minute terminal extension at 72°C. The products were resolved by gel electrophoresis on a 2% agarose gel.

2.6 Electrophoretic mobility shift assay (EMSA)

GST and GST-CDX2 fusion proteins were generated by standard procedures (Beland *et al.*, 2004). Each of the constructs, housed in the pGEX-4T-1 vector (GE Healthcare), was grown up in *Escherichia coli* BL21 cells and purified over GST-affinity columns prepared with BD BaculoGold™ Glutathione Agarose Beads (BD Biosciences Pharmingen). Double-stranded oligonucleotides were generated for the two potential CDX response elements (CDREs) from the *Dll1* promoter, and end-labeled with [γ-^{32}P]ATP (PerkinElmer). The sense oligonucleotides used for the distal and proximal elements were 5' - AGGTGAGGATTTATGGTGTGTGGG - 3' and 5'

- ATGGTGTGGCATAAATTAAGTTGG - 3' respectively, where the CDRE have been underlined. Additionally, oligonucleotides containing mutated versions of these sites were created to further analyze the specificity of binding. The sense oligonucleotides for these constructs consisted of 5' - AGGTGAGGCCCGCCTGTGTGTGGG - 3' for the distal site, and 5' - ATGGTGTGGTCCGCCCTAAGTTGG - 3' for the proximal site. Finally, a previously established CDX response element from *Hoxb8* locus, 5' - GCTATAAAAGTTTATAGGGTATAAATT - 3' (sense) (Charite *et al.*, 1998), was used as a positive control, and a DR5 retinoic acid response element (RARE) 5' - AGAGGTCACCGAAAGGTCACT - 3' (sense) served as a negative control.

EMSA was carried out as previously described (Houle *et al.*, 2000; Pilon *et al.*, 2006). In brief, 100 ng of forward primer was end-labeled by kination with 5 µl of [γ-^{32}P]ATP and passed over a Sephadex G-50 column to remove any unincorporated radioactivity. The eluate was supplemented with 200 ng of the complementary oligonucleotide prior to assessment for P-32 incorporation. 2 µg of GST-Cdx2 or 1 µg of GST were incubated with 5.6 µl of a binding reaction buffer, and to further evaluate the specificity of the potential CDX2-CDRE binding reaction, 2 µg of anti-CDX2 antibody was included in one of the samples. All tubes were incubated on ice for 30 minutes, after which time either 50,000 cpm of radioactive ("hot") probe or 200 X by mass of a non-radiolabeled ("cold") competitor was added to each sample. Tubes were incubated for another 20 minutes at room temperature while pre-running the gel. The samples were resolved over a 10% non-denaturing

polyacrylamide gel at room temperature for approximately 2.5 hours at 24 mA in 0.25 X TBE buffer (20 X stock: 215.6 g Tris base, 110.1 g Boric acid, 80 ml EDTA, pH 8.0, 863.3 ml H_2O, adjust pH to 8.3). Finally, after drying the gel the signal was developed on Kodak BioMax MS Film.

2.7 Recombinant DNA constructs

The *Dll1* proximal promoter region, encompassing the two putative CDX binding sites identified through bioinformatics, was isolated by PCR and cloned into a luciferase reporter vector. A region spanning 4,172 bp upstream of the translational start site was amplified using a nested PCR scheme and Platinum ® *Taq* DNA Polymerase High Fidelity (Invitrogen). This region was selected because it also included many of the major regulatory elements that characterized the 4.3 kb genomic region analysed by another group (Beckers *et al.*, 2000a).

The first amplification was performed with the outer primers 5' - TATACCTGAGTCTGCCCTATCCACC – 3' (sense) and 5' - TATACACAGCAGGGCAGAGACCAC - 3' (antisense), followed by a second cycle with nested primers flanked by restriction sites to facilitate later subcloning, SalI 5' - TATAGTCGACTTATTCAGATTGGGGCTGGG - 3' (sense) and BglII 5' - TATAAGATCTGGTACCGCTGGACGCC - 3' (antisense). The PCR product was isolated by gel extraction with the Wizard SV Gel and PCR Clean-Up System (Promega), and ligated by TA cloning into pCR®2.1 according to the manufacturer's instructions

(Invitrogen). The product was verified by sequencing and sub-cloned into the luciferase reporter vector, pXP2 (Nordeen, 1988).

The distal CDRE, TTTATG, was mutated by site-directed mutagenesis using a QuikChange ® II XL Site-Directed Mutagenesis Kit (Stratagene) as per the manufacturer's directions. The primers used in this amplification included 5' - GGTGAAGGTGAGGAGGATCCGTGTGTGGGGAGGGG - 3' (sense) and 5' - CCCCTCCCCACACACGGATCCTCCTCACCTTCACC - 3' (complement) and involved the introduction of a BamHI restriction site (underlined) in place of the response element in order to verify the clone.

The proximal CDX motif, CATAAA, a complement of the consensus binding site, was mutated using a two-part PCR scheme. Two overlapping fragments were amplified using primers 5' - GCCCTATCCACCCATTGCAATTATTCAGATTGGGG - 3' (sense) and 5' - GCATTCATTCTTTTCCAACTTAAGGATCCCCACACCATTCTGTATTGG - 3' (antisense) for the first strand, and 5' - CCAATACAGAATGGTGTGGGGATCCTTAAGTTGGAAAAGAATGAATGC - 3' (sense) and 5' - GGAATTTCTGCACTTCACGTCGTCATCGCCAACTC - 3' (antisense) for the second. The internal primers were complementary, and encompassed the CDX response element. The CDRE was, once again, replaced by a BamHI site (underlined) in order to identify the mutated construct. Subsequently, in the second part of this scheme, the two initial amplicons were used for an additional PCR to generate the full 1,573-bp insert by means of the outermost primers

5' - GCCCTATCCACCCATTGCAATTATTCAGATTGGGG - 3' (sense) and 5' - GGAATTTCTGCACTTCACGTCGTCATCGCCAACTC - 3' (antisense). The final PCR product was ligated into pCR®2.1 and analysed by restriction digest. Since I had previously constructed a reporter vector containing the full-length *Dll1* promoter in pXP2, I isolated a smaller 852-bp fragment containing the mutated CDRE by restriction digest with XhoI (New England BioLabs) and NcoI (new England BioLabs), and sub-cloned this fragment into the full-length *Dll1* promoter construct by a "shotgun" procedure.

To generate a plasmid containing both mutated CDREs, the altered CATAAA site was isolated from the proximal CDRE mutant vector using the same restriction enzymes, XhoI and PvuII, and subcloned into the plasmid containing the mutated distal CDRE. The final construct was verified using restriction enzyme digestion analysis.

All clones were transformed into chemically-competent DH5α *Escherichia coli* cells by a heat-shock protocol that followed standard procedures, and DNA was isolated using the PureYield™ Plasmid Maxiprep System (Promega) or the Plasmid Maxi Kit (Qiagen).

2.8 Cell lines

P19 embryocarcinoma cells (ATCC) were maintained in Alpha Modification of Eagle's Medium (αMEM, Multicell, Wisent) supplemented with 7.5% heat-

inactivated Bovine Serum (Sigma), 2.5% heat-inactivated Fetal Bovine Serum (virus and mycoplasma screened, sterile-filtered, Multicell, Wisent) and 1 X penicillin/streptomycin (Multicell, Wisent). Cells were passed at a ratio of approximately 1:10 every two days and maintained in a humidified chamber at 37°C and 5% CO_2.

2.9 Transient transfections

Transfections were performed using a modified calcium phosphate protocol. Briefly, on the day of transfection media was replenished approximately 1-3 hours prior to seeding. DNA was prepared using 1 μg of a reporter vector, 0.75 μg of CDX2 expression vector, 0.2 μg of RSV-β-galactosidase (RSV-βGAL) to normalize for transfection efficiency, and pCDNA3.1 to obtain a final mass of 2 μg of DNA per well in a final volume of 125 μl using sterile water (Burdick & Jackson). Following DNA preparation, cells were seeded from one fully confluent plate into 4 x 6-well plates. Subsequently, the plates were returned to the incubator to await transfection.

In subsequent co-transfection assays, 0.75 μg of CDX2 was replaced by 0.5 μg of CDX2 in addition to 0.5 μg of each of LEF1 and βCAT or TBX6. The mixtures were substituted with pCDNA3.1 to obtain a total of 2.5 μg or 3 μg of DNA per transfection for the TBX6 and LEF1/βCAT assays respectively. In the CDX2-TBX6 dose-seeking study, up to 1 μg of each expression vector was used, and the final mass was increased to 4 μg of DNA per well.

In the laminar flow hood, 125 µl of 4 X $CaCl_2$ was combined with the DNA preparation, and this was then added to 250 µl of 2 X HBS (HEPES buffered saline) (Fisher) dropwise while vortexing. The DNA-calcium phosphate mixture was allowed to incubate for 15 minutes then added to the cells. The media was replenished 24 hours post-transfection, and cells harvested at 48 hours. 150 µl of 1 X Reporter Lysis Buffer (Promega) was used to harvest the cells and Luciferase Assay Reagent (Promega) was added to the cell lysate at a ratio of 6:1, 30 µl of Luciferase Assay Reagent (Promega) to 5 µl of cell lysate. Luciferase activity was analysed using an LMax ™ II microplate reader and SOFTmax ® PRO Software Version 4.7 (Molecular Devices). β–galactosidase activity was assessed using a colourimetric liquid assay that employs chlorophenolred-β-D-galactopyranoside (CPRG) (Calbiochem) as a substrate. Absorbance was measured at a wavelength of 585 nm on a SpectraMax ® M2 microplate reader using SOFTmax ® PRO Software Version 4.7 (Molecular Devices). All transfection experiments were performed in triplicate.

CHAPTER 3

RESULTS

3.1 Expression of certain Wnt and Notch pathway members are dependent on CDX

Using the CRE/*loxP* recombinase system our lab generated a conditional *Cdx1/2* null mouse line, allowing us to circumvent the requirement for CDX2 in implantation (Chawengsaksophak *et al.*, 1997) and investigate its roles in later development. In addition, the deletion of *Cdx1* and *Cdx2* led to loss of CDX4 expression, resulting in the absence of all CDX members (our unpublished findings) and enabling us to explore the full extent of their function during postimplantation development.

Cdx1/2 double null homozygotes were characterized by an open neural tube, a severe caudal truncation, and broader, often asymmetrical somites (our unpublished data). A cDNA microarray analysis was subsequently conducted on the caudal, presomitic portion of E8.5 embryos to begin to define the basis for this phenotype. From these data, a number of known or suspected CDX targets were recovered, including members of the *Hox* family and other non-*Hox* target genes, like brachyury (*T*), previously identified by our group (Table 3.1) (Savory *et al.*, 2009a).

As mentioned previously, the microarray also yielded a number of candidates that are members of the canonical Wnt and Notch signaling pathways, both of which are integral to somitogenesis (Table 3.2 A and B respectively). Wnt pathway members included Frizzled-related protein (FRZB), a secreted Wnt-antagonist (Leyns *et al.*,

Table 3.1: Identification of known CDX target genes from the microarray screen on *Cdx1*$^{-/-}$*Cdx2*$^{-/-}$ embryos.

Previously characterized target genes of murine CDX isolated from the microarray screen. Log2 fc RMA indicates projected fold change in gene transcription as determined by the RMA algorithm, in compound *Cdx1/2* mutants relative to littermate controls. Known targets include many members of the *Hox* family, as well as other non-*Hox* genes previously investigated by our lab (Savory *et al.*, 2009a).

KNOWN TARGETS

Symbol	Gene Name	Biological function	Unigene	Fold Change (RMA log2) dko/wt	t-test pv (RMA)
Hoxa5	Homeo box A5	Transcription factor	Mm.173	-1.637	0.01326
Hoxa9	Homeo box A9	Transcription factor	Mm.4694	-4.276	0.00007
Hoxb8	Homeo box B8	Transcription factor	Mm.4822	-0.522	0.00817
Hoxc8	Homeo box C8	Transcription factor	Mm.6167	-3.624	0.00009
Hoxc9	Homeo box C9	Transcription factor	Mm.4765	-0.942	0.00244
Cyp26a1	Cytochrome P450, family 26, subfamily a, polypeptide 1	Enzyme in RA degradation	Mm.42230	-1.648	0.02355
T	Brachyury	Transcription factor	Mm.913	-0.953	0.13300

Table 3.1

Table 3.2: Identification of genes involved in the Wnt and Notch signaling pathways identified by the microarray screen.

A: Genes affiliated with the canonical Wnt signaling pathway that are potentially misregulated in the absence of CDX1 and CDX2. Notably, the microarray screen isolated several critical Wnt players, including genes encoding the ligand Frizzled homolog 7 (FZD7), and transcription factor Lymphoid enhancer binding factor 1 (LEF1).

B: Potential CDX target genes, identified by microarray analysis, that have been implicated in the Notch signaling pathway. Like the Wnt pathway, the microarray isolated several notable candidates, including genes encoding the ligands Delta-like 1 (DLL1) and Jagged 1 (JAG1), as well as Notch targets Hairy and enhancer of split 7 (HES7) and Notch-regulated ankyrin repeat protein (NRARP).

A WNT

Symbol	Gene Name	Role in canonical Wnt signaling	Unigene	Fold Change (RMA log2) dko/wt	t-test pv (RMA)
APC					
Apcdd1	Adenomatosis polyposis coli down-regulated 1	Target gene	Mm 391102	-1 073	0 00172
Fz					
Fzd7	Frizzled homolog 7 (Drosophila)	Receptor	Mm 297906	0 717	0 01699
Frzb	Frizzled-related protein	Secreted Wnt inhibitor	Mm 314721	-0 434	0 00650
Lef1					
Lef1	Lymphoid enhancer binding factor 1	Transcription factor	Mm 255219	-1 198	0 03057
Pitx2					
Pitx2	Paired-like homeodomain transcription factor 2	Target gene, Transcription factor	Mm 246804	0 636	0 01225
PP2					
Ppp2r5c	Protein phosphatase 2, regulatory subunit B (B56), gamma isoform	Agonist	Mm 240396	-0 506	0 33969
Rspo3					
Rspo3	R-spondin 3 homolog (Xenopus laevis)	Agonist	Mm 45191	-1 429	0 00159
Smad					
Smad1	MAD homolog 1 (Drosophila)	Antagonist assoc with Dvl1	Mm 223717	-0 315	0 02658
TCF					
Tcf20	Transcription factor 20	Transcription factor	Mm 252156	-0 327	0 36650
Tsh					
Tshz1	Teashirt zinc finger family member 1	Transcription factor	Mm 102136	1 095	0 22520

B NOTCH

Symbol	Gene Name	Role in canonical Notch signaling	Unigene	Fold Change (RMA log2) dko/wt	t-test pv (RMA)
Dll1	Delta-like 1 (Drosophila)	Ligand	Mm 4875	-0 897	0 03469
Jag1	Jagged 1	Ligand	Mm 22398	-0 522	0 07403
Hes7	Hairy and enhancer of split 7 (Drosophila)	Target gene, Transcriptional repressor	Mm 98505	-0 732	0 01474
Nrarp	Notch-regulated ankyrin repeat protein	Target gene Antagonist – negative feedback regulator	Mm 46539	-1 062	0 03866

Table 3.2

1997), LEF1, Paired-like homeodomain transcription factor 2 (PITX2), and Teashirt zinc finger family member 1 (TSHZ1); the latter three transcription factors are involved in conveying the Wnt signal (Angers and Moon, 2009; Core *et al.*, 2007; Gallet *et al.*, 1998; Gallet *et al.*, 1999; Kioussi *et al.*, 2002; MacDonald *et al.*, 2009). In addition, previous work in our laboratory identified Wingless-related MMTV integration site 3A (WNT3A), a Wnt ligand, as a potential CDX2 target gene (Savory *et al.*, 2009a).

Notch candidates recovered from the microarray included Delta-like 1 (DLL1) and Jagged 1 (JAG1), two of the principal Notch ligands (Fortini, 2009; Kopan and Ilagan, 2009), as well as Notch-regulated ankyrin repeat protein (NRARP), a target gene and antagonist of NOTCH1 (Weerkamp *et al.*, 2006; Yun and Bevan, 2003). Notably, out of the aforementioned Wnt and Notch targets, *Dll1* null mutants displayed prominent defects in somitogenesis (Hrabe de Angelis *et al.*, 1997).

In order to confirm that the above Wnt and Notch candidates predicted by the microarray analysis were indeed CDX-dependent, I performed whole mount *in situ* hybridization to assess their expression. To this end, E8.5 *Cdx1*$^{-/-}$*Cdx2*$^{-/-}$ mutant embryos were processed in tandem with *Cdx1*$^{-/-}$*Cdx2*$^{f/f}$ littermate controls, which are essentially *Cdx1*$^{-/-}$ embryos. *Cdx1* null mutants display anterior vertebral homeoses but otherwise exhibit normal caudal development. Additionally, with the exception of posterior shifts in *Hox* gene expression, *Cdx1* null embryos do not demonstrate altered expression of any Notch or Wnt pathway members (our unpublished data).

As predicted from the microarray data, among the canonical Wnt pathway players expression levels of *Frzb* and *Lef1* were markedly reduced in the caudal embryo, while *Pitx2* and *Tshz1* exhibited an induction in the mutant background (Figure 3.1 A, Figure 3.2).

As members of the CDX family generally enhance the transcriptional activation of target genes (Charite *et al.*, 1998; Knittel *et al.*, 1995; Savory *et al.*, 2009a), the induction of *Pitx2* and *Tshz1* in the *Cdx1/2* null mutants is contrary to what would be expected of direct CDX targets. Although these genes may not transpire to be *bona fide* CDX targets, on the other hand their confirmed patterns of expression further validate the microarray screen. Additionally, the upregulation of these players demonstrates that not all genes are reduced in the *Cdx1/2* null mutants, and accordingly, that observed decreases in gene expression are not necessarily a byproduct of the loss of paraxial mesoderm.

Similarly, the Notch pathway players *Dll1* and *Nrarp* were markedly downregulated, as was anticipated, although *Jag1* remained unchanged in the neural tube and presomitic mesoderm (Figure 3.1 B). To date, *Jag1* remains the only false positive identified from the microarray analysis. Overall, the validation rate by ISH was approximately 90% among the candidates tested (data not shown).

Following assessment of the Wnt and Notch candidates by whole mount *in situ* hybridization, each of the validated genes was assessed for CDX response elements

Figure 3.1: Validation of potential targets by whole mount *in situ* hybridization.

A: Whole mount *in situ* hybridization (ISH) was performed on E8.5 embryos of *Cdx1/Cdx2* null mutants and littermate controls in order to confirm the altered gene expression predicted by microarray analysis. A number of players in the canonical Wnt signaling pathway were investigated including frizzled-related protein (*Frzb*), lymphoid enhancer binding factor 1 (*Lef1*), paired-like homeodomain transcription factor 2 (*Pitx2*) and teashirt zinc finger family member 1 (*Tshz1*).

B: Whole mount *in situ* hybridization was also performed on a number of potential target genes from the canonical Notch signaling pathway. Using E8.5 *Cdx1/2* null mutant and control embryos, transcript levels were examined for delta-like 1 (*Dll1*), notch-regulated ankyrin repeat protein (*Nrarp*), and jagged 1 (*Jag1*).

A

WNT

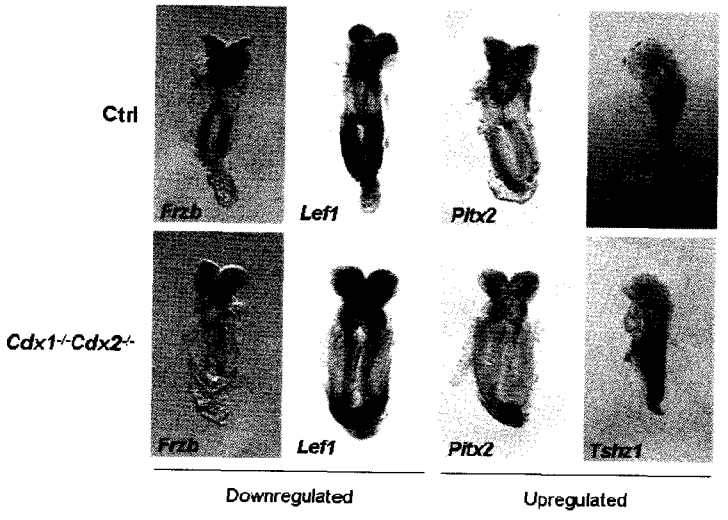

Gene	log2 fc RMA
Frzb	-0.434
Lef1	-1.198
Pitx2a	0.636
Tshz1	1.095

B

NOTCH

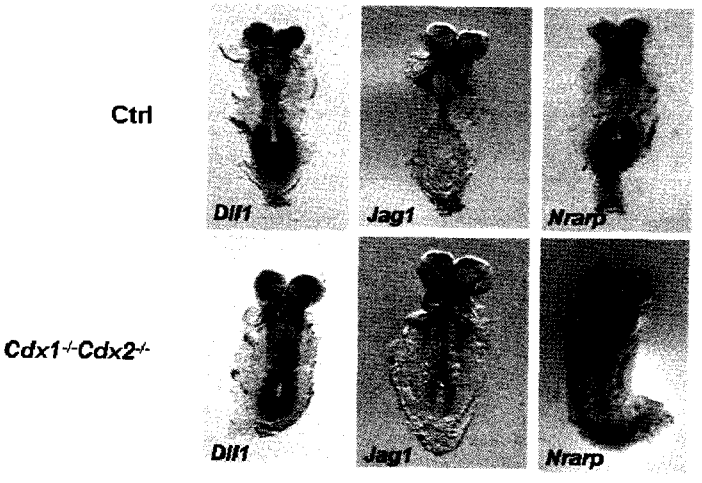

Gene	log2 fc RMA
Dll1	-0.897
Jag1	-0.522
Nrarp	-1.062

Figure 3.1

Figure 3.2: Analysis of *Lef1* expression by whole mount *in situ* hybridization.

A: Whole mount *in situ* hybridization was performed on *Cdx1/2* null embryos and their littermate controls. Individual embryos are pictured for stage E8.25 and E8.5.

B: Group pictures with dorsal (top) and lateral (bottom) views of *Lef1* transcript levels in mutants ($Cdx1^{-/-}Cdx2^{-/-}$) compared to controls ($Cdx1^{-/-}Cdx2^{f/f}$).

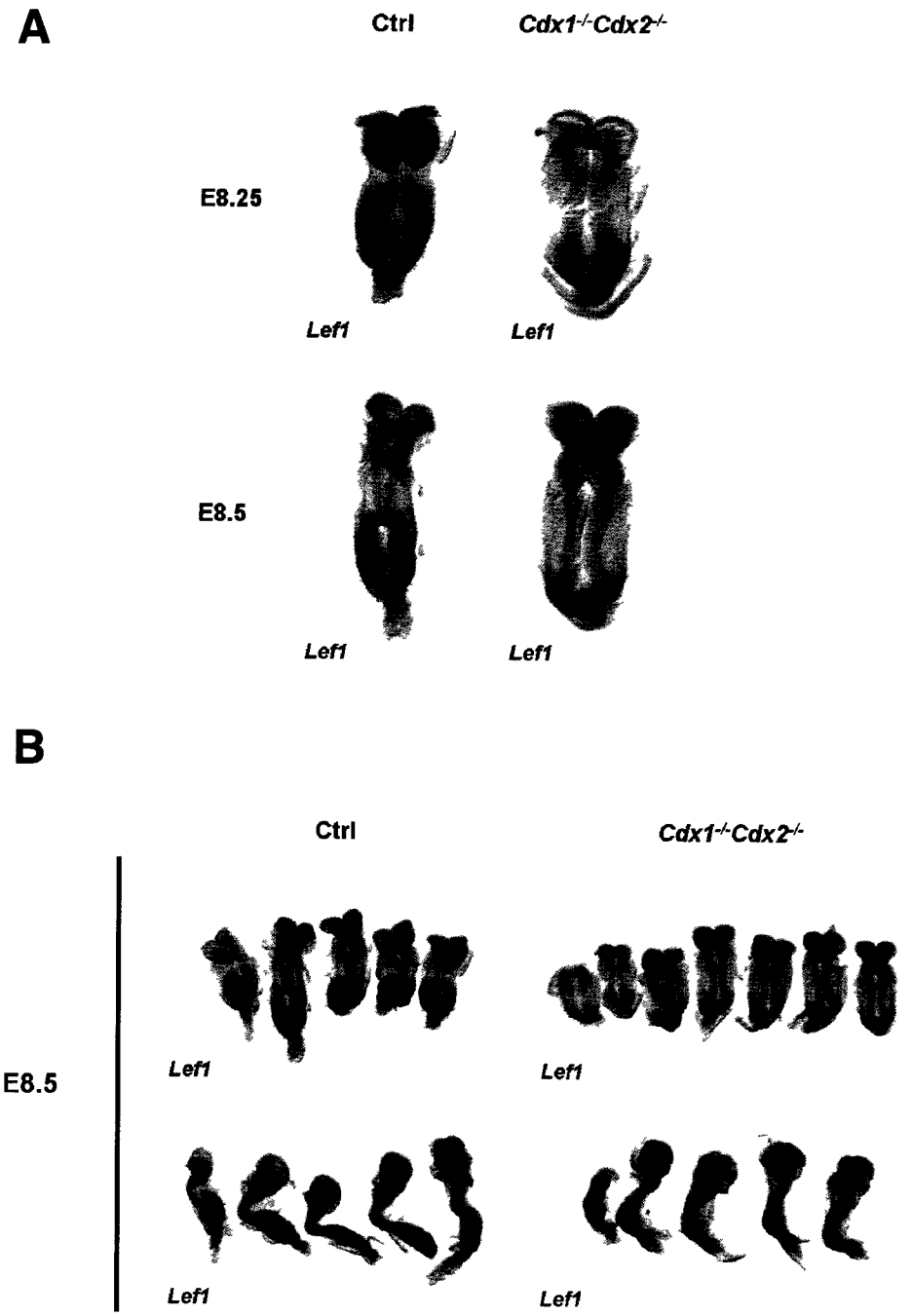
A
Ctrl
Cdx1-/-Cdx2-/-
E8.25
Lef1
Lef1
E8.5
Lef1
Lef1
B
Ctrl
Cdx1-/-Cdx2-/-
E8.5
Lef1
Lef1
Lef1
Lef1

Figure 3.2

(CDREs). Since regulatory elements are often located within a few kilobases of the initiation of transcription, genomic sequences starting at approximately 5 kb upstream of the 5' untranslated region (5'UTR) were analyzed using the Transcription Element Search System (TESS) (Schug, 2008). Amongst the Wnt candidates, only the analysis of the *Lef1* promoter tendered the sequence TTTATG, a consensus CDX response element (Dearolf *et al.*, 1989; Funakoshi *et al.*, 2008; Savory *et al.*, 2009a), although additional elements were found in the *Frzb* promoter upon a manual search for the TTTATG motif (Figure 3.3 A). Amid the validated Notch genes, the *Dll1* promoter contained the consensus sequence (Figure 3.3 B). However, the TESS screens of both *Dll1* and *Nrarp* also revealed the complement to this sequence, CATAAA. In the end, each of the validated genes contained a canonical or variant of the consensus CDX binding site in their proximal promoters. Combined with the high fidelity of the microarray screen as verified through *in situ* hybridization, these findings lend further support to the concept that this screen enriched for direct target genes.

3.2 *Dll1* as a potential CDX target

Following the above evaluations, studies were focused on one gene in particular, delta-like 1 (*Dll1*). A number of factors lead to this decision. To begin, CDX as a family of transcription factors has generally been shown to enhance transcriptional activity, therefore candidates whose expression was downregulated in the absence of CDX were prioritized. Whole mount *in situ* hybridization confirmed *Dll1*

Figure 3.3: Analysis of 5' proximal promoter regions for CDX response elements.

A: The promoter regions of potential Wnt target genes were scanned for putative CDX response elements (CDREs) using the Transcription Element Search System (TESS) as well as a manual search for the TTTATG motif. Genomic regions spanning approximately 5 kb upstream of the transcriptional start site were analysed for *Frzb* and *Lef1*, and each of these regions was found to contain consensus TTTATG binding sites.

B: The putative promoter regions of Notch candidates *Dll1* and *Nrarp* were also analysed using TESS. The *Dll1* proximal promoter contained the consensus CDX response element TTTATG, while both *Dll1* and *Nrarp* carried its complementary sequence CATAAA.

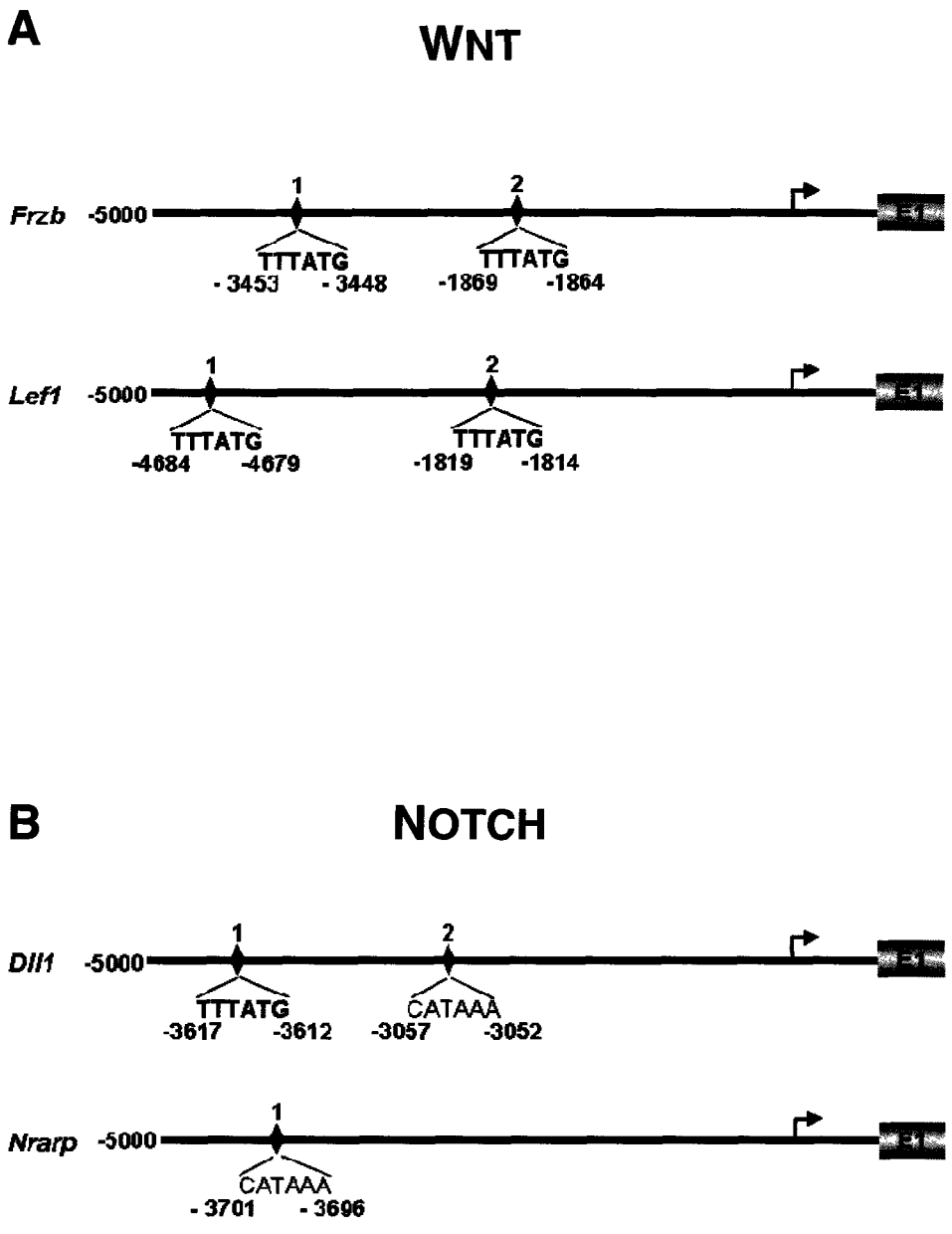
A
WNT
Frzb
-5000
1
2
TTTATG
- 3453
- 3448
TTTATG
-1869
-1864
Lef1
-5000
1
2
TTTATG
-4684
-4679
TTTATG
-1819
-1814
B
NOTCH
Dll1
-5000
1
2
TTTATG
-3617
-3612
CATAAA
-3057
-3052
Nrarp
-5000
1
CATAAA
- 3701
- 3696

Figure 3.3

expression to be markedly reduced in the CDX1/2 mutants compared to littermate controls. Importantly, *Dll1* transcript domains overlapped with the areas of *Cdx* expression (Bettenhausen *et al.*, 1995; Lohnes, 2003), making it a plausible target for direct regulatory control.

DLL1 is a major ligand in the Notch pathway, as well as one of a group of oscillating genes in the molecular somitogenic clock (Fortini, 2009; Kopan and Ilagan, 2009). The role of DLL1 in somite condensation, as well as in the establishment of cranio-caudal segment polarity (Bettenhausen *et al.*, 1995), make it a logical candidate to account for certain somitic defects seen in *Cdx1/2* null mutants. Finally, the finding of a consensus TTTATG CDX binding site in the *Dll1* promoter, as well as its complement, CATAAA, offer further support for a direct regulatory relationship between CDX and *Dll1*. The potential for cross-talk between CDX and Notch signaling during somite segmentation could be of great significance to the current model of somitogenesis and add to our understanding of CDX function in development.

3.3 *Dll1* is dependent on CDX2

As mentioned previously, a strong reduction in *Dll1* expression was detected in $Cdx1^{-/-}Cdx2^{-/-}$ mutants relative to their littermate controls (Figure 3.4 A and B). However, the exact contribution of each member of the CDX family to the observed levels of *Dll1* transcript was not clear. Accordingly, additional ISH were performed

Figure 3.4: Analysis of *Dll1* expression by whole mount *in situ* hybridization.

A: Whole mount *in situ* hybridization was performed on E8.5 embryos of *Cdx1/2* null and littermate controls in order to confirm alterations in the levels of *Dll1* transcript as predicted by the microarray screen. A sense riboprobe control was also used on CD-1 embryos in order to confirm that the displayed expression pattern was specifically associated with *Dll1* and not a result of background staining.

B: Group photos displaying *Dll1* expression in *Cdx1/2* null embryos and controls at E8.5 from a dorsal view (left) and a lateral view (right).

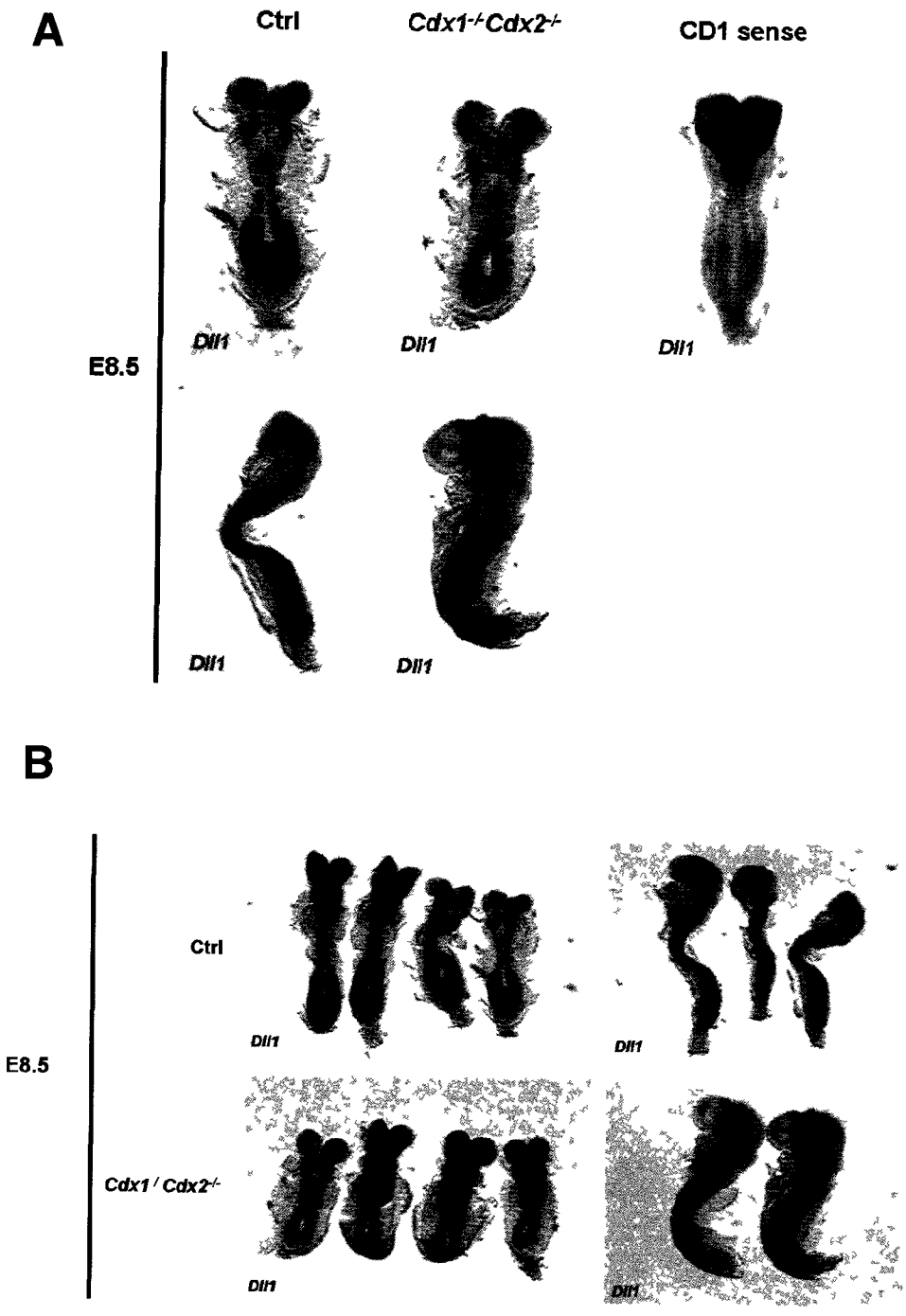
A
Ctrl
Cdx1-/-Cdx2-/-
CD1 sense
E8.5
Dll1
Dll1
Dll1
Dll1
Dll1
B
E8.5
Ctrl
Cdx1 / Cdx2-/-
Dll1
Dll1
Dll1
Dll1

Figure 3.4

to address this issue. Previous studies in our laboratory have determined that the *Cdx2* floxed allele has no effect on levels of *Dll1* transcript (Savory *et al.*, 2009a). A relative comparison of the extent and intensity of *Dll1* expression in *Cdx2*$^{f/f}$ (Ctrl) mutants (Figure 3.5 A) as compared to their *Cdx2* floxed mice that were also devoid of *Cdx1*, *Cdx1*$^{-/-}$*Cdx2*$^{f/f}$ (Ctrl) (Figure 3.4 A and B) suggested that *Dll1* expression was unaffected by the loss of *Cdx1*. Examination of *Dll1* expression in *Cdx2*$^{-/-}$ embryos relative to controls (Figure 3.5 A) revealed that *Dll1* transcript was downregulated, albeit not as severely as in *Cdx1*$^{-/-}$*Cdx2*$^{-/-}$ mutants.

Overall, these experiments revealed that neither the *Cdx2*$^{f/f}$ allele nor the deletion of *Cdx1* had any effect on the expression of *Dll1*, confirming the validity of *Cdx1*$^{-/-}$*Cdx2*$^{f/f}$ littermates as an experimental control. Additionally, the severity of *Dll1* downregulation in the *Cdx1/2* null mutants compared to other *Cdx* allelic lines supported the functional complementarity between members of the CDX family, and suggested that the *Cdx2* allele appeared to have the most penetrant effects.

Recent unpublished studies in our laboratory have demonstrated that CDX2 is expressed earlier than currently described in the literature, initiating at E7.5 in the primitive streak instead of E8.5 as previously reported (Beck *et al.*, 1995). As expression of *Dll1* is also initiated prior to E8.5 we decided to investigate its expression in *Cdx1/2* null mutants at an earlier timepoint. Surprisingly, no distinguishable difference was observed between the domain or intensity of *Dll1*

Figure 3.5: Supplementary analysis of *Dll1* expression by whole mount *in situ* hybridization.

A: Analysis of *Dll1* expression in E8.5 *Cdx2* single null embryos and littermate controls by whole mount *in situ* hybridization.

B: Analysis of *Dll1* transcript levels in E7.5 *Cdx1/2* null mutants and littermate controls. Three sets of embryos have been pictured.

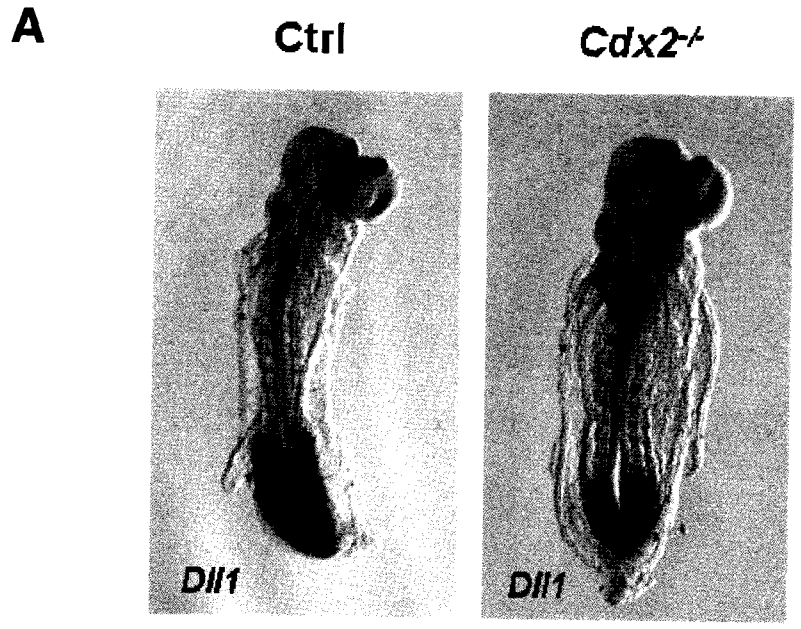

courtesy of
Joanne Savory

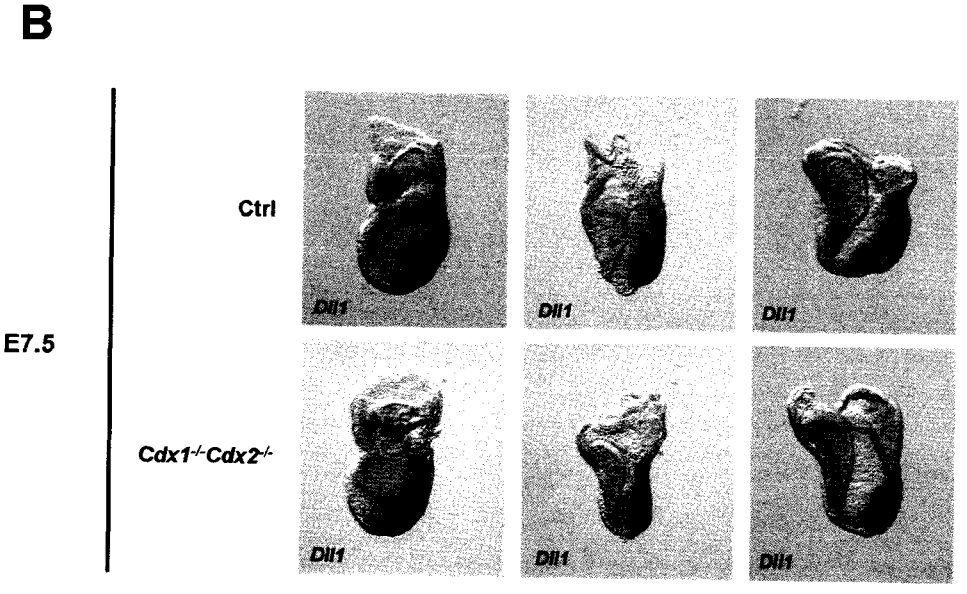

Figure 3.5

expression at E7.5 in *Cdx1/2* null mutants compared to littermate controls (Figure 3.5 B), suggesting potentially a different mechanism of regulation during this period.

To provide a more quantitative assessment of the effect of CDX1/2 loss on *Dll1* expression seen in whole mount ISH, semi-quantitative reverse-transcriptase polymerase chain reaction (RT-PCR) was performed using cDNA generated from E8.5 *Cdx1*$^{-/-}$*Cdx2*$^{-/-}$ mutant embryos and littermate controls (Figure 3.6 A). β-actin was used to normalize loading, and quantitation of expression levels was achieved using ImageJ software. No statistical difference was detected between levels of *Dll1* transcript in mutant and littermate controls ($p = 0.16$), however, the slight reduction of expression observed in *Cdx1/2* null mutants recapitulated the consistent downregulation of *Dll1* detected using whole mount *in situ* hybridization (Figure 3.4 A and B). On account of its resolution *in situ*, whole mount ISH is a more powerful technique, and it is reasonable to infer that the decrease in *Dll1* expression by RT-PCR is indeed relevant and substantiates the trend observed by ISH. Taken together, these data provide additional evidence to suggest that *Dll1* is downstream of CDX.

3.4 The *Dll1* promoter contains consensus, conserved CDX response elements

As mentioned previously, the 5-kb genomic region upstream of the *Dll1* transcriptional start site was analysed for the presence of CDX binding sites (CDRE). This proximal promoter region encompassed a 4.3-kb area containing most of the

Figure 3.6: Semi-quantitative analysis of *Dll1* expression levels.

A: Semi-quantitative analysis of *Dll1* transcript levels between *Cdx1/2* null mutants and littermate controls. E8.5 embryos were harvested for cDNA, and samples were analysed using reverse-transcriptase PCR (RT-PCR). Amplification of β-actin was used as a loading control. Quantitation using ImageJ software did not reveal a significant difference ($p = 0.16$) between transcript levels, however, the slight observable reduction in *Dll1* expression in *Cdx1/2* null mutants recapitulated the consistent downregulation detected by whole mount *in situ* hybridization.

Bioinformatics and phylogenetic analysis of the *Dll1* promoter.

B: The two potential CDRE identified in the *Dll1* 5' proximal promoter region, using the Transcription Element Search System, were investigated for evolutionary conservation using ClustalW2 software. Comparisons were made with highly related species such as the rat, as well as more evolutionary distant species like zebrafish.

A

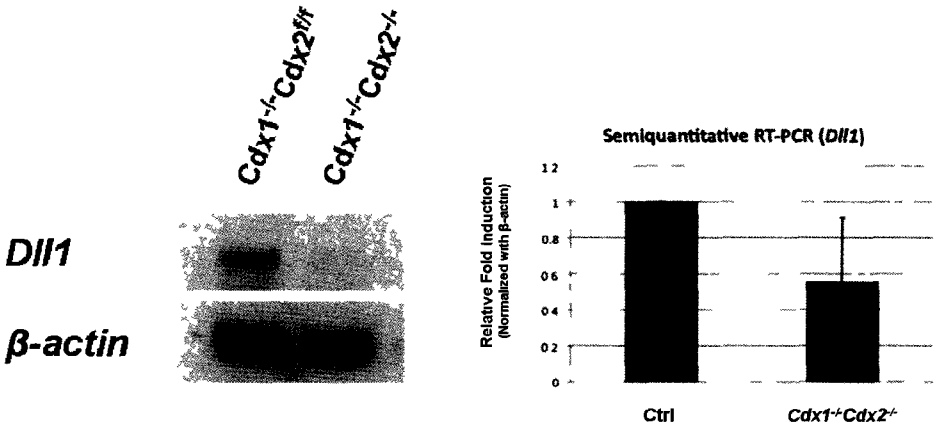

B

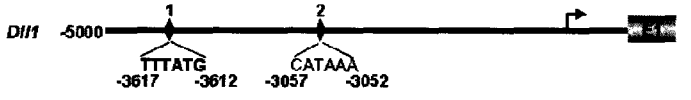

Distal CDRE (CDRE1), TTTATG:

```
Mouse      AAAGCA TTAAAACAAAG TTCC--T  TI  TC TAA G TGAAG--  TGACGATTTATG 1042
Rat        AAAG A TTAAAA AAAG TCC--TC  TI  TT  TAA G TGAAC--  TCA GATTTATG 1034
Human      AAAGTA TTAAAA AAAG T  --T TTI  TC TAA GAG AAG--  TGA GATTTATA 929
Frog       CAT CATCCATTC TGTA CA C TTG AT  CA C ATCTTCACT ATCATGAGAAATA 668
Zebrafish  GAAAAAAAAAAA-TAAAGA TTTTACAAAA C  AATA TAAG AC AATAT  CAC ATA 825
```

Proximal CDRE (CDRE2), CATAAA:

```
Mouse      T TG T GATTT CCC AATACAGAATGCT G CATAAATTAAGTTGGAAAA AATGAAT 1623
Rat        T T  T GATTT  CAATA AGAATGGTG C CATAAATTAAGTTGGAAAAGAAT AAT 1617
Human      T TG T GATTTCCCCAATACAGAATCG GTG CATAAATTAAGTTGGAAAA AATGAAC 1578
Frog       T TG T GATTT CC AATACAGAATCG G G CATAAATTAAGTTG  A  AATAAGT 1233
Zebrafish  CATTTAGAGGAAAACATTAGATA CATTTACAGGT  AT TAAA TCTTCATACATATA 1416
```

Figure 3.6

information required to reflect endogenous *Dll1* expression in transgenic reporter assays, including *Dll1* expression in the somites and presomitic mesoderm (Beckers *et al.*, 2000a). Using the Transcription Element Search System (TESS) (Schug, 2008), two potential CDX binding sites were identified (Figure 3.3 B and Figure 3.6 B). The distal CDRE, TTTATG, was located 3,617 bp upstream of the transcriptional start site, while the proximal motif, CATAAA, was located at 3,057 bp.

A phylogenetic study was subsequently conducted on the two CDRE using ClustalW2 software (Boffelli *et al.*, 2004; Larkin *et al.*, 2007), in order to determine the relative conservation of these sites. Homologues of *Dll1* from mice (*Mus musculus*), rats (*Rattus norvegicus*), humans (*Homo sapiens*), frogs (*Xenopus laevis*) and zebrafish (*Danio rerio*) were selected for comparison (Figure 3.6 B). The analysis revealed that the distal CDX response element was conserved in rats and only the final base pair was altered in humans. The region surrounding this site was also well-preserved between the various species. Interestingly, the proximal CDRE was even more highly conserved, and appeared to be identical in rats, humans and frogs. The flanking area also exhibited a high degree of conservation, with the frog exhibiting the greatest divergence. In the case of both CDX response elements, the degree of conservation between species was reflective of their phylogenetic relationship. This conservation is consistent with a direct regulatory relationship between CDX and *Dll1*.

3.5 CDX2 binds the *Dll1* promoter *in vivo* and *in vitro*

Having identified potential CDREs in the *Dll1* promoter, several assays were performed in order to assess the ability of CDX to bind to the promoter *in vivo* and *in vitro*. Given the results of *in situ* hybridization and the contribution of CDX2 to *Dll1* expression, as assessed by the mutant phenotypes, I decided to focus on CDX2 activity in the following analyses. First, chromatin immunoprecipitation (ChIP) was used to determine whether CDX2 occupied the *Dll1* promoter region *in vivo*. In this experiment proteins were cross-linked to chromatin elements, sheared into approximately 1-kb fragments by sonication, immunoprecipitated with CDX2 antibody, and the purified DNA from these precipitates was assessed by PCR for the presence of amplicons in the vicinity of the putative CDX binding sites. Fifty wildtype CD-1embryos at E8.5 were pooled for this analysis, as CDX2 loss had a clear effect on *Dll1* expression at this stage. For the PCR amplification, an interval was selected between the two closely-situated CDRE (within 560 bps of each other) on the *Dll1* promoter, in order to detect CDX-binding in the vicinity of either of the elements. The presence of a robust band in the CDX2 antibody pull-down suggested that CDX2 occupied the promoter in this region (Figure 3.7 A). This binding was likely specific, as indicated by comparison to a number of controls. These controls included the absence of CDX2 antibody or immunoprecipitation with rabbit pre-immune serum (PIS). A mock reaction and water control were also used to control for contamination. Finally, comparison with an amplicon from an upstream sequence was used to gauge the specificity of binding. Altogether, these controls demonstrated that the observed binding reaction appeared to be specific to the

Figure 3.7: Examination of CDX2 binding to the *Dll1* promoter *in vivo* and *in vitro*.

A: *In vivo* analysis of CDX2 binding by chromatin immunoprecipitation (ChIP). This screen was performed on chromatin generated from approximately 50 CD-1 embryos at E8.5, and immunoprecipitated with CDX2 antibody (αCDX2). A 457-bp genomic region between the closely situated CDREs was amplified by PCR in order to assess the ability of CDX2 to occupy the *Dll1* promoter in the vicinity of the putative binding sites. Amplification of an area 15 kb upstream of the transcriptional start site served as a negative control. The specificity of the CDX2 interaction was also confirmed by the absence of a band or an amplicon of reduced intensity in several supplementary controls. Samples were precipitated without CDX2 antibody (no Ab), in the absence of chromatin (mock), and with rabbit pre-immune serum (PIS), all to account for background amplification.

B: The specificity of CDX2 binding to the putative CDREs was assessed *in vitro* using electrophoretic mobility shift assay (EMSA). This assay was used to validate CDX2 binding to each of the putative response elements (lanes 10 and 18), and verified the specificity of results through a variety of controls. Incubation with GST protein alone was included to ensure that the binding component was the CDX2 portion of the fusion protein (lanes 9 and 17), and this was further confirmed by the observation of a "supershift" (SS, lanes 11 and 19) upon incubation with anti-CDX2 antibody. A mutated version of the binding motif was employed to confirm that the sequence in question was responsible for CDX2-binding (lanes 12 and 20), and a 200 fold excess of a radioinert self-competitor (lanes 14 and 22) as well as a known CDX target (lanes 13 and 21) and a non-CDX motif RARE (lanes 15 and 23) were included as further validation of binding specificity. CDREs in the *Dll1* promoter were compared with a characterized CDRE from *Hoxb8*, in order to contrast the pattern and affinity of CDX2 association (lanes 1-7).

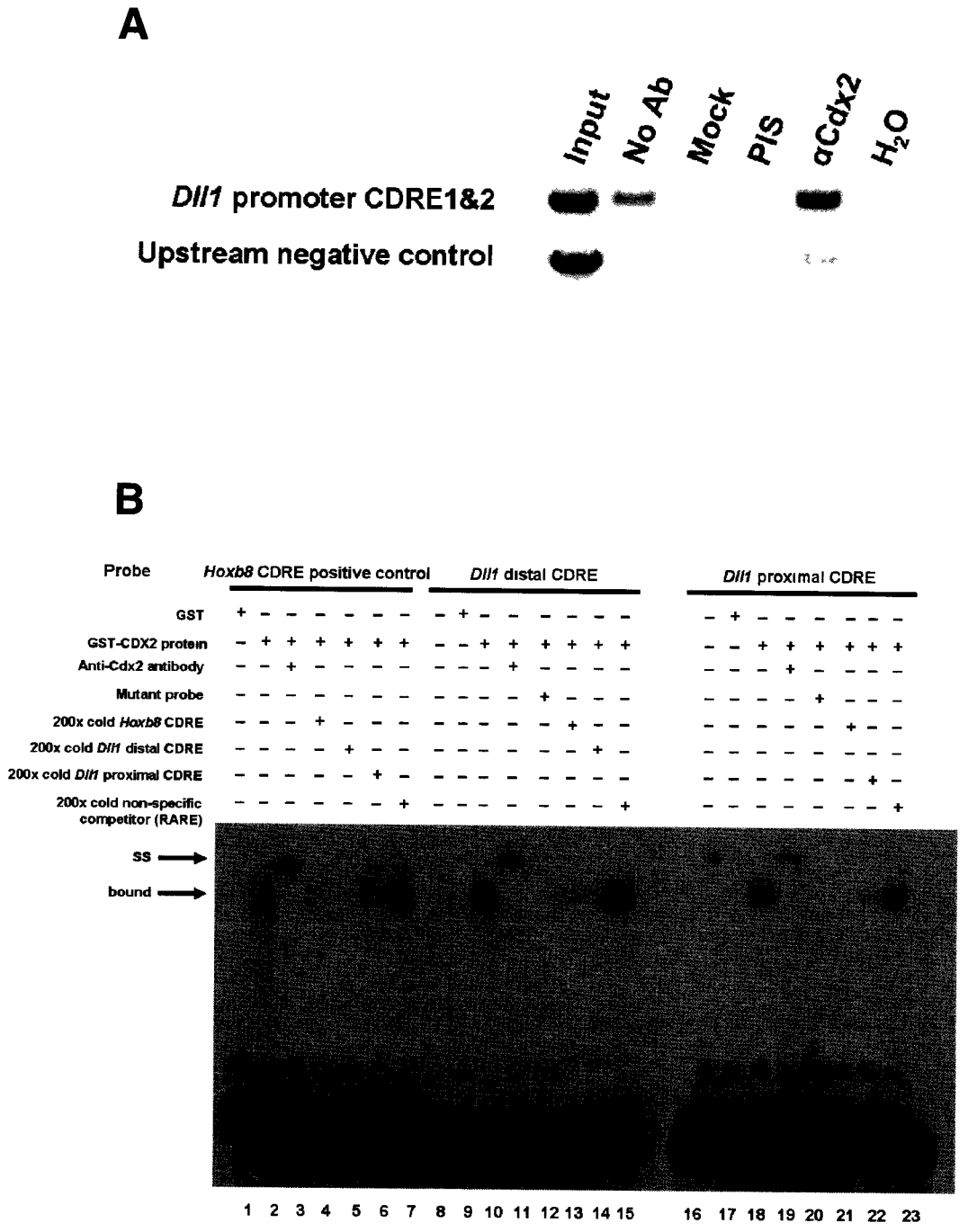
A
Input
No Ab
Mock
PIS
αCdx2
H2O
Dll1 promoter CDRE1&2
Upstream negative control
B
Probe
Hoxb8 CDRE positive control
Dll1 distal CDRE
Dll1 proximal CDRE
GST
GST-CDX2 protein
Anti-Cdx2 antibody
Mutant probe
200x cold Hoxb8 CDRE
200x cold Dll1 distal CDRE
200x cold Dll1 proximal CDRE
200x cold non-specific competitor (RARE)
SS
bound
1 2 3 4 5 6 7 8 9 10 11 12 13 14 15 16 17 18 19 20 21 22 23

Figure 3.7

region of the *Dll1* promoter containing the two putative CDREs, consistent with *Dll1* being a direct CDX2 target.

Subsequently, electrophoretic mobility shift assay (EMSA) was used to investigate whether CDX2 could specifically bind the CDX response elements identified in the *Dll1* promoter. Short double-stranded oligonucleotides corresponding to the potential binding sites, as well as mutated versions of these elements, were end-labeled with [γ-^{32}P]ATP, and binding of GST-CDX2 fusion protein to these motifs was assessed *in vitro*. GST-CDX2 adhered to probes representing either the proximal or distal CDREs (Figure 3.7 B lanes 10 and 18), resulting in a decrease in mobility of the radioactive probes relative to the free probes alones (Figure 3.7 B lanes 8 and 16). The specificity of these interactions was verified through the addition of anti-CDX2 antibody, which resulted in a further retardation of the GST-CDX2-probe complexes, also known as a "supershift" (SS) (Figure 3.7 B lanes 11 and 19). GST protein alone was incapable of associating with the probes (Figure 3.7 B lanes 9 and 17). Furthermore, GST-CDX2 proteins were unable to bind to mutated versions of the CDREs (Figure 3.7 B lanes 12 and 20), further demonstrating the exclusivity of the interaction. Competition assays also provided confirmation of the specificity and authenticity of the observed binding reaction, with radioinert competitor probes representative of either *Dll1* CDRE or a previously characterized CDRE (Charite *et al.*, 1998) both able to outcompete the radiolabeled probe in binding reactions (Figure 3.7 B lanes 13,14 and 21,22). Conversely, a cold competitor generated from an unrelated retinoic acid receptor binding motif (RARE) (Houle *et*

al., 2003) was unable to compete (Figure 3.7 B lanes 15 and 23). Finally, the binding patterns of both the distal and proximal CDREs from the *Dll1* promoter were similar to the pattern of the previously characterized element from the *Hoxb8* promoter (Figure 3.7 B lanes 1-7). Interestingly, the distal *Dll1* CDRE had an affinity comparable to the *Hoxb8* motif, while the proximal CDRE appeared to be less tightly associated. Together, these findings are consistent with a direct regulatory interaction between CDX2 and the putative CDREs in the *Dll1* promoter.

3.6 Functional analysis of the CDX response elements in the *Dll1* promoter

To address the functional relevance of the CDRE, the *Dll1* promoter was cloned into a promoterless luciferase reporter vector, pXP2. After generating mutations of the CDREs, plasmids were transiently transfected into P19 embryonal carcinoma cells alone or with a CDX2 expression vector, and luciferase activity was assessed.

The full-length *Dll1* promoter was shown to be responsive to CDX2, further supporting the hypothesis of a direct regulatory relationship (Figure 3.8 A and B). Additionally, mutation of the proximal CATAAA response element resulted in a significant ($p = 0.03$) reduction in luciferase activity, again substantiating the functional relevance of the binding site and a role for CDX2 in *Dll1* transcription. Conversely, when the distal CDRE was altered, luciferase activity increased relative to the wildtype promoter, although this was not statistically significant ($p = 0.055$). However, this increase in induction was also seen upon mutation of both

Figure 3.8: Functional analysis of putative CDREs in the *Dll1* promoter.

A: Induction of luciferase activity from the *Dll1* promoter by CDX2 was optimized using the wild-type reporter construct. The highest induction was achieved using 0.75 μg of CDX2 expression vector, and this quantity was selected for further experimentation.

B: Examination of the *Dll1* promoter through transient transfection analysis in P19 embryonal carcinoma cells. The wildtype *Dll1* proximal promoter region was cloned into a pXP2 luciferase reporter vector, and one or both of the putative CDRE were mutated for analysis. Subsequently, the series of *Dll1* reporters was transfected into P19 cells in the presence or absence of a *Cdx2* expression vector. RSV-βgal was included to correct for transfection efficiency, and luciferase activity was assessed as fold induction of RSV-βgal-corrected luciferase values, over reporter-alone controls. This experiment was performed in triplicate and repetition of the experiment produced similar results. Statistical analysis revealed a significant reduction in luciferase activity upon mutation of the proximal site (CDRE2, *: $p = 0.03$), but a significant increase when both sites were altered (**: $p = 0.02$).

A

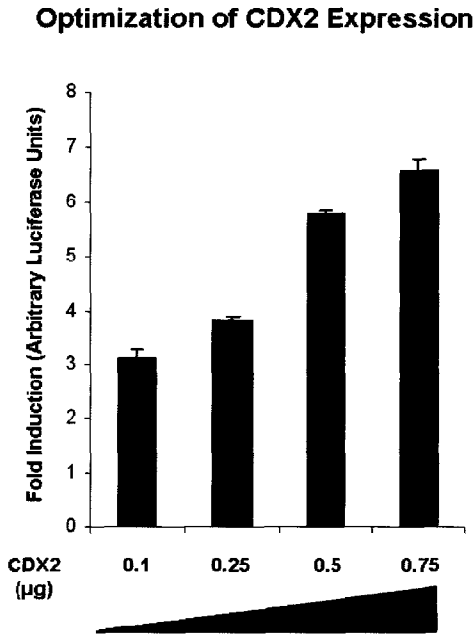
Optimization of CDX2 Expression
Fold Induction (Arbitrary Luciferase Units)
0
1
2
3
4
5
6
7
8
CDX2 (µg)
0.1
0.25
0.5
0.75

B

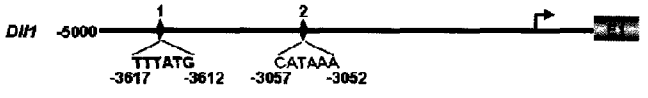
Dll1
-5000
1
2
TTTATG
-3617
-3612
CATAAA
-3057
-3052

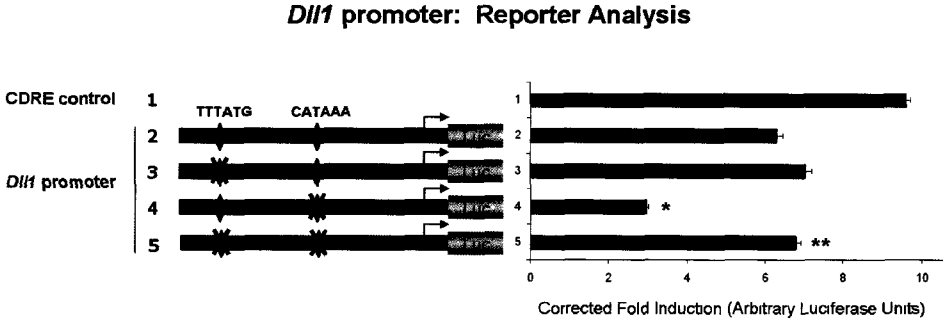
Dll1 promoter: Reporter Analysis
CDRE control
Dll1 promoter
1
2
3
4
5
TTTATG
CATAAA
*
**
0
2
4
6
8
10
Corrected Fold Induction (Arbitrary Luciferase Units)

Figure 3.8

CDX motifs, and was found to be statistically significant ($p = 0.02$). Overall, these results, and particularly the induction of *Dll1* upon mutation of the distal and both CDX binding sites, was not in agreement with the reduced transcription of *Dll1* observed in the absence of CDX players. These findings also did not reflect the decreased activity of the *Dll1* promoter seen upon mutation of a response element that overlaps with the distal CDRE (Hofmann *et al.*, 2004). Collectively, these inconsistencies prompted reconsideration of the transfection analysis.

P19 cells are an immortalized cell line derived from pluripotent embryonal carcinoma cells (McBurney, 1993). As such, they may not express the necessary co-factors to support all mesoderm transcription programs. Transcription factors do not act in isolation but elicit their effects as part of a larger complex of proteins, or in combination with other transcription factor input(s). It is therefore quite possible that CDX-dependent regulation of *Dll1* expression requires ancillary factors that are not accounted for in the P19 transfection studies. In this regard, LEF1 and TBX6 are also direct regulators of *Dll1* expression (Galceran *et al.*, 2004; Hofmann *et al.*, 2004; White and Chapman, 2005), and our group has previously shown interactions between LEF1 and CDX1 (Beland *et al.*, 2004). Therefore, I assessed the possibility of interactions between CDX2 and either one of these factors on the *Dll1* promoter. In order to achieve this, the combination of LEF1 and β-catenin or TBX6 was transfected in the presence or absence of a CDX2 expression vector into P19 embryocarcinoma cells (Figure 3.9 A and B). Although LEF1/β-cat or TBX6 alone had modest effects on *Dll1* promoter activity, the induction was not significant

Figure 3.9: Co-transfection assays in P19 embryonal carcinoma cells.

A: In this experiment, the *Dll1* wildtype reporter was transfected with CDX2 in addition to LEF1 and β-catenin expression vectors in order to assess the potential for combinatorial regulation. RSV-βgal was used to control for transfection efficiency. One microgram of the reporter was used in conjunction with 0.5 μg of each of the expression vectors. In this assay, individual luciferase values are picture following correction for RSV-βgal. Transfection with CDX2 alone as well as CDX2 in combination with LEF1 and β-catenin resulted in a significant increase in luciferase activity (* and **: $p = 0.0009$) relative to basal levels.

B: Similar to the above experiment with CDX2, LEF1 and β-catenin, the *Dll1* wildtype reporter vector was transfected with CDX2 in addition to TBX6 and assessed for luciferase activity. One microgram of the reporter was used in conjunction with 0.5 μg of each of the expression vectors. Transfection with CDX2 alone as well as CDX2 in combination with TBX6 resulted in a significant increase in luciferase activity (*: $p = 0.007$; **: $p = 0.003$) relative to basal levels. Furthermore, induction of luciferase by CDX2 and TBX6 in combination appeared to be synergistic, and was submitted to further analysis for possible combinatorial regulation.

C: A dose-response study was performed, in light of a potential combinatorial regulation of the *Dll1* promoter by CDX2 and TBX6, in order to elucidate the optimal levels of each expression vector to be used in transient transfection as well as the reproducibility of the synergistic interaction. One microgram of the reporter was used in conjunction with 0.125 μg, 0.25 μg, 0.5 μg, and 1.0 μg of each of the expression vectors, and RSV-βgal was used to control for transfection efficiency.

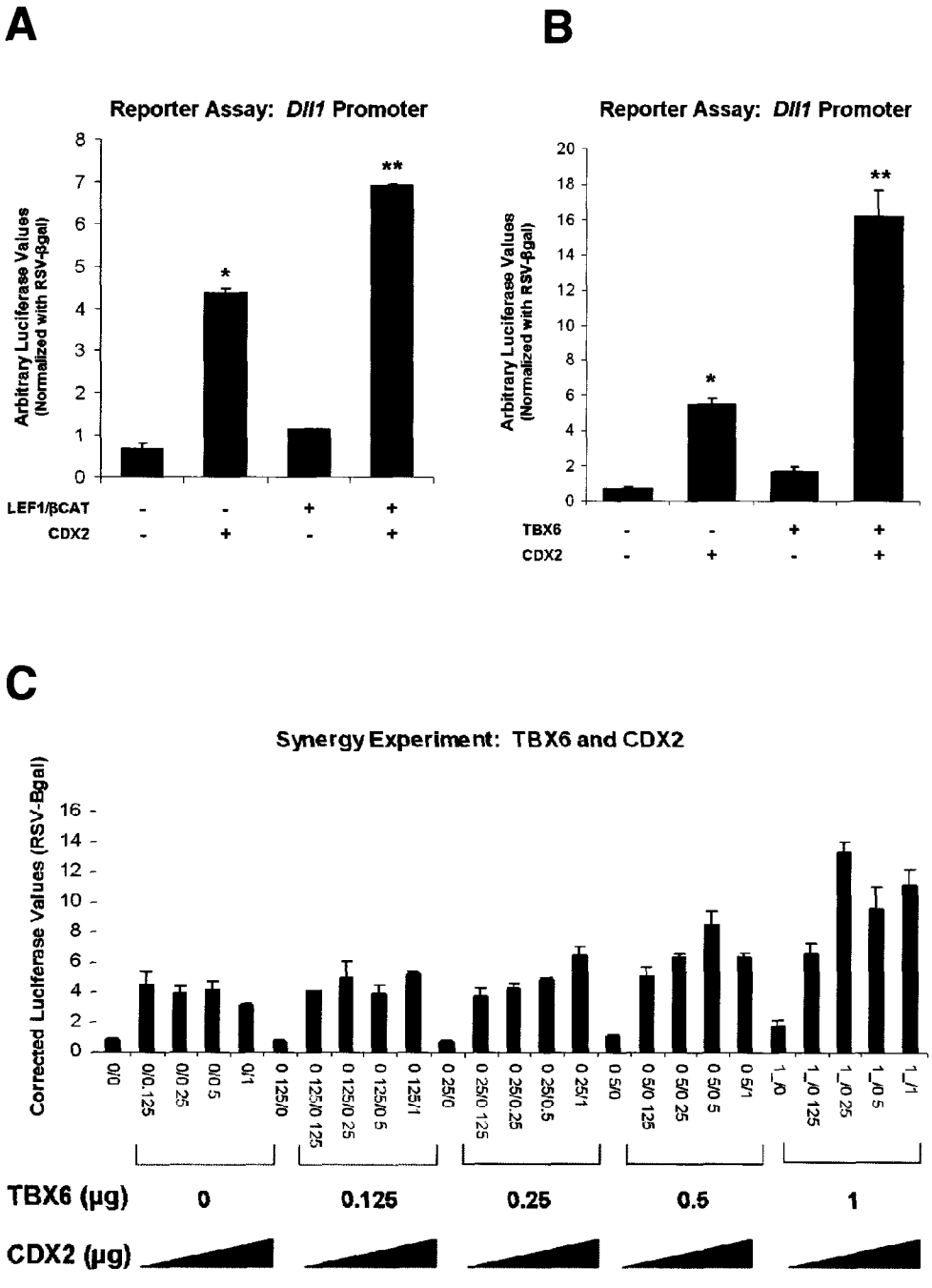
A
Reporter Assay: Dll1 Promoter
Arbitrary Luciferase Values (Normalized with RSV-βgal)
LEF1/βCAT
CDX2
B
Reporter Assay: Dll1 Promoter
Arbitrary Luciferase Values (Normalized with RSV-βgal)
TBX6
CDX2
C
Synergy Experiment: TBX6 and CDX2
Corrected Luciferase Values (RSV-Bgal)
0/0
0/0.125
0/0 25
0/0 5
0/1
0 125/0
0 125/0 125
0 125/0 25
0 125/0 5
0 125/1
0 25/0
0 25/0 125
0 25/0.25
0 25/0.5
0 25/1
0 5/0
0 5/0 125
0 5/0 25
0 5/0 5
0 5/1
1_/0
1_/0 125
1_/0 25
1_/0 5
1_/1
TBX6 (µg)
0
0.125
0.25
0.5
1
CDX2 (µg)

Figure 3.9

(LEF1/β-cat and TBX6 p = 0.06). On the other hand, transfection with CDX2 resulted in a significant increase in transcription (LEF1/β-cat assay p = 0.0009; TBX6 assay p = 0.007). Upon further addition of LEF1/β-catenin the increase in luciferase activity seemed to be additive (p = 0.0009). Co-transfection of CDX2 with TBX6, in contrast, appeared to result in a synergistic activation of the *Dll1* promoter (p = 0.003). As synergy is often indicative of a concerted function between two transcription factors (Merika and Orkin, 1995), this finding supported the hypothesis of a combinatorial interaction.

Subsequent to this result, a dose-seeking study was performed to define the combination of CDX2 and TBX6 that achieved the greatest activity and whether there was a threshold for this induction. Maximal activation of luciferase occurred at approximately 1 μg of CDX2 protein in association with 0.25 μg of TBX6. Beyond these levels, induction began to decline (Figure 3.9 C). The reduction in luciferase beyond the elucidated parameters is likely a result of oversaturation. Thus, future experiments will use the optimized parameters for CDX2-TBX6 co-transfection to readdress the issue of *Dll1* expression upon mutation of the putative CDX binding sites.

Overall, the above data support *Dll1* as a CDX target gene, potentially in synergy with TBX6. *Dll1* expression is markedly reduced in *Cdx1/2* null mutants, and CDX2 can bind to the *Dll1* promoter region *in vivo*. *In vitro,* CDX2 can associate with specific CDX response elements identified by bioinformatics in the 5' proximal

promoter region. Additionally, evidence from combinatorial regulation studies indicates that CDX2 can induce transcriptional activity from the *Dll1* promoter, and that this activity is greatly enhanced in the presence of TBX6. Collectively, these observations support a direct regulatory relationship between CDX2 and *Dll1*.

CHAPTER 4

DISCUSSION

4.1 *Dll1*: a novel CDX target gene

Standard genetic models give a limited view of CDX function as *Cdx2* null embryos die between E3.5 and 5.5 due to a failure to implant (Chawengsaksophak *et al.*, 1997). Additionally, the functional redundancy between CDX1, CDX2, and CDX4 introduces the problem of functional compensation in the mutant models described to date. The generation of a conditional *Cdx2* knockout line by our laboratory has helped to address some of these limitations. In addition, the creation of CDX1/2 double mutants using this line has produced mice that also exhibit loss of CDX4 (our unpublished data). Accordingly, these mice represent the absence of the full cohort of CDX expression. Together, these new mutant lines provide a powerful vehicle to explore previously uninvestigated roles of CDX transcription factors during development.

The *Cdx2* single null mutant is distinguished by a severe caudal truncation likely associated with the premature termination of paraxial mesoderm (Savory *et al.*, 2009a). This truncation was even more progressive in *Cdx1/2* double nulls (our unpublished data). Additionally, CDX1/2 mutants were characterized by disrupted somitogenesis, and the somites that did form had an aberrant morphology (Figure 1.5).

Microarray analysis of CDX1/2 double mutants revealed several known or suspected direct CDX targets, including a number of *Hox* genes (our unpublished data). This screen also identified a number of players from Wnt and Notch

signaling, pathways known to be involved in somitogenesis, offering a potential mechanism to explain the somitic defects. One of these genes, *Dll1*, a central ligand in the Notch pathway, was selected for additional scrutiny. *Dll1* exhibits overlapping expression domains with CDX members, and its loss leads to somite defects reminiscent of certain abnormalities seen in *Cdx1/2* null mutants.

CDX2 was able to bind the *Dll1* promoter region *in vivo* as well as conserved CDRE *in vitro*. To date, functional analysis of these motifs has proven inconclusive, however a preliminary investigation suggests that CDX2 and TBX6 may function in combination on the *Dll1* promoter. While further experimentation is necessary to confirm these relationships, the current findings are consistent with *Dll1* as a direct target of CDX2.

4.2 CDX in somitogenesis

The process of somitogenesis is currently an area of great interest in development. Despite an influx of information, our understanding of the mechanisms governing somite formation and patterning is limited. Several of the pathways involved in posterior development are also implicated in somitogenesis, including the fibroblast growth factor (Fgf), retinoic acid (RA), Wnt and Notch signaling pathways. To this end, CDX transcription factors are also posterior effectors. Their potential complicity in somitogenesis is supported by the broader morphology of somites in *Cdx1/2* homozygotes (our unpublished data) (Figure 1.5) and the precocious

termination of somite formation in *Cdx2* null mutants (Chawengsaksophak *et al.*, 2004; Savory *et al.*, 2009a). However, the mechanistic basis for this phenotype is not understood.

Previous research has established that CDX factors regulate the expression of *Hox* genes, and thereby influence vertebral AP patterning (Davidson *et al.*, 2003; van Nes *et al.*, 2006). However, this association fails to explain the effect of CDX factors on somite morphology and segmentation. Interestingly, earlier studies in our laboratory have placed CDX2 in direct control of *Wnt3a* and *Cyp26a1*, which are important regulators of Wnt and RA signaling, pathways with established links to somitogenesis (Savory *et al.*, 2009a). The identification of additional Wnt and Notch pathway members (Table 3.1 A and B) through the microarray screen of *Cdx1/2* compound null mutants, supports a potential role for CDX factors upstream of these genes, and may offer a mechanistic basis for the somite defects in CDX1/2 mutants.

Prospective CDX targets from the microarray screen included *Lef1*, a member of the family of LEF/TCF transcription factors and a central player in Wnt signaling. *Lef1* null mutants do not exhibit somite defects (van Genderen *et al.*, 1994), although *Lef1* is present at E8.5 in the presomitic mesoderm of wildtype embryos (Figure 3.1 A and Figure 3.2 A and B) and overlaps with the expression of all three CDX members (Beck *et al.*, 1995; Gamer and Wright, 1993; Meyer and Gruss, 1993). The absence of somitic defects in *Lef1* mutants or a direct phenocopy with the cohort of CDX knockout lines, can likely be attributed to functional overlap of *Lef1* with other *Tcf*

genes (van Genderen *et al.*, 1994). Indeed, *Lef1/Tcf1* homozygotes are characterized by irregular somites with abnormal morphology anterior to the forelimb bud, as well as mis-specification of paraxial mesoderm to a neural fate at more posterior levels (Galceran *et al.*, 1999). In addition to reduced *Lef1* expression levels in the absence of CDX, as confirmed by whole mount ISH (Figure 3.1 A and Figure 3.2 A and B), consensus CDX binding sites were located in the *Lef1* 5-kb proximal promoter region. While this data is certainly not substantive of a direct regulatory relationship, it sustains the possibility of one, and further experimentation will be necessary to determine the precise mechanism of CDX factors in *Lef1* regulation.

Finally, important candidates were also identified from the Notch signaling pathway, including *Nrarp*, a target gene and antagonist of the NOTCH1 receptor (Weerkamp *et al.*, 2006; Yun and Bevan, 2003), as well as the genes encoding ligands DLL1 and JAG1. Of all the prospective targets analysed thus far, *Jag1* was the only false positive identified, and was excluded from all further analysis. In contrast, *Nrarp* and *Dll1* expression were misregulated in whole mount ISH in accordance with the predictions of the microarray (Figure 3.1 B). The identification of CDX response elements in their proximal promoter regions, in particular the consensus TTTATG motif in *Dll1*, was consistent with a potential direct regulation by CDX (Figure 3.3 B).

Nrarp homozygous null embryos display retinal vascular defects but normal paraxial mesoderm (Phng *et al.*, 2009). While these defects do not phenocopy the

somitic and caudal anomalies inherent to the *Cdx1/2* null line, it is possible that *Nrarp* homozygotes are functionally compensated. In ay case, *Nrarp* is expressed in the correct region for direct regulation by CDX, with two strong bands in the presomitic mesoderm of wildtype embryos at E8.5 (Figure 3.1 B) (Krebs *et al.*, 2001).

Dll1 also demonstrates intense staining throughout the presomitic mesoderm at this time (Figure 3.1 B). *Dll1* null mutants, $Dll1^{lacZ/lacZ}$, are characterized by aberrant somites in the trunk region, which become progressively worse in the caudal embryo to the point where no somites can be discerned. Additionally, the posterior halves of somites fail to condense, disrupting their craniocaudal polarity (Hrabe de Angelis *et al.*, 1997). These anomalies bear some resemblance to the defects in *Cdx1/2* null mutants. In addition, $Dll1^{lacZ}$ rib-vertebrae (*rv*) compound mutants exhibit tail kinks or a caudal truncation (Beckers *et al.*, 2000b) similar to the defects seen in *Cdx1/2* null mutants (our unpublished data) and the tail kinks and caudal truncation in *Cdx2* heterozygotes and homozygotes (Chawengsaksophak *et al.*, 1997; Chawengsaksophak *et al.*, 2004; Savory *et al.*, 2009a). Notably, the rib-vertebrae allele was later identified as a hypomorph of *Tbx6* (Watabe-Rudolph *et al.*, 2002; White *et al.*, 2003), a direct regulator of *Dll1* activity. *Dll1* is therefore a promising candidate as a direct target of CDX.

4.3 *Dll1* as a direct target of CDX2

In addition to demonstrating the expected decrease in transcript levels in CDX1/2 mutants, *Dll1* is expressed throughout the presomitic mesoderm, the anlagen of the somites, in a pattern that overlaps with each of the CDX members (Beck *et al.*, 1995; Gamer and Wright, 1993; Meyer and Gruss, 1993). The homozygous mutant of *Dll1* is also the only candidate to display somitic defects, as well as a caudal truncation in combination with *rv*, the hypomorphic allele of *Tbx6* (Watabe-Rudolph *et al.*, 2002; White *et al.*, 2003). These defects are similar to the anomalies observed in the *Cdx1/2* null mutants. While earlier studies in our laboratory proposed that decreased levels of *Dll1* transcript in conditional *Cdx2* null embryos might be an indirect effect of reduced *Wnt3a* (Savory *et al.*, 2009a), the identification of two potential CDREs in the 5' proximal promoter region, one of which was the consensus TTTATG motif, are consistent with direct regulation of *Dll1* by CDX.

To further investigate *Dll1* as a direct CDX target, additional ISH were performed. From the initial ISH screens at E8.5, reduction of *Dll1* expression in *Cdx1/2* null mutants suggested that CDX factors were acting as transcriptional enhancers on the *Dll1* promoter. Interestingly, and despite concurrent expression of CDX1/2 and *Dll1* at earlier stages, levels of *Dll1* expression were indistinguishable between mutants and controls at E7.5 (Figure 3.5 B). This result might suggest that CDX is involved in the maintenance but not the initiation of *Dll1* activity, and that other signaling cascades regulate *Dll1* expression at these earlier timepoints. On the other hand, sufficient levels of CDX4 may persist in the double mutants at earlier stages to

sustain *Dll1* activity. In a similar way, reverse transcriptase PCR revealed a modest decrease in *Dll1* transcript levels in *Cdx1/2* null mutants relative to controls, but this reduction was not significant upon statistical analysis. While this result was also not expected, on comparison of these data with the pictures from whole mount ISH, a methodology with greater resolution, it appears that this decrease is nonetheless relevant, as it is consistent and the domain of *Dll1* expression is observably and reproducibly smaller *in situ*.

Analysis of the *Dll1* 5' proximal promoter region returned two potential CDX binding sites. A phylogenetic analysis was undertaken in order to analyse the evolutionary conservation of these motifs (Boffelli *et al.*, 2004). Conservation is often used as a benchmark for functional significance since essential regulatory elements are often retained throughout the course of evolution. In a comparison of 5 species that included organisms both closely related (rats and humans) and evolutionary distant (frogs and fish) from mice, the distal CDRE from the mouse *Dll1* promoter region was conserved in rats and only one base pair was altered in humans. The proximal site was highly conserved in rats, humans, and frogs (Figure 3.6 B). While the human genome retains 40% sequence identity with mice (Boffelli *et al.*, 2004), preservation of the proximal site in the frog genome, a much more distantly-related species, supports its functional relevance. It is curious that neither CDRE was retained in zebrafish given a previous study that showed high homology of upstream regulatory regions between mouse and zebrafish particularly in association with *Dll1* (Hans and Campos-Ortega, 2002), however, it is possible that

the CDX-dependent *Dll1* regulation diverged between species even as other activities on the *Dll1* promoter were retained.

Additional analyses provided further support for direct regulation of *Dll1* by members of the CDX family. Chromatin immunoprecipitation (ChIP) indicated that CDX2 occupied the *Dll1* promoter *in vivo* in the region of the two putative CDRE (Figure 3.7 A). This was consistent with a role for CDX2 in the direct regulation of *Dll1*. Electrophoretic mobility shift assay (EMSA) was performed to determine whether CDX2 could specifically bind the putative motifs in isolation. This analysis revealed an interaction between CDX2 and the *Dll1* CDRE sequences (Figure 3.7 B), supporting the proposition that CDX2 binds the identified motifs.

While the above findings were encouraging, the binding detected in EMSA does not guarantee identical associations *in vivo*. Moreover, while ChIP revealed that CDX2 occupies the *Dll1* promoter *in vivo* in the vicinity of the putative CDREs, this assay does not ensure that binding was actually occurring at the determined motifs as opposed to unidentified response elements. Additionally, neither ChIP nor EMSA demonstrate that this binding was productive. In order to begin to address certain of these issues I cloned the wildtype *Dll1* promoter and generated a series of site-directed mutants ablating the putative CDREs to derive luciferase reporter constructs. Co-transfection of each reporter with a CDX2 expression vector was used to assess whether a particular motif was functionally relevant. Mutation of either motif alone or in combination modified the fold change in luciferase activity

relative to the wild-type promoter following co-transfection with CDX2 (Figure 3.8 B). Induction by the distal motif in isolation was not statistically significant ($p = 0.55$), however, mutation of both CDX response elements in concert resulted in an increase in luciferase activity that was statistically significant ($p = 0.02$). This result implied a repressive role for CDX on the *Dll1* promoter, but is in contrast with previous findings. Studies of *Hox* and other CDX targets have generally shown CDX to function in transcriptional activation (Subramanian *et al.*, 1995; Taylor *et al.*, 1997). What's more, this increase in transcriptional activity does not correlate with the reduction in *Dll1* transcripts observed using whole mount ISH. In addition, this finding seems to contract a study by Hofmann *et al.* where mutation of a T-box response element (that overlaps with the distal CDRE) results in complete loss of *Dll1* expression outside of the tailbud (Hofmann *et al.*, 2004).

While historical and empirical evidence seem to point to the contrary, the possibility that CDX2 is acting as a repressor is not without precedent. CAD has been shown to repress the activity of *Abdominal-B* (*Abd-B*), the caudal-most *Hox* gene in *Drosophila* (Moreno and Morata, 1999), while xcad can suppress the expression of more rostral *hox* genes in *Xenopus* (Isaacs *et al.*, 1998). Additionally, murine CDX4 can restrict the posterior domain of *Hoxa5* expression through two CDX binding sites in a mesodermal enhancer domain (MES) downstream of the coding region (Tabaries *et al.*, 2005). Interestingly, one of these elements is the consensus sequence TTTATG, identical to the distal CDRE. Since identical TTTATG motifs also confer transcriptional activation on CDX target genes such as *Wnt3a*, *Cyp26a1*, and *T*

(Savory *et al.*, 2009a), this study indicates that co-factors may be involved in CDX repression versus induction of a given target gene. In this regard, P19 cells may not be an appropriate model to reflect transcriptional programs inherent to presomitic mesoderm.

As evidenced through the indistinguishable levels of *Dll1* transcript at E7.5 in *Cdx1/2* null mutants and controls (Figure 3.5 B), the presence of CDX2 alone is not sufficient to enhance *Dll1* activity. In this regard, previous work has shown that both LEF1 and TBX6 are important regulators of *Dll1* in the presomitic mesoderm and tailbud (Galceran *et al.*, 2004; Hofmann *et al.*, 2004; White and Chapman, 2005). In addition, we have previously shown that LEF1-CDX1 complexes can impact on transcription (Beland *et al.*, 2004), making LEF1 an attractive candidate for further investigation. However, preliminary experiments suggested that LEF1/βCAT and CDX2 only resulted in an additive effect on *Dll1* promoter activity (Figure 3.9 A).

TBX6, as mentioned previously, has a binding motif in the *Dll1* promoter that overlaps with the sequence of the distal CDRE. This particular T-box motif is essential for expression of *Dll1* in the tailbud (Hofmann *et al.*, 2004), and the physical proximity between the two response elements is suggestive of a functional interaction between TBX6 and CDX2. Indeed, the co-transfection of CDX2 with TBX6 gave rise to a synergistic activation of the *Dll1* promoter (Figure 3.9 B). Further elucidation of the TBX6 effect with a dose-seeking study determined the amounts of CDX2 and TBX6 expression vectors necessary to achieve the optimal induction of

luciferase activity, and recapitulated the synergistic activity observed in the pilot experiment at varying concentrations of expression vectors (Figure 3.9 C). To date, the mutated *Dll1* reporter constructs have not been tested in the presence of both CDX2 and TBX6, but future experiments will determine whether the inclusion of TBX6 has any impact on CDX-regulation of *Dll1* activity by transient transfection.

Although LEF1 and CDX2 did not synergize in my transfection assays, it is interesting to note that LEF1 synergizes with TBX6 on the mesodermal enhancer region of the *Dll1* promoter (Hofmann *et al.*, 2004). Since TBX6 and CDX2 synergized in the present experiments, it is also possible that LEF1 may interact with TBX6 and CDX2.

Another approach to address the issue of a suitable tissue culture model was to use a cell line more reflective of presomitic mesoderm. Wnt signaling is active in the presomitic and somitic mesoderm, and attempts were made to test *Dll1* expression in cells where Wnt signaling is constitutively active. Two different methodologies were selected to achieve this end. First, cells stably transfected to overexpress β-catenin were used for transient transfection analyses. Additionally, plates of P19 cells were treated with lithium chloride to antagonize GSK3 and stabilize cytoplasmic β-catenin (Klein and Melton, 1996). These experiments are still in the process of being optimized, and as such the findings remain inconclusive (data not shown).

Still other attempts have been made to differentiate P19 cells into a mesoderm-like lineage (Savage *et al.*, 2010). Aggregation of cells in the presence of DMSO has been shown to initiate the expression of an array of genes that are present in the primitive streak and early somite stage embryo *in vivo* (Buckingham, 2007). Following aggregation, cells were subsequently transfected with the *Dll1* reporter and CDX2 expression vectors. Transfection of the wildtype *Dll1* reporter in aggregated and non-aggregated controls has revealed greater induction in the differentiated samples, but it remains to be seen what effect aggregation will have on the overall trend of *Dll1* expression following mutation of the CDREs. Nevertheless, this assay as well as the constitutive expression of Wnt in P19 cells, present promising avenues to investigate the irregularities of the original transfection data.

Collectively, the findings from this report call for a new model of CDX activity. In addition to roles in vertebral patterning it is now evident that CDX members impact on earlier stages such as somitogenesis, potentially through direct regulation of genes like *Dll1* (Figure 4.1). Previous study from our lab has also identified *T* and *Wnt3a* as potential CDX targets (Savory *et al.*, 2009a). Interestingly, these genes also happen to be upstream regulators of *Dll1*, implying the potential for a concerted feed-forward mechanism. Given this, I performed experiments on additional upstream regulators of *Dll1* to assess their potential as CDX2 target genes (Supplementary Figures 1-5). Notably, ChIP experiments on *Lef1* (Supplementary Figure 2 A) and *Tbx6* (Supplementary Figure 5 A) suggested that CDX2 occupied

Figure 4.1: Proposed model for CDX2 regulation of somitic activity through *Dll1* and other members of the Wnt and Notch pathways.

This model suggests that CDX2 may act through *Dll1* to impact processes involved in the formation of somites. Previous study by our laboratory has identified *T* and *Wnt3a*, players upstream of *Dll1*, as likely CDX2 target genes, and evidence from preliminary experiments suggests that direct regulators of *Dll1* activity, *Lef1* and *Tbx6* may also be direct CDX2 targets. The potential for regulation by CDX2 at multiple levels of this pathway is consistent with CDX2 playing a central and integral role in the regulation of somitogenesis.

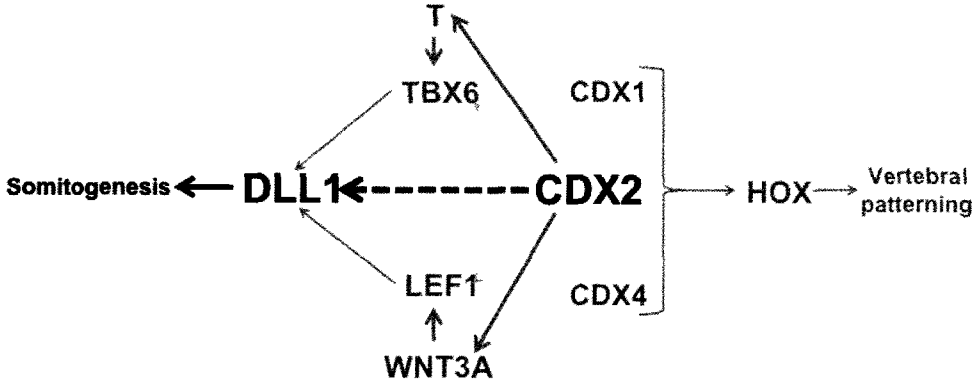
T
TBX6
CDX1
Somitogenesis
DLL1
CDX2
HOX
Vertebral patterning
LEF1
CDX4
WNT3A

Figure 4.1

the proximal promoter region of each of these genes. However, additional studies will be necessary to establish whether this occupation is functional, and how these interactions might integrate into a regulatory network.

4.4 Future directions

Given the number of preliminary experiments relating to the transient transfection of the *Dll1* promoter that have yet to be optimized and assessed, initial work will focus on completing these assays. Following the optimization of the various cell lines and experimental conditions, it will be necessary to test the series of mutated *Dll1* reporters in each of these systems. Additionally, given the finding of potential combinatorial regulation between CDX2 and TBX6, a reporter construct wherein the T-box binding site is mutated may shed further light on this interaction. Protein-protein interactions between TBX6 and CDX2 could also be explored. Given the synergistic interaction of LEF1 and TBX6 on the mesodermal enhancer region, it would also be interesting to assess interaction between CDX2, LEF1/β-CATENIN, and TBX6. Double chromatin immunoprecipitation (ChIP) experiments, where the purified substrate following initial immunoprecipitation is subsequently re-precipitated with the second antibody might be used to define co-occupation of *Dll1* by TBX6, CDX2 and/or LEF1 in embryos *in vivo*.

The most definitive way to assess the functional relevance of the *Dll1* CDRE is through transgenic reporter analysis. By mutating each of the CDX response

elements in the context of a *LacZ* transgenic reporter, it would be possible to evaluate whether these elements, and therefore CDX2 are critical to transcription of *Dll1*. Altered expression in the mutant constructs would validate not only the functionality of these, but also the functional nature of CDX2 on each of these motifs.

Finally, and in order to further validate the significance of a regulatory relationship between CDX2 and *Dll1*, I can investigate the authenticity of a genetic interaction between the two genes through the generation of mutant mouse lines. By creating $Cdx2^{+/-}Dll1^{+/lacZ}$ double heterozygous embryos, the appearance of a more penetrant phenotype compared to single heterozygous controls would be a good indication that the two genes interact in the same pathway. Functional complementarity between *Cdx2* and *Dll1* could also be tested through a rescue experiment. For instance, using transgenesis to drive *Dll1* expression in *Cdx1/2* null mutants would allow assessment of the ability of exogenous *Dll1* to rescue the somite defects inherent to the *Cdx1/2* null line.

In conclusion, considerable work remains to more fully characterize the relationship between CDX2 and *Dll1*. However, the possibility of genetic interaction between Notch and Cdx pathways is significant, and would contribute towards a better understanding of somitogenesis and other aspects of embryogenesis.

4.5 Summary

In this thesis I present evidence to suggest that members of the CDX family, and particularly CDX2, may be involved in the regulation of players in Wnt and Notch signaling. Additional characterization of one of these genes, *Dll1*, further suggests that this regulation may be direct. We had hypothesized that CDX members were able to modulate the process of somitogenesis through the regulation of Wnt and Notch genes, and the identification and characterization of *Dll1*, a Notch ligand known to play a critical role in somite boundary formation and polarity, supports the possibility of such a mechanism of action. *Dll1* expression was markedly downregulated in the absence of CDX players, and the proximal promoter region was shown to contain two putative and highly conserved CDX response elements. CDX2 was demonstrated to occupy the proximal promoter in the vicinity of these binding sites and to associate specifically with the identified motifs *in vitro*. These results are consistent with a potential direct regulatory interaction between CDX2 and *Dll1*, and preliminary functional analysis suggests that this may be mediated by the co-regulation of TBX6.

Future investigation should focus on the completion of functional analyses including the development of a transgenic model expressing mutated versions of one or both CDX binding motifs. This particular technique would allow us to confirm the functionality of the identified response elements as well as the requirement for CDX2 in *Dll1* expression *in vivo*. The outcome of this work may reveal a novel CDX target gene as well as an integral role for CDX transcription factors in the complex

regulatory network of somitogenesis. Verification of one or both of these functions could be invaluable to the field of CDX investigation as well as embryonic development as a whole.

CHAPTER 5

APPENDIX

Supplementary Figure 1: Semi-quantitative analysis of *Lef1* expression levels.

A: Semi-quantitative analysis of *Lef1* transcript levels between *Cdx1/2* null mutants and littermate controls. E8.5 embryos were harvested for cDNA, and samples were analysed using reverse-transcriptase PCR (RT-PCR). Amplification of β-actin was employed as a loading control. Quantification of amplicon levels was achieved using ImageJ software, and revealed a significant (*: $p = 0.008$) decrease in *Lef1* in the $Cdx1^{-/-}Cdx2^{-/-}$ mutants compared to littermate controls.

Bioinformatics and phylogenetic analysis of the *Lef1* promoter.

B: The two potential CDRE identified in the *Lef1* 5' proximal promoter region, using the Transcription Element Search System, were investigated for evolutionary conservation, using ClustalW2 software. Comparisons were made with highly related species such as the rat, as well as more evolutionary distant species like zebrafish.

A

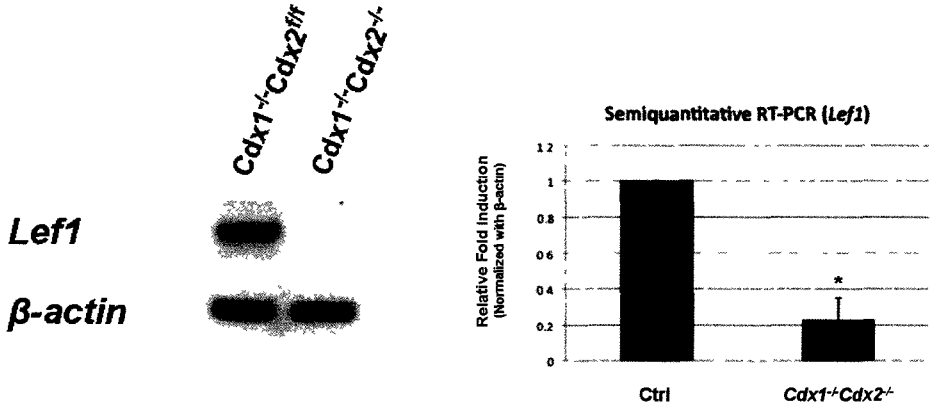

B

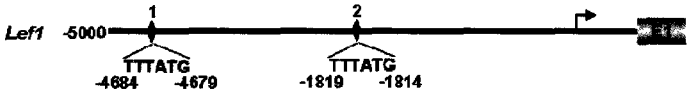

Distal CDRE (CDRE1), TTTATG:

```
Mouse       ---AGCAGGC--TGGAAGAAGACAATATTT-ATGGCTAAAGAAATTCAGC---CTCA-CA 344
Rat         ---AACATGC--TGGAAGAAGACAATATTT-ATGGCTGAAGAAATTCAGC---CTCA-CA 258
Human       ---AGCATGC--TGAAATAAGACAGTATTT-ACGGCTAAGGAAATTCGGC---TTCA-CA 107
Frog        CAAGAAGGTCTTTGAAAAAGGGCTGCACCTGCTGGATGATGAAGTCCAGAAAATTCTGGG 116
Zebrafish   ---CTCCAACCTCAATCAAACACACAGGAA-CCAGCTAATCAAACTCTTT---CTTGGTA 147
```

Proximal CDRE (CDRE2), TTTATG:

```
Mouse       TTTGTC---AAATTTATGCTAGCA--GGAGCTGTA-AACGTCTGAAACTATGTCCCTTTG 3226
Rat         TTTGTC---AAACGTATGCTAGCA--GGAGCTGTA-AACGTCTGAAAAGTCTGTCCCTTG 3223
Human       TGTTTTCCCATGTGTCTTTTAAGAATGGGGCTATA-AATGTCTGACACAGCTACAC---G 3191
Frog        TGTTTTCATGATCTAATCCATGCTATATATTTGTGCGACACTTAATGATATAACTTCACA 3213
Zebrafish   GTTCATAAAAAGGTTAGACTTTCAGAGGAACCAT----TATGTAAAGTAATACAGACTGG 3156
```

Supplementary Figure 1

Supplementary Figure 2: Examination of CDX2 binding to the *Lef1* promoter *in vivo* and *in vitro*.

A: Chromatin immunoprecipitation (ChIP) was used to analyse the ability of CDX2 to bind to the *Lef1* promoter *in vivo*. Specifically, the region containing the distal CDX response element was examined. The specificity of the CDX2 interaction was confirmed by the absence of a band or an amplicon of reduced intensity in several supplementary controls. Samples were precipitated without the CDX2 antibody (no Ab), in the absence of chromatin (mock), with rabbit pre-immune serum (PIS), as well as a non-specific antibody (αGAL4 (DBD)), all to account for background amplification.

B: EMSA was performed to assess the specificity of binding by CDX2 to the putative CDREs in the *Lef1* promoter. This assay was used to validate CDX2 binding to each of the putative response elements (lanes 10 and 18), and verified the specificity of results through a variety of controls. Incubation with GST protein alone was included to ensure that the binding component was the CDX2 portion of the fusion protein (lanes 9 and 17), and this was further confirmed by the observation of a "supershift" (SS, lanes 11 and 19) upon incubation with anti-CDX2 antibody. A mutated version of the binding motif was employed to confirm that the sequence in question was responsible for CDX2-binding (lanes 12 and 20), and a 200 fold excess of a radioinert self-competitor (lanes 14 and 22) as well as a known CDX target (lanes 13 and 21) and a non-CDX motif RARE (lanes 15 and 23) were included as further validation of binding specificity. CDREs in the *Dll1* promoter were compared with a characterized CDRE from *Hoxb8*, in order to contrast the pattern and affinity of CDX2 association (lanes 1-7).

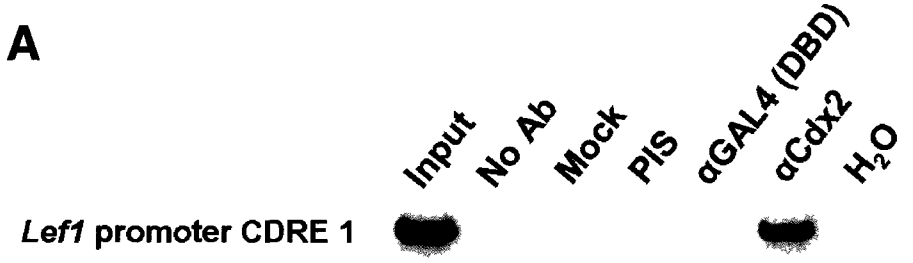

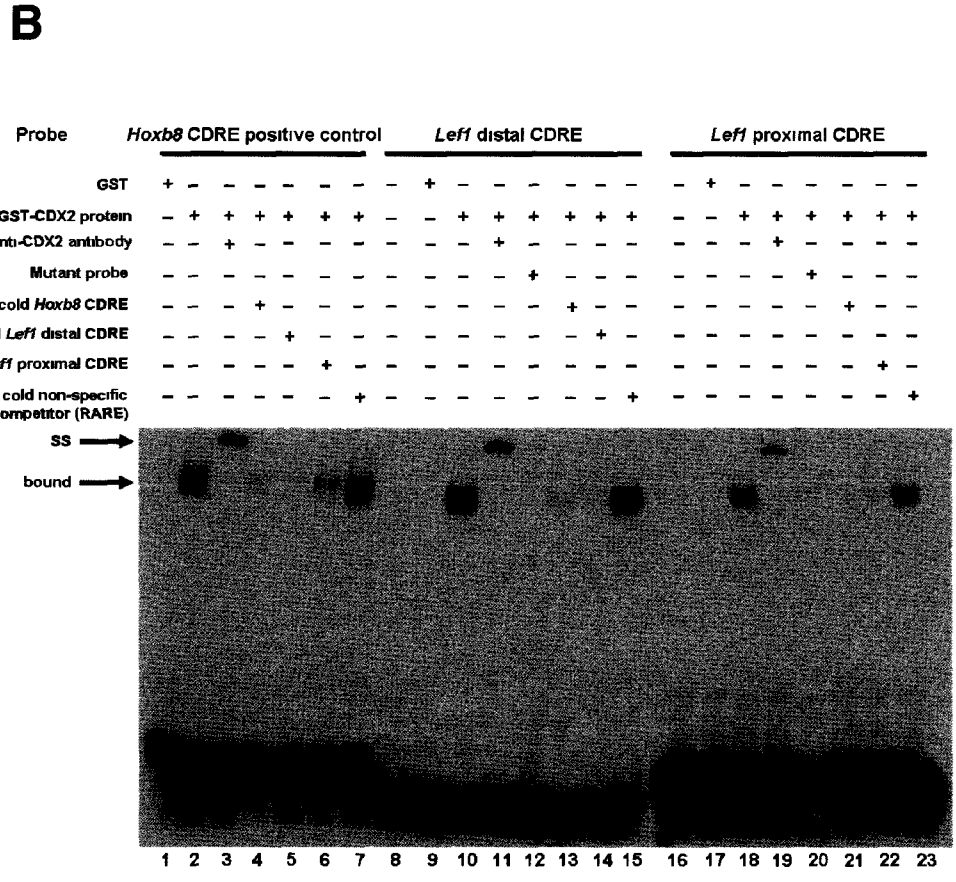

Supplementary Figure 2

Supplementary Figure 3: Analysis of *Tbx6* expression by whole mount *in situ* hybridization.

A: Whole mount *in situ* hybridization was performed on *Cdx1/2* null embryos and their littermate controls, as well as CD-1 wildtype embryos at E8.5. Individual embryos are depicted in dorsal (top) and lateral (view).

B: Group pictures with dorsal (top) and lateral (bottom) views of *Tbx6* transcript levels in wildtype (CD-1), control ($Cdx1^{-/-}Cdx2^{f/f}$) and mutant ($Cdx1^{-/-}Cdx2^{-/-}$) embryos.

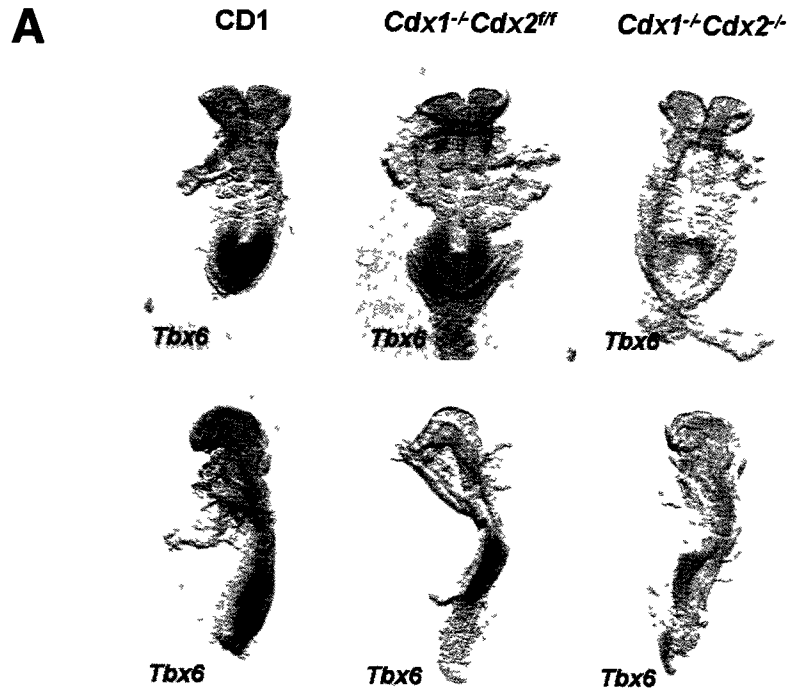

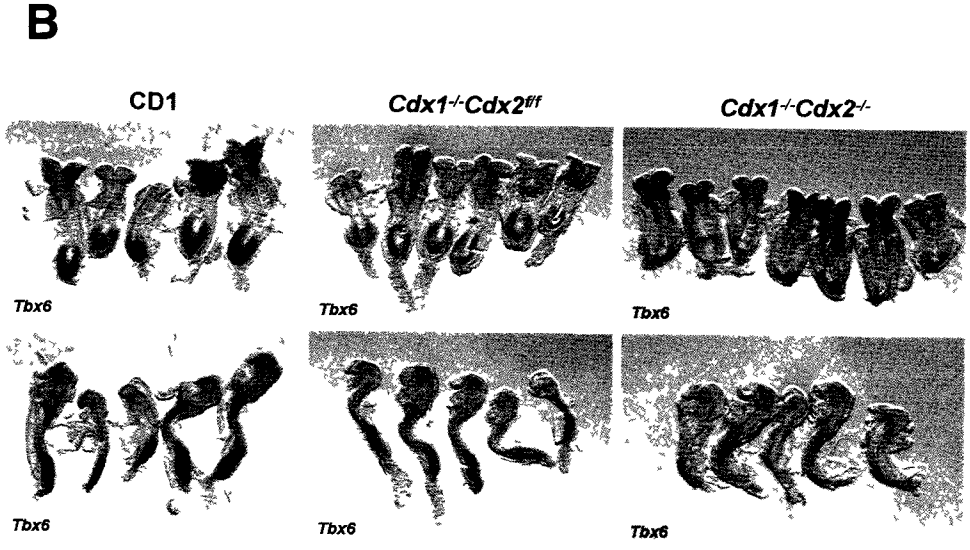

Supplementary Figure 3

Supplementary Figure 4: Semi-quantitative analysis of *Tbx6* expression levels.

A: Semi-quantitative analysis of *Tbx6* transcript levels between *Cdx1/2* null mutants and littermate controls. E8.5 embryos were harvested for cDNA, and samples were analysed using reverse-transcriptase PCR (RT-PCR). Amplification of β-actin was used as a loading control. Quantification was achieved using ImageJ software, and revealed a significant (*: $p = 0.004$) reduction in *Tbx6* transcript in $Cdx1^{-/-}Cdx2^{-/-}$ mutants compared to littermate controls.

Bioinformatics and phylogenetic analysis of the *Tbx6* promoter.

B: The two potential CDRE identified in the *Tbx6* 5' proximal promoter region, using the Transcription Element Search System, were investigated for evolutionary conservation, using ClustalW2 software. Comparisons were made with highly related species such as the rat, as well as more evolutionary distant species like zebrafish.

A

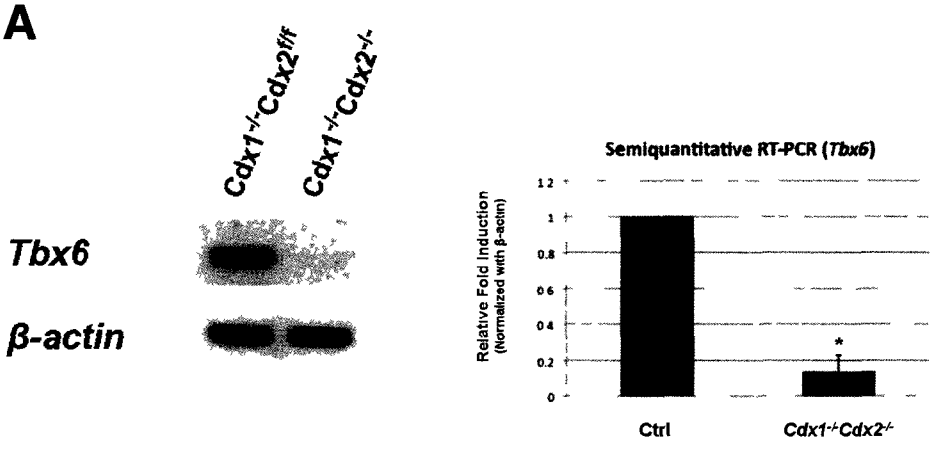

B

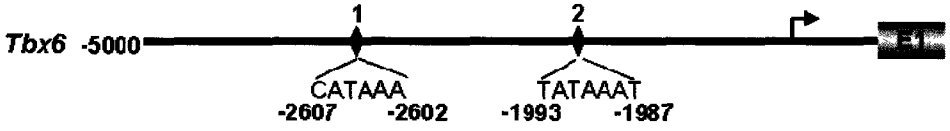

C

Distal CDRE (CDRE1), CATAAA:

```
Mouse        T A AAC TCAA T  TAT---C TAC TGGCAT GA CATAAAG TAC AC TGCA 413
Rat          TTA AAC TC--TC TAT---C TCA TTGCAT GCA CATTAAC TAC T TGC A 641
Human        T A TA-  TTAATC TAGCA T-T T-GGAGGC GAGG  TG A----TCA AAG T- 375
Zebrafish    TCTGATCCACGGLAAAAAAAACACATCATTCG TCTTGAGCATATTCACATGCCC 403
                **  * **       *  *       *    *   *    *  *
```

Proximal CDRE (CDRE2), TATAAA:

```
Mouse        AAAAACAAAACAAAAAAAGAGCAAGCAGATATCGTCGGTTTATAAACGCG--TAGATATA 1025
Rat          ----------------------------TACCGTGGATTTATAAACGGCGTAGATTTA 1078
Human        ----------------------------TTTCAAAACCAAACAAACAAA--AAAACCTC 939
Zebrafish    TCAAATTTLGCT TACTCTATTTGAC CTTATCCTAACTTATTTTCCTAGATAAGCTTTA 1046
                                          *                  *   *
```

Supplementary Figure 4

Supplementary Figure 5: Analysis of CDX2 binding to the *Tbx6* promoter *in vivo* and *in vitro*.

A: Chromatin immunoprecipitation (ChIP) was performed on the *Tbx6* promoter in order to validate the binding of CDX2 to the region containing the two CDX response elements *in vivo*. Due to the proximity of the binding motifs, a genomic region was selected in-between the two sites. The specificity of the CDX2 interaction was confirmed by the absence of a band or an amplicon of reduced intensity in several supplementary controls. Samples were precipitated without the CDX2 antibody (no Ab), in the absence of chromatin (mock), with rabbit pre-immune serum (PIS), as well as a non-specific antibody (αGAL4 (DBD)), all to account for background amplification.

B: EMSA was performed to assess the specificity of binding by CDX2 to the putative CDREs in the *Tbx6* promoter. This assay was used to validate CDX2 binding to each of the putative response elements (lanes 10 and 18), and verified the specificity of results through a variety of controls. Incubation with GST protein alone was included to ensure that the binding component was the CDX2 portion of the fusion protein (lanes 9 and 17), and this was further confirmed by the observation of a "supershift" (SS, lanes 11 and 19) upon incubation with anti-CDX2 antibody. A mutated version of the binding motif was employed to confirm that the sequence in question was responsible for CDX2-binding (lanes 12 and 20), and a 200 fold excess of a radioinert self-competitor (lanes 14 and 22) as well as a known CDX target (lanes 13 and 21) and a non-CDX motif RARE (lanes 15 and 23) were included as further validation of binding specificity. CDREs in the *Dll1* promoter were compared with a characterized CDRE from *Hoxb8*, in order to contrast the pattern and affinity of CDX2 association (lanes 1-7).

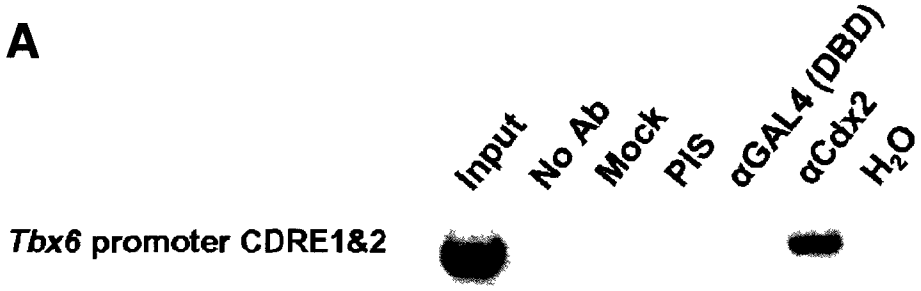

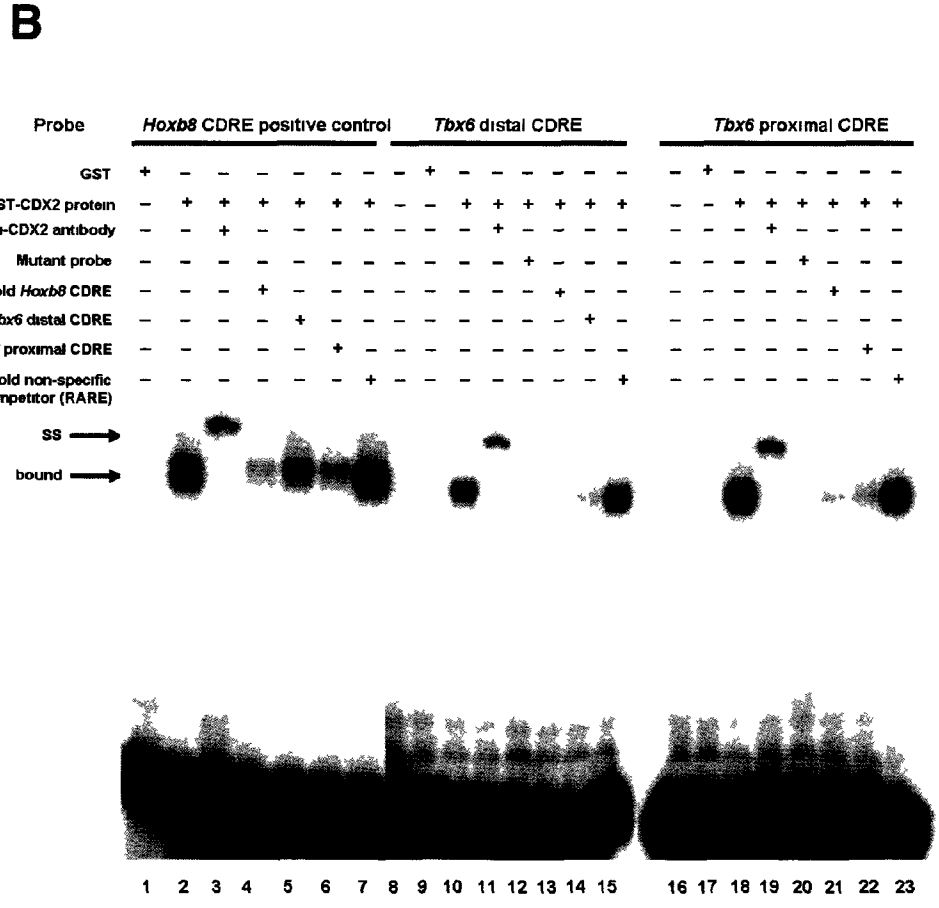

Supplementary Figure 5

REFERENCES

Ahimou, F., Mok, L.P., Bardot, B., and Wesley, C. (2004). The adhesion force of Notch with Delta and the rate of Notch signaling. J. Cell Biol. *167,* 1217-1229.

Alexander, T., Nolte, C., and Krumlauf, R. (2009). Hox genes and segmentation of the hindbrain and axial skeleton. Annu. Rev. Cell Dev. Biol. *25,* 431-456.

Angers, S., and Moon, R.T. (2009). Proximal events in Wnt signal transduction. Nat. Rev. Mol. Cell Biol. *10,* 468-477.

Arce, L., Yokoyama, N.N., and Waterman, M.L. (2006). Diversity of LEF/TCF action in development and disease. Oncogene *25,* 7492-7504.

Aulehla, A., Wehrle, C., Brand-Saberi, B., Kemler, R., Gossler, A., Kanzler, B., and Herrmann, B.G. (2003). Wnt3a plays a major role in the segmentation clock controlling somitogenesis. Dev Cell *4,* 395-406.

Aulehla, A., Wiegraebe, W., Baubet, V., Wahl, M.B., Deng, C., Taketo, M., Lewandoski, M., and Pourquie, O. (2008). A beta-catenin gradient links the clock and wavefront systems in mouse embryo segmentation. Nat Cell Biol *10,* 186-93.

Baig-Lewis, S., Peterson-Nedry, W., and Wehrli, M. (2007). Wingless/Wnt signal transduction requires distinct initiation and amplification steps that both depend on Arrow/LRP. Dev. Biol. *306,* 94-111.

Beck, F., Erler, T., Russell, A., and James, R. (1995). Expression of Cdx-2 in the mouse embryo and placenta: possible role in patterning of the extra-embryonic membranes. Dev. Dyn. *204,* 219-227.

Beckers, J., Caron, A., Hrabe de Angelis, M., Hans, S., Campos-Ortega, J.A., and Gossler, A. (2000a). Distinct regulatory elements direct delta1 expression in the nervous system and paraxial mesoderm of transgenic mice. Mech Dev *95,* 23-34.

Beckers, J., Schlautmann, N., and Gossler, A. (2000b). The mouse rib-vertebrae mutation disrupts anterior-posterior somite patterning and genetically interacts with a Delta1 null allele. Mech Dev *95,* 35-46.

Beddington, R.S., and Robertson, E.J. (1998). Anterior patterning in mouse. Trends Genet. *14,* 277-284.

Beland, M., Pilon, N., Houle, M., Oh, K., Sylvestre, J.R., Prinos, P., and Lohnes, D. (2004). Cdx1 autoregulation is governed by a novel Cdx1-LEF1 transcription complex. Mol Cell Biol *24,* 5028-38.

Bettenhausen, B., Hrabe de Angelis, M., Simon, D., Guenet, J.L., and Gossler, A. (1995). Transient and restricted expression during mouse embryogenesis of Dll1, a murine gene closely related to Drosophila Delta. Development *121,* 2407-18.

Binnerts, M.E., Kim, K.A., Bright, J.M., Patel, S.M., Tran, K., Zhou, M., Leung, J.M., Liu, Y., Lomas, W.E.,3rd, Dixon, M., *et al.* (2007). R-Spondin1 regulates Wnt signaling by inhibiting internalization of LRP6. Proc. Natl. Acad. Sci. U. S. A. *104,* 14700-14705.

Bjarnadottir, T.K., Gloriam, D.E., Hellstrand, S.H., Kristiansson, H., Fredriksson, R., and Schioth, H.B. (2006). Comprehensive repertoire and phylogenetic analysis of the G protein-coupled receptors in human and mouse. Genomics *88,* 263-273.

Boffelli, D., Nobrega, M.A., and Rubin, E.M. (2004). Comparative genomics at the vertebrate extremes. Nat. Rev. Genet. *5,* 456-465.

Bray, S.J. (2006). Notch signalling: a simple pathway becomes complex. Nat. Rev. Mol. Cell Biol. *7,* 678-689.

Buckingham, M. (2007). Skeletal muscle progenitor cells and the role of Pax genes. C. R. Biol. *330,* 530-533.

Cambray, N., and Wilson, V. (2007). Two distinct sources for a population of maturing axial progenitors. Development *134,* 2829-2840.

Chapman, D.L., Agulnik, I., Hancock, S., Silver, L.M., and Papaioannou, V.E. (1996). Tbx6, a mouse T-Box gene implicated in paraxial mesoderm formation at gastrulation. Dev Biol *180,* 534-42.

Chapman, D.L., and Papaioannou, V.E. (1998). Three neural tubes in mouse embryos with mutations in the T-box gene Tbx6. Nature *391,* 695-697.

Charite, J., de Graaff, W., Consten, D., Reijnen, M.J., Korving, J., and Deschamps, J. (1998). Transducing positional information to the Hox genes: critical interaction of cdx gene products with position-sensitive regulatory elements. Development *125,* 4349-58.

Chawengsaksophak, K., de Graaff, W., Rossant, J., Deschamps, J., and Beck, F. (2004). Cdx2 is essential for axial elongation in mouse development. Proc. Natl. Acad. Sci. U. S. A. *101,* 7641-7645.

Chawengsaksophak, K., James, R., Hammond, V.E., Kontgen, F., and Beck, F. (1997). Homeosis and intestinal tumours in Cdx2 mutant mice. Nature *386,* 84-7.

Clevers, H. (2006). Wnt/beta-catenin signaling in development and disease. Cell *127,* 469-80.

Cordle, J., Johnson, S., Tay, J.Z., Roversi, P., Wilkin, M.B., de Madrid, B.H., Shimizu, H., Jensen, S., Whiteman, P., Jin, B., *et al.* (2008). A conserved face of the Jagged/Serrate DSL domain is involved in Notch trans-activation and cis-inhibition. Nat. Struct. Mol. Biol. *15,* 849-857.

Core, N., Caubit, X., Metchat, A., Boned, A., Djabali, M., and Fasano, L. (2007). Tshz1 is required for axial skeleton, soft palate and middle ear development in mice. Dev. Biol. *308,* 407-420.

Cornier A.S., Staehling-Hampton K., Delventhal K.M., Saga Y., Caubet J.F., Ellard S., Young E., Carlo S.E., Emans J.B., Turnpenny P.D., Pourquié O. (2008). Mutations in the MESP2 gene cause Spondylothoracic Dysostosis/Jarcho-Levin syndrome. Am J Hum Genet. *82,* 1334–41.

Davidson, A.J., Ernst, P., Wang, Y., Dekens, M.P., Kingsley, P.D., Palis, J., Korsmeyer, S.J., Daley, G.Q., and Zon, L.I. (2003). Cdx4 Mutants Fail to Specify Blood Progenitors and can be Rescued by Multiple Hox Genes. Nature *425,* 300-306.

Davidson, G., Wu, W., Shen, J., Bilic, J., Fenger, U., Stannek, P., Glinka, A., and Niehrs, C. (2005). Casein kinase 1 gamma couples Wnt receptor activation to cytoplasmic signal transduction. Nature *438,* 867-872.

Dearolf, C.R., Topol, J., and Parker, C.S. (1989). The caudal gene product is a direct activator of fushi tarazu transcription during Drosophila embryogenesis. Nature *341,* 340-343.

Dequeant, M.L., Glynn, E., Gaudenz, K., Wahl, M., Chen, J., Mushegian, A., and Pourquie, O. (2006). A complex oscillating network of signaling genes underlies the mouse segmentation clock. Science *314,* 1595-8.

Dequeant, M.L., and Pourquie, O. (2008). Segmental patterning of the vertebrate embryonic axis. Nat. Rev. Genet. *9,* 370-382.

D'Souza, B., Miyamoto, A., and Weinmaster, G. (2008). The many facets of Notch ligands. Oncogene *27,* 5148-67.

Duboule, D. (1998). Vertebrate hox gene regulation: clustering and/or colinearity? Curr. Opin. Genet. Dev. *8,* 514-518.

Duboule, D., and Dolle, P. (1989). The structural and functional organization of the murine HOX gene family resembles that of Drosophila homeotic genes. EMBO J. *8,* 1497-1505.

Dubrulle, J., and Pourquie, O. (2004). Coupling segmentation to axis formation. Development *131,* 5783-5793.

Dunwoodie, S.L., Henrique, D., Harrison, S.M., and Beddington, R.S. (1997). Mouse Dll3: a novel divergent Delta gene which may complement the function of other Delta homologues during early pattern formation in the mouse embryo. Development *124,* 3065-3076.

Duprey, P., Chowdhury, K., Dressler, G.R., Balling, R., Simon, D., Guenet, J.L., and Gruss, P. (1988). A mouse gene homologous to the Drosophila gene caudal is expressed in epithelial cells from the embryonic intestine. Genes Dev. *2,* 1647-1654.

Feller, J., Schneider, A., Schuster-Gossler, K., and Gossler, A. (2008). Noncyclic Notch activity in the presomitic mesoderm demonstrates uncoupling of somite compartmentalization and boundary formation. Genes Dev *22,* 2166-71.

Ferrier, D.E., and Holland, P.W. (2001). Ancient origin of the Hox gene cluster. Nat. Rev. Genet. *2,* 33-38.

Fortini, M.E. (2009). Notch signaling: the core pathway and its posttranslational regulation. Dev. Cell. *16,* 633-647.

Freund, J.N., Domon-Dell, C., Kedinger, M., and Duluc, I. (1998). The Cdx-1 and Cdx-2 homeobox genes in the intestine. Biochem. Cell Biol. *76,* 957-969.

Fryer, C.J., Lamar, E., Turbachova, I., Kintner, C., and Jones, K.A. (2002). Mastermind mediates chromatin-specific transcription and turnover of the Notch enhancer complex. Genes Dev. *16,* 1397-1411.

Funakoshi, S., Ezaki, T., Kong, J., Guo, R.J., and Lynch, J.P. (2008). Repression of the desmocollin 2 gene expression in human colon cancer cells is relieved by the homeodomain transcription factors Cdx1 and Cdx2. Mol. Cancer. Res. *6,* 1478-1490.

Galceran, J., Farinas, I., Depew, M.J., Clevers, H., and Grosschedl, R. (1999). Wnt3a-/--like phenotype and limb deficiency in Lef1(-/-)Tcf1(-/-) mice. Genes Dev *13,* 709-17.

Galceran, J., Sustmann, C., Hsu, S.C., Folberth, S., and Grosschedl, R. (2004). LEF1-mediated regulation of Delta-like1 links Wnt and Notch signaling in somitogenesis. Genes Dev *18,* 2718-23.

Gallet, A., Angelats, C., Erkner, A., Charroux, B., Fasano, L., and Kerridge, S. (1999). The C-terminal domain of armadillo binds to hypophosphorylated teashirt to modulate wingless signalling in Drosophila. EMBO J. *18,* 2208-2217.

Gallet, A., Erkner, A., Charroux, B., Fasano, L., and Kerridge, S. (1998). Trunk-specific modulation of wingless signalling in Drosophila by teashirt binding to armadillo. Curr. Biol. *8,* 893-902.

Gamer, L.W., and Wright, C.V. (1993). Murine Cdx-4 bears striking similarities to the Drosophila caudal gene in its homeodomain sequence and early expression pattern. Mech. Dev. *43,* 71-81.

Geffers, I., Serth, K., Chapman, G., Jaekel, R., Schuster-Gossler, K., Cordes, R., Sparrow, D.B., Kremmer, E., Dunwoodie, S.L., Klein, T., and Gossler, A. (2007). Divergent functions and distinct localization of the Notch ligands DLL1 and DLL3 in vivo. J Cell Biol *178,* 465-76.

Ghysen, A., and Dambly-Chaudiere, C. (1988). From DNA to form: the achaete-scute complex. Genes Dev. *2,* 495-501.

Gomez, C., Ozbudak, E.M., Wunderlich, J., Baumann, D., Lewis, J., and Pourquie, O. (2008). Control of segment number in vertebrate embryos. Nature *454,* 335-9.

Gordon, W.R., Arnett, K.L., and Blacklow, S.C. (2008). The molecular logic of Notch signaling--a structural and biochemical perspective. J. Cell. Sci. *121,* 3109-3119.

Grainger, S., Savory, J.G., and Lohnes, D. (2009). Cdx2 regulates patterning of the intestinal epithelium. Dev. Biol. *339,* 155-165.

Grant, S.F., Thorleifsson, G., Reynisdottir, I., Benediktsson, R., Manolescu, A., Sainz, J., Helgason, A., Stefansson, H., Emilsson, V., Helgadottir, A., *et al.* (2006). Variant of transcription factor 7-like 2 (TCF7L2) gene confers risk of type 2 diabetes. Nat. Genet. *38,* 320-323.

Gridley, T. (2006). The long and short of it: somite formation in mice. Dev Dyn *235,* 2330-6.

Gridley, T. (2003). Notch signaling and inherited disease syndromes. Hum. Mol. Genet. *12 Spec No 1,* R9-13.

Guazzi, S., Lonigro, R., Pintonello, L., Boncinelli, E., Di Lauro, R., and Mavilio, F. (1994). The thyroid transcription factor-1 gene is a candidate target for regulation by Hox proteins. EMBO J. *13,* 3339-3347.

Hamilton, D.L., and Abremski, K. (1984). Site-specific recombination by the bacteriophage P1 lox-Cre system. Cre-mediated synapsis of two lox sites. J. Mol. Biol. *178,* 481-486.

Hans, S., and Campos-Ortega, J.A. (2002). On the organisation of the regulatory region of the zebrafish deltaD gene. Development *129,* 4773-4784.

Hatzis, P., van der Flier, L.G., van Driel, M.A., Guryev, V., Nielsen, F., Denissov, S., Nijman, I.J., Koster, J., Santo, E.E., Welboren, W., *et al.* (2008). Genome-wide pattern

of TCF7L2/TCF4 chromatin occupancy in colorectal cancer cells. Mol. Cell. Biol. *28,* 2732-2744.

Hausmann, G., Banziger, C., and Basler, K. (2007). Helping Wingless take flight: how WNT proteins are secreted. Nat. Rev. Mol. Cell Biol. *8,* 331-336.

Heitzler, P., Bourouis, M., Ruel, L., Carteret, C., and Simpson, P. (1996). Genes of the Enhancer of split and achaete-scute complexes are required for a regulatory loop between Notch and Delta during lateral signalling in Drosophila. Development *122,* 161-171.

Hofmann, M., Schuster-Gossler, K., Watabe-Rudolph, M., Aulehla, A., Herrmann, B.G., and Gossler, A. (2004). WNT signaling, in synergy with T/TBX6, controls Notch signaling by regulating Dll1 expression in the presomitic mesoderm of mouse embryos. Genes Dev *18,* 2712-7.

Houle, M., Prinos, P., Iulianella, A., Bouchard, N., and Lohnes, D. (2000). Retinoic acid regulation of Cdx1: an indirect mechanism for retinoids and vertebral specification. Mol Cell Biol *20,* 6579-86.

Houle, M., Sylvestre, J.R., and Lohnes, D. (2003). Retinoic acid regulates a subset of Cdx1 function in vivo. Development *130,* 6555-67.

Hrabe de Angelis, M., McIntyre, J.,2nd, and Gossler, A. (1997). Maintenance of somite borders in mice requires the Delta homologue DII1. Nature *386,* 717-21.

Huang, H., and He, X. (2008). Wnt/beta-catenin signaling: new (and old) players and new insights. Curr. Opin. Cell Biol. *20,* 119-125.

Iimura, T., and Pourquie, O. (2007). Hox genes in time and space during vertebrate body formation. Dev Growth Differ *49,* 265-75.

Isaacs, H.V., Pownall, M.E., and Slack, J.M. (1998). Regulation of Hox gene expression and posterior development by the Xenopus caudal homologue Xcad3. EMBO J *17,* 3413-27.

Jacobsen, T.L., Brennan, K., Arias, A.M., and Muskavitch, M.A. (1998). Cis-interactions between Delta and Notch modulate neurogenic signalling in Drosophila. Development *125,* 4531-4540.

James, R., and Kazenwadel, J. (1991). Homeobox gene expression in the intestinal epithelium of adult mice. J. Biol. Chem. *266,* 3246-3251.

Kageyama, R., Masamizu, Y., and Niwa, Y. (2007). Oscillator mechanism of Notch pathway in the segmentation clock. Dev. Dyn. *236,* 1403-1409.

Katanaev, V.L., Solis, G.P., Hausmann, G., Buestorf, S., Katanayeva, N., Schrock, Y., Stuermer, C.A., and Basler, K. (2008). Reggie-1/flotillin-2 promotes secretion of the long-range signalling forms of Wingless and Hedgehog in Drosophila. EMBO J. *27,* 509-521.

Kimelman, D., and Xu, W. (2006). Beta-Catenin Destruction Complex: Insights and Questions from a Structural Perspective. Oncogene *25,* 7482-7491.

Kinder, S.J., Tsang, T.E., Quinlan, G.A., Hadjantonakis, A.K., Nagy, A., and Tam, P.P. (1999). The orderly allocation of mesodermal cells to the extraembryonic structures and the anteroposterior axis during gastrulation of the mouse embryo. Development *126,* 4691-4701.

Kioussi, C., Briata, P., Baek, S.H., Rose, D.W., Hamblet, N.S., Herman, T., Ohgi, K.A., Lin, C., Gleiberman, A., Wang, J., *et al.* (2002). Identification of a Wnt/Dvl/beta-Catenin --> Pitx2 pathway mediating cell-type-specific proliferation during development. Cell *111,* 673-685.

Klein, P.S., and Melton, D.A. (1996). A molecular mechanism for the effect of lithium on development. Proc. Natl. Acad. Sci. U. S. A. *93,* 8455-8459.

Knittel, T., Kessel, M., Kim, M.H., and Gruss, P. (1995). A conserved enhancer of the human and murine Hoxa-7 gene specifies the anterior boundary of expression during embryonal development. Development *121,* 1077-1088.

Komatsu, H., Chao, M.Y., Larkins-Ford, J., Corkins, M.E., Somers, G.A., Tucey, T., Dionne, H.M., White, J.Q., Wani, K., Boxem, M., and Hart, A.C. (2008). OSM-11 facilitates LIN-12 Notch signaling during Caenorhabditis elegans vulval development. PLoS Biol. *6,* e196.

Kopan, R., and Ilagan, M.X. (2009). The canonical Notch signaling pathway: unfolding the activation mechanism. Cell *137,* 216-233.

Kovall, R.A. (2008). More complicated than it looks: assembly of Notch pathway transcription complexes. Oncogene *27,* 5099-109.

Krebs, L.T., Deftos, M.L., Bevan, M.J., and Gridley, T. (2001). The Nrarp gene encodes an ankyrin-repeat protein that is transcriptionally regulated by the notch signaling pathway. Dev Biol *238,* 110-9.

Krumlauf, R. (1994). Hox genes in vertebrate development. Cell *78,* 191-201.

Kunath, T., Gish, G., Lickert, H., Jones, N., Pawson, T., and Rossant, J. (2003). Transgenic RNA interference in ES cell-derived embryos recapitulates a genetic null phenotype. Nat. Biotechnol. *21,* 559-561.

Lai, E.C. (2004). Notch signaling: control of cell communication and cell fate. Development *131,* 965-973.

Larkin, M.A., Blackshields, G., Brown, N.P., Chenna, R., McGettigan, P.A., McWilliam, H., Valentin, F., Wallace, I.M., Wilm, A., Lopez, R., *et al.* (2007). Clustal W and Clustal X version 2.0. Bioinformatics *23,* 2947-2948.

Leyns, L., Bouwmeester, T., Kim, S.H., Piccolo, S., and De Robertis, E.M. (1997). Frzb-1 is a secreted antagonist of Wnt signaling expressed in the Spemann organizer. Cell *88,* 747-756.

Lin, X. (2004). Functions of heparan sulfate proteoglycans in cell signaling during development. Development *131,* 6009-6021.

Logan, C.Y., and Nusse, R. (2004). The Wnt signaling pathway in development and disease. Annu. Rev. Cell Dev. Biol. *20,* 781-810.

Lohnes, D. (2003). The Cdx1 homeodomain protein: an integrator of posterior signaling in the mouse. Bioessays *25,* 971-80.

Louvi, A., Arboleda-Velasquez, J.F., and Artavanis-Tsakonas, S. (2006). CADASIL: a critical look at a Notch disease. Dev. Neurosci. *28,* 5-12.

MacDonald, B.T., Tamai, K., and He, X. (2009). Wnt/beta-catenin signaling: components, mechanisms, and diseases. Dev. Cell. *17,* 9-26.

Macdonald, P.M., and Struhl, G. (1986). A molecular gradient in early Drosophila embryos and its role in specifying the body pattern. Nature *324,* 537-45.

Machka, C., Kersten, M., Zobawa, M., Harder, A., Horsch, M., Halder, T., Lottspeich, F., Hrabe de Angelis, M., and Beckers, J. (2005). Identification of Dll1 (Delta1) target genes during mouse embryogenesis using differential expression profiling. Gene Expr Patterns *6,* 94-101.

Margalit, Y., Yarus, S., Shapira, E., Gruenbaum, Y., and Fainsod, A. (1993). Isolation and characterization of target sequences of the chicken CdxA homeobox gene. Nucleic Acids Res. *21,* 4915-4922.

Maruhashi, M., Van De Putte, T., Huylebroeck, D., Kondoh, H., and Higashi, Y. (2005). Involvement of SIP1 in positioning of somite boundaries in the mouse embryo. Dev. Dyn. *234,* 332-338.

McBurney, M.W. (1993). P19 embryonal carcinoma cells. Int. J. Dev. Biol. *37,* 135-140.

McGinnis, W., and Krumlauf, R. (1992). Homeobox genes and axial patterning. Cell *68,* 283-302.

Merika, M., and Orkin, S.H. (1995). Functional synergy and physical interactions of the erythroid transcription factor GATA-1 with the Kruppel family proteins Sp1 and EKLF. Mol. Cell. Biol. *15,* 2437-2447.

Meyer, B.I., and Gruss, P. (1993). Mouse Cdx-1 expression during gastrulation. Development *117,* 191-203.

Mitiku, N., and Baker, J.C. (2007). Genomic analysis of gastrulation and organogenesis in the mouse. Dev. Cell. *13,* 897-907.

Mlodzik, M., Fjose, A., and Gehring, W.J. (1985). Isolation of caudal, a Drosophila homeo box-containing gene with maternal expression, whose transcripts form a concentration gradient at the pre-blastoderm stage. EMBO J *4,* 2961-2969.

Mlodzik, M., and Gehring, W.J. (1987). Expression of the caudal gene in the germ line of Drosophila: formation of an RNA and protein gradient during early embryogenesis. Cell *48,* 465-78.

Moreno, E., and Morata, G. (1999). Caudal is the Hox gene that specifies the most posterior Drosophile segment. Nature *400,* 873-877.

Morgan, T.H., and Bridges, C.B. (1916). Sex-linked inheritance in *Drosophila*. Publs Carnegie Instn *237,* 1-88.

Nagy, A. (2000). Cre recombinase: the universal reagent for genome tailoring. Genesis *26,* 99-109.

Nagy, A., Gocza, E., Diaz, E.M., Prideaux, V.R., Ivanyi, E., Markkula, M., and Rossant, J. (1990). Embryonic stem cells alone are able to support fetal development in the mouse. Development *110,* 815-21.

Nordeen, S.K. (1988). Luciferase reporter gene vectors for analysis of promoters and enhancers. BioTechniques *6,* 454-458.

Oellers, N., Dehio, M., and Knust, E. (1994). bHLH proteins encoded by the Enhancer of split complex of Drosophila negatively interfere with transcriptional activation mediated by proneural genes. Mol. Gen. Genet. *244,* 465-473.

Olivera-Martinez, I., and Storey, K.G. (2007). Wnt signals provide a timing mechanism for the FGF-retinoid differentiation switch during vertebrate body axis extension. Development *134,* 2125-35.

Panakova, D., Sprong, H., Marois, E., Thiele, C., and Eaton, S. (2005). Lipoprotein particles are required for Hedgehog and Wingless signalling. Nature *435,* 58-65.
Papaioannou, V.E. (2001). T-box genes in development: from hydra to humans. Int. Rev. Cytol. *207,* 1-70.

Petcherski, A.G., and Kimble, J. (2000). LAG-3 is a putative transcriptional activator in the C. elegans Notch pathway. Nature *405,* 364-368.

Phng, L.K., Potente, M., Leslie, J.D., Babbage, J., Nyqvist, D., Lobov, I., Ondr, J.K., Rao, S., Lang, R.A., Thurston, G., and Gerhardt, H. (2009). Nrarp coordinates endothelial Notch and Wnt signaling to control vessel density in angiogenesis. Dev. Cell. *16,* 70-82.

Pilon, N., Oh, K., Sylvestre, J.R., Bouchard, N., Savory, J., and Lohnes, D. (2006). Cdx4 is a direct target of the canonical Wnt pathway. Dev Biol *289,* 55-63.

Pilon, N., Oh, K., Sylvestre, J.R., Savory, J.G., and Lohnes, D. (2007). Wnt signaling is a key mediator of Cdx1 expression in vivo. Development *134,* 2315-23.

Polakis, P. (2007). The many ways of Wnt in cancer. Curr. Opin. Genet. Dev. *17,* 45-51.

Poulson, D.F. (1940). The effects of certain X-chromosome deficiencies on the embryonic development of *Drosophila melanogaster.* J. Exp. Zool. *83,* 271-325.

Prinos, P., Joseph, S., Oh, K., Meyer, B.I., Gruss, P., and Lohnes, D. (2001). Multiple pathways governing Cdx1 expression during murine development. Dev Biol *239,* 257-69.

Rao, P.K., Dorsch, M., Chickering, T., Zheng, G., Jiang, C., Goodearl, A., Kadesch, T., and McCarthy, S. (2000). Isolation and characterization of the notch ligand delta4. Exp. Cell Res. *260,* 379-386.

Rebay, I., Fleming, R.J., Fehon, R.G., Cherbas, L., Cherbas, P., and Artavanis-Tsakonas, S. (1991). Specific EGF repeats of Notch mediate interactions with Delta and Serrate: implications for Notch as a multifunctional receptor. Cell *67,* 687-699.

Rossant, J., and Spence, A. (1998). Chimeras and mosaics in mouse mutant analysis. Trends Genet. *14,* 358-363.

Rozante, L.C., Gubitoso, M.D., and Matioli, S.R. (2007). A framework for modeling of juxtacrine signaling systems. Genet. Mol. Res. *6,* 821-845.

Rubio-Aliaga, I., Przemeck, G.K., Fuchs, H., Gailus-Durner, V., Adler, T., Hans, W., Horsch, M., Rathkolb, B., Rozman, J., Schrewe, A., *et al.* (2009). Dll1

haploinsufficiency in adult mice leads to a complex phenotype affecting metabolic and immunological processes. PLoS One *4,* e6054.

Santagati, F., Minoux, M., Ren, S.Y., and Rijli, F.M. (2005). Temporal requirement of Hoxa2 in cranial neural crest skeletal morphogenesis. Development *132,* 4927-4936.

Savage, J., Voronova, A., Mehta, V., Sendi-Mukasa, F., and Skerjanc, I.S. (2010). Canonical Wnt signaling regulates Foxc1/2 expression in P19 cells. Differentiation *79,* 31-40.

Savory, J.G., Bouchard, N., Pierre, V., Rijli, F.M., De Repentigny, Y., Kothary, R., and Lohnes, D. (2009a). Cdx2 regulation of posterior development through non-Hox targets. Development *136,* 4099-4110.

Savory, J.G., Pilon, N., Grainger, S., Sylvestre, J.R., Beland, M., Houle, M., Oh, K., and Lohnes, D. (2009b). Cdx1 and Cdx2 are functionally equivalent in vertebral patterning. Dev. Biol. *330,* 114-122.

Schroder, N., and Gossler, A. (2002). Expression of Notch pathway components in fetal and adult mouse small intestine. Gene Expr. Patterns *2,* 247-250.

Schug, J. (2008). Using TESS to predict transcription factor binding sites in DNA sequence. Curr. Protoc. Bioinformatics *Chapter 2,* Unit 2.6.

Shutter, J.R., Scully, S., Fan, W., Richards, W.G., Kitajewski, J., Deblandre, G.A., Kintner, C.R., and Stark, K.L. (2000). Dll4, a novel Notch ligand expressed in arterial endothelium. Genes Dev. *14,* 1313-1318.

Silberg, D.G., Swain, G.P., Suh, E.R., and Traber, P.G. (2000). Cdx1 and cdx2 expression during intestinal development. Gastroenterology *119,* 961-971.

Subramanian, V., Meyer, B.I., and Gruss, P. (1995). Disruption of the murine homeobox gene Cdx1 affects axial skeletal identities by altering the mesodermal expression domains of Hox genes. Cell *83,* 641-53.

Tabaries, S., Lapointe, J., Besch, T., Carter, M., Woollard, J., Tuggle, C.K., and Jeannotte, L. (2005). Cdx protein interaction with Hoxa5 regulatory sequences contributes to Hoxa5 regional expression along the axial skeleton. Mol. Cell. Biol. *25,* 1389-1401.

Tam, P.P., and Behringer, R.R. (1997). Mouse gastrulation: the formation of a mammalian body plan. Mech. Dev. *68,* 3-25.

Taylor, J.K., Levy, T., Suh, E.R., and Traber, P.G. (1997). Activation of enhancer elements by the homeobox gene Cdx2 is cell line specific. Nucleic Acids Res. *25,* 2293-2300.

Thomas, K.R., and Capecchi, M.R. (1987). Site-directed mutagenesis by gene targeting in mouse embryo-derived stem cells. Cell *51,* 503-12.

Tsunematsu, R., Nakayama, K., Oike, Y., Nishiyama, M., Ishida, N., Hatakeyama, S., Bessho, Y., Kageyama, R., Suda, T., and Nakayama, K.I. (2004). Mouse Fbw7/Sel-10/Cdc4 is required for notch degradation during vascular development. J. Biol. Chem. *279,* 9417-9423.

van den Akker, E., Forlani, S., Chawengsaksophak, K., de Graaff, W., Beck, F., Meyer, B.I., and Deschamps, J. (2002). Cdx1 and Cdx2 have overlapping functions in anteroposterior patterning and posterior axis elongation. Development *129,* 2181-93.

van Es, J.H., van Gijn, M.E., Riccio, O., van den Born, M., Vooijs, M., Begthel, H., Cozijnsen, M., Robine, S., Winton, D.J., Radtke, F., and Clevers, H. (2005). Notch/gamma-secretase inhibition turns proliferative cells in intestinal crypts and adenomas into goblet cells. Nature *435,* 959-963.

van Genderen, C., Okamura, R.M., Farinas, I., Quo, R.G., Parslow, T.G., Bruhn, L., and Grosschedl, R. (1994). Development of several organs that require inductive epithelial-mesenchymal interactions is impaired in LEF-1-deficient mice. Genes Dev. *8,* 2691-2703.

van Nes, J., de Graaff, W., Lebrin, F., Gerhard, M., Beck, F., and Deschamps, J. (2006). The Cdx4 mutation affects axial development and reveals an essential role of Cdx genes in the ontogenesis of the placental labyrinth in mice. Development *133,* 419-28.

Wahl, M.B., Deng, C., Lewandoski, M., and Pourquie, O. (2007). FGF signaling acts upstream of the NOTCH and WNT signaling pathways to control segmentation clock oscillations in mouse somitogenesis. Development *134,* 4033-41.

Wallberg, A.E., Pedersen, K., Lendahl, U., and Roeder, R.G. (2002). p300 and PCAF act cooperatively to mediate transcriptional activation from chromatin templates by notch intracellular domains in vitro. Mol. Cell. Biol. *22,* 7812-7819.

Wallingford, J.B., and Habas, R. (2005). The developmental biology of Dishevelled: an enigmatic protein governing cell fate and cell polarity. Development *132,* 4421-4436.

Watabe-Rudolph, M., Schlautmann, N., Papaioannou, V.E., and Gossler, A. (2002). The mouse rib-vertebrae mutation is a hypomorphic Tbx6 allele. Mech Dev *119,* 251-6.

Weerkamp, F., Luis, T.C., Naber, B.A., Koster, E.E., Jeannotte, L., van Dongen, J.J., and Staal, F.J. (2006). Identification of Notch target genes in uncommitted T-cell

progenitors: No direct induction of a T-cell specific gene program. Leukemia *20,* 1967-1977.

Wellik, D.M. (2007). Hox patterning of the vertebrate axial skeleton. Dev Dyn *236,* 2454-63.

Weng, A.P., Ferrando, A.A., Lee, W., Morris, J.P.,4th, Silverman, L.B., Sanchez-Irizarry, C., Blacklow, S.C., Look, A.T., and Aster, J.C. (2004). Activating mutations of NOTCH1 in human T cell acute lymphoblastic leukemia. Science *306,* 269-271.

White, P.H., and Chapman, D.L. (2005). Dll1 is a downstream target of Tbx6 in the paraxial mesoderm. Genesis *42,* 193-202.

White, P.H., Farkas, D.R., McFadden, E.E., and Chapman, D.L. (2003). Defective somite patterning in mouse embryos with reduced levels of Tbx6. Development *130,* 1681-90.

Wilson, V., and Beddington, R.S. (1996). Cell fate and morphogenetic movement in the late mouse primitive streak. Mech. Dev. *55,* 79-89.

Wolfe, M.S., and Kopan, R. (2004). Intramembrane proteolysis: theme and variations. Science *305,* 1119-1123.

Wu, L., Aster, J.C., Blacklow, S.C., Lake, R., Artavanis-Tsakonas, S., and Griffin, J.D. (2000). MAML1, a human homologue of Drosophila mastermind, is a transcriptional co-activator for NOTCH receptors. Nat. Genet. *26,* 484-489.

Yun, T.J., and Bevan, M.J. (2003). Notch-regulated ankyrin-repeat protein inhibits Notch1 signaling: multiple Notch1 signaling pathways involved in T cell development. J. Immunol. *170,* 5834-5841.

Zeng, X., Huang, H., Tamai, K., Zhang, X., Harada, Y., Yokota, C., Almeida, K., Wang, J., Doble, B., Woodgett, J., *et al.* (2008). Initiation of Wnt signaling: control of Wnt coreceptor Lrp6 phosphorylation/activation via frizzled, dishevelled and axin functions. Development *135,* 367-75.

Zeng, X., Tamai, K., Doble, B., Li, S., Huang, H., Habas, R., Okamura, H., Woodgett, J., and He, X. (2005). A dual-kinase mechanism for Wnt co-receptor phosphorylation and activation. Nature *438,* 873-877.